# Rare Earth Elements (REEs) Recovery and Hydrochar Production from Hyperaccumulators

Shiyu Li

Dissertation submitted to the faculty of the Virginia Polytechnic Institute and State University in partial fulfillment of the requirements for the degree of

Doctor of Philosophy
In
Mining Engineering

Wencai Zhang, Chair
Wanting Chen
Christopher Aaron Noble
Alexander S. Brand
Haibo Huang

November 05, 2024
Blacksburg, VA

Keywords: Hyperaccumulators, Rare earth elements, Recovery, Microwave-assisted hydrothermal carbonization, Hydrochar, Biocrudes, Solvent extraction

# Rare Earth Elements (REEs) Recovery and Hydrochar Production from Hyperaccumulators

Shiyu Li

## ACADEMIC ABSTRACT

Phytomining is a promising method for metal recovery, but rare studies have been devoted to metal recovery from hyperaccumulator biomass. The objective of this study was to propose efficient and sustainable methods for treating REE hyperaccumulators, aimed at enhancing REE recovery and obtaining value-added byproducts.

Firstly, grass seeds fed with a solution containing Y, La, Ce, and Dy, were found to have the capacity to accumulate around 510 mg/kg (dry basis) of total rare earth elements (TREEs) in grass leaves. With the use of conventional hydrometallurgy, around 95% of Y, La, Ce, and Dy were extracted from the GL using 0.5 mol/L $H_2SO_4$ at a solid concentration of 5 wt.%. Subsequently, microwave-assisted hydrothermal carbonization (MHTC) was used to convert the leaching residue into hydrochar to achieve a comprehensive utilization of GL biomass. Scanning electron microscopy (SEM) analysis revealed that the original structure of GL was destructed at 180 °C during MHTC, producing numerous microspheres and pores. As the reaction temperature increased, there was a concurrent increase in carbon content, HHV, and energy densification, coupled with a decrease in hydrogen and oxygen contents of hydrochar. The results showed that the waste biomass of the GL after REE extraction can be effectively converted into energy-rich solid fuel and low-cost adsorbent via MHTC.

In addition to utilizing conventional hydrometallurgy for REE recovery and employing MHTC to convert leaching residue into hydrochar, MHTC was also applied to directly recover REEs and produce hydrochar from the GL as a more efficient approach. The effects of acid type and acid concentration on REE extraction from GL using MHTC were investigated. The utilization of 0.2 mol/L $H_2SO_4$ led to the extraction of nearly 100% of REEs from the GL into

the resulting biocrudes. Concurrently, the acid-mediated MHTC system also caused the degradation of amorphous hemicellulose and crystalline cellulose present in the GL, thereby enhancing the thermal stability of the resulting hydrochar. The physiochemical properties of the hydrochar were also influenced by acid type and acid concentration. Using 0.2 mol/L $H_2SO_4$ as the reaction medium, MHTC resulted in a yield of 28% hydrochar with enhanced high heating value and energy densification. These results suggest that MHTC in the presence of an appropriate concentration of $H_2SO_4$ is an effective way to extract REEs and produce hydrochar from the GL.

A process that combines solvent extraction and struvite precipitation was developed for the treatment of biocrudes containing REEs and other elements. In the extraction step, 95.6% of REEs were extracted using 0.05 mol/L di(2-ethylhexyl)phosphoric acid (D2EHPA) with an aqueous to organic (A/O) ratio of 1:1 at pH 3.0. However, other impurity metals were co-extracted into the organic phase with the REEs. To solve this issue, a subsequent scrubbing step using deionized water was applied, with the removal of over 98% of these impurities, while incurring negligible loss of REEs. After the scrubbing step, over 97% of REEs were ultimately stripped out from the organic phase as REE oxalates using 0.01 mol/L oxalic acid. Furthermore, phosphorous (P) was found to be retained in the raffinate after the solvent extraction process. 94.4% of the P was recovered by forming struvite precipitate at pH 9.0 and a Mg/P molar ratio of 1.5. In general, high purity and value-added REE products and struvite precipitate were eventually achieved from biocrudes in environmentally friendly and economically viable ways.

In summary, this study contributes a sustainable and efficient framework for REE hyperaccumulator treatment that integrates acid leaching, MHTC, solvent extraction, and struvite precipitation. This work supports a circular economy, minimizing waste and promoting resource reuse.

# Rare Earth Elements (REEs) Recovery and Hydrochar Production from Hyperaccumulators

Shiyu Li

## GENERAL AUDIENCE ABSTRACT

Rare Earth Elements (REEs) are essential for technologies like smartphones and electric vehicles, but traditional mining is environmentally harmful and resource-intensive. Innovations are needed to reduce waste and enhance resource reuse. In this study, grass, a natural accumulator, was found to be able to extract REEs from contaminated soils. Nearly all REEs can be recovered efficiently using a mild sulfuric acid solution, and the residual biomass was also transformed into valuable byproducts such as energy-rich solid fuel and low-cost adsorbents. Furthermore, a more sustainable and efficient method, microwave-assisted hydrothermal carbonization, was also investigated to treat grass aiming at recovering REEs and achieving value-added products. High purity REE product and phosphorous-rich fertilizer were finally produced. This method reduces the environmental impact of REE mining, utilizes renewable resources, and cuts costs, thereby supporting economic sustainability. By turning environmental challenges into opportunities, this research highlights how innovative, greener methods can drive a more sustainable future in resource management.

## Acknowledgments

I have seen the acknowledgments of graduates. They like to summarize their Ph.D. journey with the phrase, “A light boat has passed through ten thousand heavy mountains.” At first, I did not grasp the meaning of the tune; upon listening again, I found myself within its story. It has been a hard journey. Good job, Shiyu Li.

The trials and tribulations along the way have long been scenery to me, yet I still want to thank my father, Xiaotao Li, and my mother, Jianhua Zhang, who have steadfastly stood behind me and supported me. My dad has always been the strongest support when I encounter difficulties, and my mom has always patiently listened to me when I am happy, down, anxious, or breaking down. Without them, I could not have grown into who I am today.

How fortunate I am that I have met many talented spotters during my Ph.D. journey. Thanks to my advisor, Dr. Wencai Zhang, for giving me the opportunity to pursue a Ph.D. degree at Virginia Tech three years ago. Every step on the path of scientific research in the past three years is closely related to his guidance and advice. It is he who made me understand what real effort and passion should look like.

Thanks to my senior, Bin Ji, under his careful guidance, I quickly overcame the initial unease of arriving in Blacksburg and smoothly integrated into the study and research work at VT. Thank you for the companionship and support beside me over the past three years.

Thanks to Dr. Wan-Ting (Grace) Chen, Dr. Aaron Noble, Dr. Alexander S. Brand, and Dr. Haibo Huang, for their efforts as my Ph.D. thesis committee members. Thanks to the members of my research group, as well as everyone who has appeared on my path of growth. Thanks to VT, studying and living in the beautiful VT has been a bright color in my life.

Thanks to the project, “Recovery of ZnO from End-of-Life Tires for Enhanced and Effective Waste Material Utilization” funded by the Center for Tire Research as well as “Low-Cost, Eco-friendly Recovery of Rare Earth Elements (REEs) from Coal Mine Wastes through

Phytomining" funded by the Office of Surface Mining Reclamation and Enforcement, for supporting me to complete my dissertation work.

Compared to "time is everything," in my eyes, "time is nothing." I never dictate that I must grow into a rose; I am jasmine, I am a daisy, I am an unnamed flower, I am countless others, and I am myself. The universe is infinite, technology is limitless, Shiyu Li, you should go and see.

# Table of Contents

# List of Figures

# List of Tables

# Preface

This dissertation is submitted as a completion of the degree of Doctor of Philosophy at Virginia Polytechnic Institute and State University. This research was conducted by the author, Shiyu Li, under the supervision of Dr. Wencai Zhang at the Department of Mining and Minerals Engineering.

This dissertation is established based on four manuscripts. Altogether, the dissertation includes four peer-reviewed journal articles.

Chapter 1 has been published as "Li, S., Ji, B., & Zhang, W. (2023). A review on the thermochemical treatments of biomass: Implications for hydrochar production and rare earth element recovery from hyperaccumulators. Chemosphere, 140140." https://doi.org/10.1016/j.chemosphere.2023.140140 (Shiyu Li: Conceptualization, Methodology, Investigation, Writing –original draft. Bin Ji: Methodology, Writing – review & editing. Wencai Zhang: Conceptualization, Methodology, Supervision, Validation, Writing – review & editing.)

Chapter 2 has been published as "Li, S., Ji, B., & Zhang, W. (2024). Rare Earth Element Recovery and Hydrochar Evaluation from Hyperaccumulator by Acid Leaching and Microwave-Assisted Hydrothermal Carbonization. Minerals, 14(3), 277." https://doi.org/10.3390/min14030277 (Shiyu Li: Conceptualization, Methodology, Validation, Investigation, Writing –original draft preparation. Bin Ji: Conceptualization, Validation, Writing – review & editing. Wencai Zhang: Conceptualization, Validation, Resources, Validation, Writing – review & editing, Supervision, Project administration, Funding Acquisition.)

Chapter 3 has been published as "Li, S., & Zhang, W. (2024). REE recovery and hydrochar production from a hyperaccumulator by microwave-assisted hydrothermal carbonization. Minerals Engineering, 208, 108595." https://doi.org/10.1016/j.mineng.2024.108595 (Shiyu Li: Conceptualization, Data curation, Formal analysis, Investigation, Methodology, Writing – original draft. Wencai Zhang: Conceptualization, Supervision, Writing – review & editing.)

Chapter 4 has been published as “Li, S., Zhang, W. (2024). Process Development for the Recovery of Rare Earth Elements and the Production of Struvite Precipitate from Biocrudes. Journal of Sustainable Metallurgy. 10, 1621–1633.” https://doi.org/10.3390/min14030277 (Shiyu Li: Conceptualization, Data curation, Formal analysis, Investigation, Methodology, Writing – original draft. Wencai Zhang: Conceptualization, Supervision, Writing – review & editing.)

# Chapter 1 Brief Introduction

## 1.1 Background

Rare earth elements (REEs) have wide applications in modern life as a result of their unique magnetic, optical, and electrical properties in advanced technologies (Jowitt et al. 2018; L. Wang et al. 2017; Yin et al. 2021). The extensive utilization of REEs has resulted in a large amount of REE waste. The increasing discharge of REE waste into the environment has raised concerns about the environment and human health (Dinh, Dobo, and Kovacs 2022a; Dutta et al. 2016; J. T. Li et al. 2018; Wu et al. 2019; Yu et al. 2020). From the perspective of environmental friendliness, it is necessary to consider the disposal of contaminated soils that contain REEs.

A few feasible technical routes have been proposed for the recovery of REEs from contaminated soils. For instance, hydrometallurgical methods were previously extensively employed to recover REEs from polluted soils due to their practical operability. However, studies on this aspect are decreased due to the substantial costs, high energy requirements, and minimal amounts of REEs production from the process (Lima and Ottosen 2021; Liu and Naidu 2014). Therefore, phytomining is increasingly gaining recognition and being extensively studied as an eco-friendly method for treating contaminated soil.

Plants require certain metals for their growth, while excessive amounts of metals can become toxic to plants (Asati, Pichhode, and Nikhil 2016). In the 20$^{th}$ century, it was found that certain plants have the ability to accumulate excessive metals present in contaminated soils (Lai et al. 2005; J. T. Li et al. 2018; Pollard, Reeves, and Baker 2014; Sheoran, Sheoran, and Poonia 2009; W. Sun et al. 2018). For example, *Sedum alfredii* population obtained from Quzhou, China can accumulate >10,000 mg/kg of Zn in its shoots. *Dicranopteris linearis*, growing in an REE mining area located in Fujian Province, China, accumulates up to 3,045 mg/kg of REEs (J. T. Li et al. 2018).

The plants that can accumulate metals in roots and above-ground tissues (e.g., shoots, flowers, stems, and leaves) are termed hyperaccumulators (Cosio, Martinoia, and Keller 2004; Jankovská et al. 2016). After a certain period of accumulation, the hyperaccumulators are harvested and processed through different methods to recover the metals. Several studies have indicated the feasibility of phytomining of REEs from contaminated soils by hyperaccumulators, and it was found that REE concentrations in the hyperaccumulators can reach up to over 1,000 mg/kg (Echevarria 2018). Given the fact that the REE content in the Upper Continental Crust (UCC) is only about 168.4 mg/kg (Housh, Bowring, and Villeneuve 1985), REE recovery from hyperaccumulators holds immense promise (Anderson et al. 1999; Dinh, Dobo, and Kovacs 2022b; Robinson et al. 1997; Sheoran, S.Sheoran, and Poonia 2013; Wang et al. 2020).

Among waste biomass treatment methods, thermochemical treatments are the most promising approaches, driven by their high efficiency and economic viability (Chai, Chen, et al. 2022a; Cui, Zhang, Wang, Pan, Lin, Khan, Yan, Li, He, Yang, et al. 2021; Yuan et al. 2011a). Thermochemical treatments can be classified into dry thermal treatments and hydrothermal treatments. Dry thermal treatments encompass incineration, gasification, and pyrolysis, while hydrothermal treatments consist of hydrothermal carbonization, hydrothermal liquefaction, and hydrothermal gasification (Cui, Zhang, Wang, Pan, Lin, Khan, Yan, Li, He, Yang, et al. 2021). Despite the significant reduction of waste volume, incineration and gasification can lead to severe environmental problems, such as air pollution, wastewater production, and energy consumption, due to the destruction of organic compounds and the release of non-destructive metal species (Fericelli 2011; Zhang et al. 2021). Therefore, in recent years, researchers have turned their direction to the application of pyrolysis and hydrothermal methods to treat waste biomass (Evcil et al. 2020a; Gollakota, Kishore, and Gu 2018; Guo et al. 2016; Jiang et al. 2022; LIU et al. 2017; Liu and Zhang 2008; S. Wang et al. 2017). In addition, compared with hydrothermal treatment, microwave-assisted hydrothermal treatment emerges as a more promising method due to its lower energy consumption and rapid volumetric heating (Afolabi and Sohail 2017).

Regarding hyperaccumulator disposal, previous studies mainly focused on the parametric optimization of using different thermochemical treatment technologies to produce high-value products with minimal metal content, including biogas, biocrudes (consisting of bio-oil and an aqueous phase containing value-added chemicals: sugars, furans, and carboxylic acids), and biochar or hydrochar (Cui, Zhang, Wang, Pan, Lin, Khan, Yan, Li, He, Yang, et al. 2021; Reza et al. 2013; Al Shra'Ah and Helleur 2014). The presence of metals in the products will negatively affect their downstream utilizations (Shen et al. 2021). Therefore, previous studies mainly aimed at immobilizing metals in biochar or hydrochar to improve the quality of bio-oil that can be used as fuel (Lang et al. 2019; Phytolaccaceae 2017; Qian et al. 2018; S. Sun et al. 2018; Zhang et al. 2017). For example, by the liquefaction of construction wood, the majority of heavy metals (Cr, Co, Ni, and Zn) transferred to the solid residue, and negligible amounts of heavy metals were presented in the biocrudes. The obtained biocrudes with minimal heavy metals are valued as higher quality products. In addition, metals sequestered in biochar or hydrochar exhibit a notable resistance to mobilization, thus protecting the environment with low release potential (Seehar et al. 2021).

Nowadays in the US, the price of ethanol fluctuates in the range of 0.4 to 0.8 $/L, but the unit price of biochar is incredibly high ($1600 per ton) (Berazneva, Woolf, and Lee 2021). Therefore, transferring the metals present in waste biomass to the liquid phase through thermochemical treatments to achieve high-quality biochar or hydrochar with low metal content seems to be a promising approach due to the price advantage. Furthermore, the advantage of not necessitating high temperatures for the generation of biochar or hydrochar enhances the environmental friendliness of the process aiming at converting waste biomass into more hydrochar. In general, it is promising to investigate efficient thermal treatment methods that can be integrated into a process for valuable metal recovery while generating useful products from hyperaccumulators (Cui, Zhang, Wang, Pan, Lin, Khan, Yan, Li, He, Yang, et al. 2021).

### 1.2 Research objectives

The overall objective of this research is to recover REEs and produce hydrochar from the REE hyperaccumulator. The specific objectives included:

(1) Optimize the REE recovery from the GL using conventional leaching method.

(2) Investigate the feasibility of transforming GL residue after the REE extraction into value-added hydrochar by MHTC.

(3) Investigate a sustainable technique (MHTC) to recover REEs into biocrudes and produce hydrochar from the GL.

(4) Propose a process flowsheet for the recovery of REEs and the production of struvite from biocrudes.

This study contributes a novel, sustainable, and efficient framework for REE hyperaccumulator treatment and supports a circular economy, minimizing waste and promoting resource reuse. The intellectual Merit of this study is to advance the knowledge of using sustainable and efficient ways to treat hyperaccumulators with the aim of recovering valuable elements and producing value-added byproducts. The broader impact of this work is to extend beyond the specific field of metal recovery, contributing significantly to environmental sustainability, economic development, and technological innovation in the area of mineral processing.

### 1.3 Dissertation outline

This dissertation comprises five chapters, the outline of each chapter is as follows:

Chapter 1 gave a brief introduction to the use of phytomining for REE recovery from contaminated soils. Emerging thermochemical technologies were systematically reviewed, and the effects of operating parameters on product characteristics and metal fate during thermochemical treatment of waste biomass were summarized.

In Chapter 2, objectives (1) and (2) were addressed. The effect of various factors on REE recovery from GL was investigated during the conventional hydrometallurgy process. The effect of MHTC temperature on the chemical and structural characteristics of hydrochar was explored, to evaluate the potential fuel properties as well as sequestration and adsorption abilities of the hydrochar product.

In Chapter 3, objective (3) was addressed. MHTC experiments of the GL were performed with the addition of acids and acid concentration to identify the optimal acid and acid concentration yielding the maximum recovery of REEs into biocrudes. X-ray diffraction (XRD) and thermogravimetric analysis (TGA) analyses were performed to characterize the structural changes and thermal decomposition behavior of the GL and the hydrochar produced from the MHTC process. Hydrochar and biocrudes were comprehensively characterized with the use of TGA and gas chromatography-mass spectrometry (GC-MS), respectively.

In Chapter 4, objective (4) was addressed. A process flowsheet for the recovery of REEs and the production of struvite from biocrudes was elaborated. The separation and purification of REEs from the biocrudes were accomplished via a solvent extraction process that encompassed stages of extraction, scrubbing, and precipitation stripping, with each phase undergoing parametric optimization to enhance operational efficiency. The struvite precipitation experiments were performed through adjustments of pH and Mg/P molar ratio to identify optimum conditions aiming at maximizing P recovery.

Chapter 5 summarizes this dissertation and provides perspectives for further improvement of the current study.

# Chapter 2 Rare Earth Element Recovery and Hydrochar Evaluation from Grass Leaves by Acid Leaching and Microwave-assisted Hydrothermal Carbonization

**Abstract**

Phytomining is a sustainable approach that uses hyperaccumulators for critical element extraction from various substrates, such as contaminated soils, mine tailings, and aqueous solutions. In this study, grass seeds were fed with a solution containing Y, La, Ce, and Dy, resulting in around 510 mg/kg (dry basis) of total rare earth elements (TREEs) accumulated in grass leaves. Electron probe microanalyzer (EPMA) analysis showed that REEs in the GL predominantly complexed with phosphorous (P). Around 95% of Y, 93% of La, 92% of Ce, and 93% of Dy were extracted from the GL using 0.5 mol/L $H_2SO_4$ at a solid concentration of 5 wt.%. Subsequently, microwave-assisted hydrothermal carbonization (MHTC) was used to convert the leaching residue into hydrochar to achieve a comprehensive utilization of GL biomass. The effect of temperature on the structural properties and chemical composition of the resulting hydrochar was evaluated. Scanning electron microscopy (SEM) analysis revealed that the original structure of GL was destructed at 180 °C during MHTC, producing numerous microspheres and pores. As the reaction temperature increased, there was a concurrent increase in carbon content, HHV, and energy densification, coupled with a decrease in hydrogen and oxygen contents of hydrochar. The evolution of H/C and O/C ratios indicated that dehydration and decarboxylation occurred during MHTC. The results showed that the waste biomass of the GL after REE extraction can be effectively converted into energy-rich solid fuel and low-cost adsorbent via MHTC.

## 2.1 Introduction

Several processes have been developed for the recovery of REEs from hyperaccumulators due to the increasing importance of REEs (Jally et al. 2021a). For instance, *D. dichotoma* is a REE hyperaccumulator that can accumulate 1.9 ~ 4.4 g/kg of REEs on a dry matter basis. 78% of the REEs present in the hyperaccumulator were recovered into a product with 81.4% purity by an ion exchange leaching step using 0.5 M $HNO_3$ solution, followed by removing competing ions with water and 0.75 M $HNO_3$, and a final one-stage elution step using 3 M $HNO_3$ (Chour et al. 2018). *Dicranopteris linearis* naturally growing on waste mine tailings in Southern China is classified as an REE hyperaccumulator that the total REE concentration in its frond can reach 2~3 g/kg of REEs on a dry matter basis. In order to recover REEs, *Dicranopteris linearis* was firstly incinerated to ash, and 6 mol/L sodium hydroxide was used to dissolve Al from the *Dicranopteris linearis* at a temperature of 80 ºC. Subsequently, the REEs were extracted under mildly acidic conditions using $HNO_3$ (25 ºC, pH 4.8), producing a valuable solution that contained relatively pure REEs (Jally et al. 2021b). These studies provide ideas for extracting REEs from hyperaccumulators. However, it is obvious that the incineration process contributes to carbon emissions and air pollution. Therefore, the extraction of REEs from hyperaccumulators needs to be reconsidered to make it more environmentally friendly.

The disposal of hyperaccumulator residue after REE extraction needs to be considered from a sustainable perspective. Currently, thermochemical treatments, such as pyrolysis and hydrothermal processing, are gaining more attention for waste biomass treatment due to their high efficiency, economic viability, and environmental friendliness (Chai, Chen, et al. 2022b; Cui, Zhang, Wang, Pan, Lin, Khan, Yan, Li, He, and Yang 2021; Yuan et al. 2011b). Among all thermochemical treatment methods, hydrothermal carbonization (HTC) has been extensively researched due to its relatively mild reaction conditions (160 ºC-270 ºC) and capability to convert waste biomass into a valuable solid product (hydrochar) (Shao et al. 2019; Tag, Duman, and Yanik 2018; Zhang et al. 2019). The produced hydrochar can be used as a fuel source, soil amendment, carbon-based catalyst, or adsorbent material (Zhang et al. 2019). Compared to HTC, microwave-assisted hydrothermal carbonization (MHTC) promotes the reaction kinetics as a result of rapid volumetric heating and consumes less energy (approximately 50% energy consumption compared with the HTC process) (Shao et al. 2020). It was found that 57.9% hydrochar was generated from MHTC-treated rice straw at 180 ºC for 20 min with a fixed solid concentration of 7% (Nizamuddin, Qureshi, Baloch, Siddiqui, Takkalkar, Mubarak, Deepa K Dumbre, et al. 2019). The higher heating value (HHV), carbon content, and fixed carbon (FC) values increased from 12.3 MJ/kg, 37.19%, and 14.37% to 17.6 MJ/kg, 48.8%, and 35.4%, respectively after MHTC. The porosity, crystallinity, and thermal stability of the hydrochar obtained from MHTC were also improved significantly.

In this chapter, grass was found to be a promising REE hyperaccumulator, and the electron probe microanalyzer (EPMA) analysis was conducted to characterize the occurrence of REEs in the grass leaves (GL). The effect of acid types, solid concentration, and acid concentration on REE recovery from GL was investigated. In addition, this study investigated the feasibility of transforming GL residue after the REE extraction into valuable hydrochar by MHTC. The effect of MHTC temperature on the chemical and structural characteristics of hydrochar was explored, to evaluate the potential fuel properties as well as sequestration and adsorption abilities of the hydrochar product.

## 2.2 Materials and methods

### 2.2.1 Chemicals and reagents

The chemicals used in this chapter include nitric acid ($HNO_3$, 67 wt.% to 70 wt.%), hydrochloric acid (HCl, 37 wt.%), sulfuric acid ($H_2SO_4$, 93 wt.% to 98 wt.%), and 50% w/w sodium hydroxide solution (NaOH, ≥ 97 wt.%). $Y(NO_3)_3·6H_2O$, $La(NO_3)_3·6H_2O$, $Ce(NO_3)_3·6H_2O$, and $Dy(NO_3)_3·6H_2O$ were used to prepare the feeding solution of grass seeds. All the chemicals were of trace metal grade and purchased from Thermo Fisher Scientific, USA.

Type I deionized water with a resistivity of 18.2 MΩ·cm at 25 °C was prepared by Direct-Q Water Purification System (Millipore, USA).

### 2.2.2 Hyperaccumulator plant

Grass seeds were grown in "potting mix" that contains a mixture of organic materials such as peat moss, drainage-assisted materials, and slow-release fertilizers. Both the grass seeds (The Rebels, PENNINGTON) and potting mix (Potting Mix, Miracle-Gro) were purchased from The Home Depot, USA. The grass seeds were grown under natural light and an average temperature of 25 ± 3 ºC. A solution containing Y, La, Ce, and Dy of 50 mg/L was used to feed the seeds once every two days. After 14 days of growth, the GL was harvested, thoroughly rinsed with deionized water, dried at 80 ºC for 48 h, and ground by a high-speed multifunction grinder. The ground product was collected and used as the feed for leaching tests. The product was predominantly distributed in the size range of 53 to 297 µm. The product of 0.2 g was mixed with 12 mL of $HNO_3$ and placed in a 50 mL digestion vessel (HVT50, Anton Paar, Austria). The vessel was then placed in a microwave digestor (Multiwave GO Plus, Anton Paar, Austria) and subjected to microwave digestion with a heating rate of 18.5 ºC/min. The digestion was carried out at 185 ºC with a residence time of 40 min. After digestion, the vessel was cooled completely, and then the digestion liquor was collected and centrifuged. The resulting supernatant was diluted 100 times with a solution containing 5% (v/v) $HNO_3$. Elemental concentrations of the diluted solution were analyzed using an inductively coupled plasma emission mass spectrometer (ICP-MS, Thermo Electron iCAP-RQ, Thermo Scientific, USA). ICP-MS analysis data was used to calculate the elemental composition of the GL.

JEOL JXA-iHP200F field emission electron probe microanalyzer (EPMA) was used for the quantitative elemental analysis of the GL. The sample was fit onto a 1-inch diameter sample holder with a vertical profile not exceeding 1 mm and was coated with carbon using a mini sputter coater (QUORUM, Model EMS 7620, USA) (Misch et al. 2016; Smolders and Degryse 2002). The sample holder was placed in a vacuum chamber to avoid the interactions between air and the electron beam during observation using the microprobe. 30 $mm^2$ energy-dispersive silicon drift detector (SDD EDS) was used for rapid phase identification, and wavelength-dispersive spectrometers (WDS) was used for fast, high-resolution, quantitative chemical analyses of elements.

### 2.2.3 Acid leaching tests

All leaching tests were carried out at 25 ºC for a duration of 30 min. The effect of acid types ($HNO_3$, HCl, and $H_2SO_4$) on REE recovery from the GL was first investigated to identify the most promising lixiviant. The acid concentration and solid concentration were fixed at 0.5 mol/L and 5 wt.%, respectively. The mixture was agitated using a magnetic stirrer at 450 rpm for 30 min. After the reaction, the mixture was centrifuged at 5000 rpm for 5 min using a SorvallTM Legend X1 centrifuge (Thermo Fisher Scientific, USA). The resulting supernatant was collected and diluted 100 times with a 5% (v/v) $HNO_3$ solution for REE concentration measurement using ICP-MS. The remaining solid was thoroughly rinsed with deionized water and then dried at 80 ºC for 48 hours. The dried solid was then digested following the same procedure as the raw GL (see section 2.2).

After determining the most promising lixiviant, the effects of solid concentration and acid concentration on the recovery of REEs from the GL were investigated. The acid concentration was fixed at 0.5 mol/L with the solid concentration varying from 1 to 10 wt.% (i.e., 1 wt.%, 2 wt.%, 5 wt.%, and 10 wt.%). When investigating the effect of acid concentration (0.1 mol/L, 0.5 mol/L, 1 mol/L, and 2 mol/L), the solid concentration was maintained at 5 wt.%. After the reaction, the solid and liquid were separated by centrifugation and then subjected to elemental concentration analysis. In addition, the dry solid residue was used for further characterizations as well as the feed for the MHTC experiments.

The fraction of REEs in the feed GL that was extracted into the solution during the leaching process was defined as REE leaching recovery ($R_L$, %). The recovery was calculated using the following Equation (2.1).

$$R_L = \frac{C_L \times 0.1}{C_L \times 0.1 + C_S \times M_S} \times 100 \tag{2.1}$$

where $C_S$ and $C_L$ represent REE concentrations in the leaching residue (mg/kg) and leaching solution (mg/L), respectively; $M_S$ (kg) represents the mass of the leaching residue, and 0.1 (L) is the volume of the leaching solution.

The most effective lixiviant, solid concentration, and acid concentration for REE recovery from the GL were identified after optimizing these factors. To maximize the potential value of the GL, MHTC was used for the conversion of the GL residue obtained from acid leaching into hydrochar.

### 2.2.4 Microwave-assisted hydrothermal carbonization (MHTC)

MHTC was conducted in a microwave reactor (Multiwave GO Plus, Anton Paar GmbH, Austria) with a magnetron frequency of 2450 MHz. The effect of temperature on the characteristics of the obtained hydrochar was investigated. Briefly, GL residue of 0.5 g was mixed with 10 mL deionized water in a 50 mL reaction vessel. A heating rate of 10 ºC/min and a residence time of 60 min were applied during the reaction at different temperatures (i.e., 120 ºC, 140 ºC, 160 ºC, and 180 ºC). After the completion of reaction, the suspension was collected and centrifuged at 5000 rpm for 5 min. The solid residue was rinsed thoroughly with deionized water and dried at 80 ºC for 48 hours. After drying, the solid was weighed and stored for characterizations.

### 2.2.5 Hydrochar characterization

#### 2.2.5.1 Proximate analysis

Thermogravimetric analysis (TGA) (TGA 5500, TA Instruments CO., USA) was used for the proximate analysis of the samples obtained from MHTC, in which the sample was heated to constant weight under ASTM specified conditions (Donahue and Rais 2009; Khoo et al. 2020). A sample weighing approximately 5 mg underwent thermal analysis in a controlled atmosphere of high-purity $N_2$ with a flow rate of 20 mL/min. To eliminate any moisture, the sample was heated to 110 ºC and held for at least 30 min. The temperature was then increased to 900 ºC at a ramp rate of 10 ºC/min, which was maintained for 60 min. The weight loss during this step was attributed to the volatile matter (VM) present in the sample. Subsequently, the $N_2$ gas flow was replaced with dry air, and the temperature was increased to 925 ºC at the same heating rate of 10 ºC/min. The sample was then held at this temperature for 60 min. Any oxidizable matter lost at this step was considered fixed carbon (FC), while the remaining mass represented the ash content of the sample.

#### 2.2.5.2 Elemental composition

The percentages of key elements (C, H, and O) were calculated using the Parikh formula(Parikh, Channiwala, and Ghosal 2007). These correlations can calculate elemental compositions of biomass materials from simple proximate analysis. The correlations were determined based on Equations (2.2) ~ (2.4).

$$C = 0.637FC + 0.455VM \tag{2.2}$$

$$H = 0.052FC + 0.062VM \tag{2.3}$$

$$O = 0.304FC + 0.476VM \tag{2.4}$$

### 2.2.5.3 High heating value calculation

The high heating value (HHV; in MJ/kg) of the samples was calculated based on Jenkins's formula (Channiwala and Parikh 2002; Ebeling and Jenkins 1985)(Equation (2.5)).

$$HHV = -0.763 + 0.301C + 0.525H + 0.064O \tag{2.5}$$

This correlation is derived based on 57 data points of biomass material and using multiple regression analysis.

### 2.2.5.4 Definitions

The hydrochar yield (*Hy*, %), energy densification (*Ed*), and energy recovery efficiency (*ERE*, %) were calculated using Equations (2.6) ~ (2.8), respectively (Kim, Lee, and Park 2014).

$$Hy = \frac{M_h}{M_{GLR}} \times 100 \tag{2.6}$$

$$Ed = \frac{HHV_h}{HHV_{GLR}} \tag{2.7}$$

$$ERE = E_d \times H_y \tag{2.8}$$

where, $M_h$ is the hydrochar weight (g), $M_{GLR}$ is the mass of the GL residue (g), $HHV_h$ is the high heating value of the hydrochar (MJ/kg), and $HHV_{GLR}$ is the high heating value of the GL residue (MJ/kg).

### 2.2.5.5 Characterization

A JSM-IT500 scanning electron microscope (SEM) equipped with a backscattered electron (BSE) system was used to determine changes in the structure and morphology of the samples. The samples were spread on carbon tapes and sputtered with palladium/platinum (5 nm thickness) with the use of a sputter coater (208HR, Cressington Scientific Instrument, England, UK) to increase their electron conductivity.

The Brunauer-Emmett-Teller (BET) surface area and pore volume of the samples were measured by $N_2$ sorption on a Quantachrome Autosorb-1. Samples were degassed under vacuum for 24 h at 120 ºC prior to the analysis. The surface area was calculated according to BET theory using adsorption data in the 0.05-0.30 relative pressure range (equilibrium pressure (kPa)/saturation pressure (kPa) ($P/P_0$)), and the volume of $N_2$ adsorbed at the relative pressure of 0.99 was used to calculate the pore volume of the samples.

## 2.3 Results and discussion

### 2.3.1 Elemental composition of GL

Elemental concentrations of the GL are presented in Table 2.1. The concentration of total REEs (TREEs) in the GL was 510.5 mg/kg, while the total concentration of the four REEs (Y, La, Ce, and Dy) added to the watering solution was 503.4 mg/kg, accounting for the majority of the TREEs present in the GL. In addition, the TREE concentration of the GL watered with deionized water was around 0 mg/kg (Figure 2.1). Therefore, these results suggested that the GL can effectively accumulate REEs. Moreover, the concentration of La and Ce in the GL was 242.1 mg/kg, which was close to the concentrations of Y and Dy (261.3 mg/kg). Therefore, it can be concluded that the GL exhibited a comparable accumulation capacity for light REEs (LREEs) and heavy REEs (HREEs). A plant can be called an REE hyperaccumulator when the concentration of REEs in the aboveground shoot exceeds 1000 mg/kg (Liu et al. 2021). As can be seen from Figure 2.1, when increasing the concentration of the four different REEs in the watering solution from 50 mg/L to 500 mg/L, the concentration of TREEs in GL shows an almost similar proportional increase from 510.5 mg/kg to 5801.9 mg/kg, indicating that GL can accumulate over 1000 mg/kg of REEs in the aboveground shoot. The concentration of four different REEs in the GL also increased proportionally with the increase of REE concentration in the watering solution. Therefore, the grass used in this study can be regarded as an REE hyperaccumulator.

Table 2.1 Elemental concentrations (mg/kg) of GL.

| | | | | | | | | | |
|---|---|---|---|---|---|---|---|---|---|
| K | Ca | P | Mg | Na | Fe | Al | Si | Mn | Zn |
| 48730.2 | 12360.5 | 7725.4 | 3628.8 | 544.5 | 255.7 | 266.2 | 182.0 | 73.7 | 45.6 |
| Sr | Ba | Ti | TREEs | LREEs | HREEs | Y | La | Ce | Dy |
| 20.1 | 18.8 | 10.3 | 510.5 | 247.1 | 263.1 | 125.4 | 119.9 | 122.2 | 135.9 |

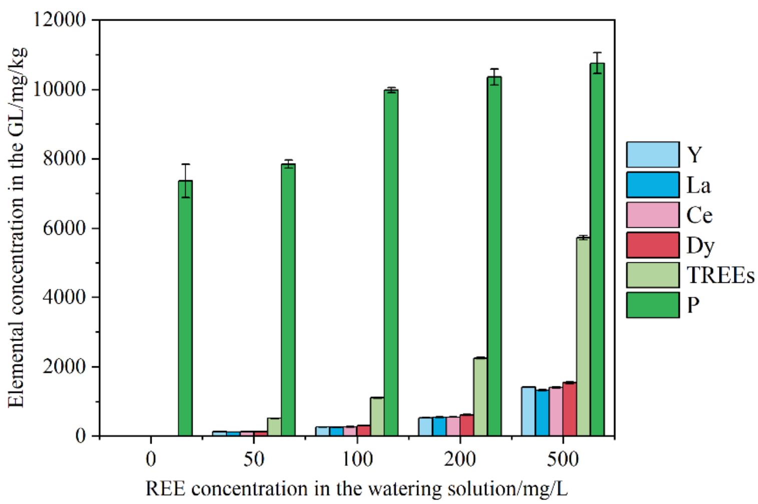


Figure 2.1 Effect of REE concentration in watering solution on the elemental concentration in the GL.

In addition to REEs, the concentration of some major (>1000 mg/kg) and other trace (10-1000 mg/kg) elements in the GL was also listed in Table 2.1. It was found that GL was rich in K, Ca, and Mg, with a concentration of 48730.2 mg/kg, 12360.5 mg/kg, and 3628.8 mg/kg, respectively. This phenomenon is consistent with the general finding that plants are rich in these elements  (Chour et al. 2020). The concentration of P in GL was 7725.4 mg/kg, which was higher than any other elements except for K and Ca. In addition, Figure 2.1 illustrates that with the increase of REE concentration in the feeding solution from 0 mg/L to 500 mg/L, the concentration of P in the GL increases from 4117.5 mg/kg to 8899.9 mg/kg. This phenomenon can be explained by the formation of complexes between REE and P in the GL (Ding et al. 2006;

Liu et al. 2020). As more REEs were accumulated, they complexed with more P in the GL, leading to the undernourishment of P, which prompted the adsorption for the nutrition requirement of plant growth.

EPMA characterization was employed to conduct quantitative chemical analysis of various elements, with a particular focus on Y, La, Ce, Dy, and P, in the GL. Heavy elements appear as bright spots in the SEM images, while light elements are known to show up as dark spots (Z.-M. Wang et al. 2017). A relatively bright particle of the GL was selected for the characterization (in the red rectangle in Figure 2.2(a)). The Point & ID mode with the use of an EDS detector was first employed to have a quick elemental composition analysis at a specific point of this bright particle (Ji, Li, and Zhang 2022). It was found that the molar percentages of $Y_2O_3$, $La_2O_3$, $CeO_2$, and $Dy_2O_3$ were 3.79%, 1.25%, 2.23%, and 0.99%, indicating that REEs were presented in this bright particle (Table 2.2). The SEM image of a region of interest on that particle was shown in Figure 2.2(a), and the distribution of elements in this area of interest was known by developing elemental maps with Map mode using a WDS detector. Compared with EDS, WDS was more suitable for mapping at low concentrations owing to its greater peak-to-background ratios (Borghi et al. 1998; Reed and Buckley 1998). Therefore, considering the trace quantity of REEs (~500 mg/kg) in the GL, elemental mapping of this area was analyzed using the WDS in the Map mode. A higher concentration of the corresponding element is indicated by the presence of a brighter color at a specific location on the map (Ji et al. 2022). As can be seen from Figure 2.2(b)~(e), four specific REEs (Y, La, Ce, and Dy) are rich in the area of red rectangle and circle. It was also found that these REE-enriched locations also had the enrichment of P (Figure 2.2(f)). However, some areas enriched in P did not have the enrichment of REEs in the GL. This phenomenon indicated that REEs accumulated in the GL tended to be in the complexation with a portion of P in the GL. Furthermore, It was found that the areas containing high concentrations of REEs and P also contained some other metals, such as K, Ca, Mg, Na, Fe, Al, and Mn (Figure 2.3).

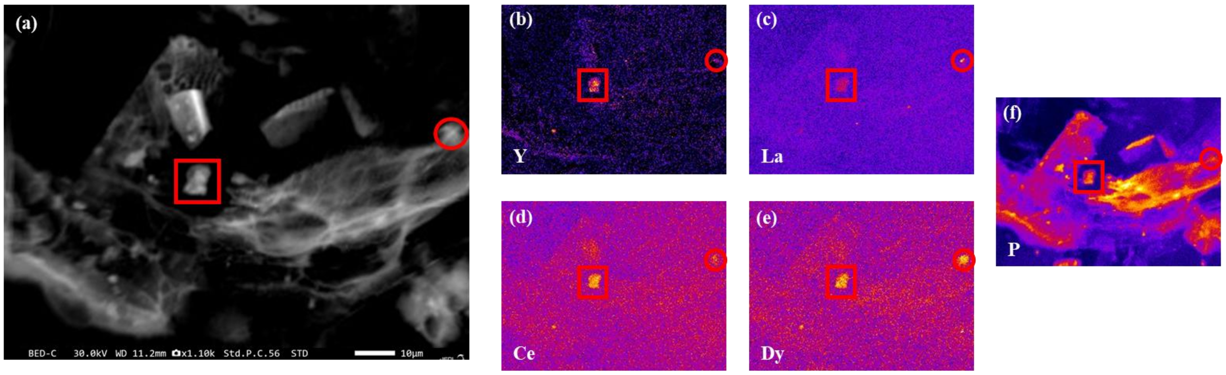


Figure 2.2 SEM image of the GL (a) and WDS mapping of different elements (b)~(f).

Table 2.2 Chemical compositions (Mol%) of the GL analyzed by EDS spectrum.

| Chemicals | MgO | $SiO_2$ | $P_2O_5$ | Cl | $K_2O$ | CaO | $Y_2O_3$ | $La_2O_3$ | $CeO_2$ | $Dy_2O_3$ |
|---|---|---|---|---|---|---|---|---|---|---|
| Mol% | 14.65 | 10.00 | 21.84 | 12.26 | 12.80 | 20.18 | 3.79 | 1.25 | 2.23 | 0.99 |

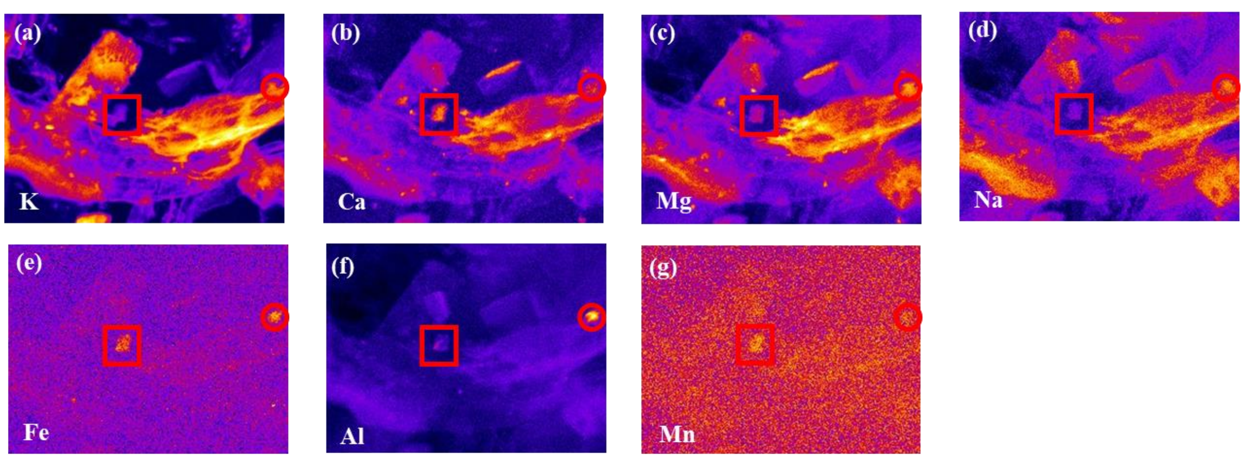


Figure 2.3 WDS mapping of different elements in the GL (a)~(h).

### 2.3.2 Acid leaching

#### 2.3.2.1 Effect of acid types

Different acid types may lead to different leaching characteristics at the same molar concentration due to differences in normality and anionic components. Therefore, the influence of acid type on the recovery of REEs and P from the GL was investigated. Figure 2.4 shows the leaching recoveries of REEs from the GL using three different acids, including $HNO_3$, HCl, and $H_2SO_4$. The solid concentration and acid concentration were fixed at 5 wt.% and 0.5 mol/L, respectively. When using $HNO_3$ as the lixiviant, 67%, 73%, 67%, and 63% of Y, La, Ce, and Dy were leached, respectively. Similar recoveries of 66%, 69%, 63%, and 61% were obtained when using HCl as the lixiviant. However, it can be seen from Figure 2.4 that the recoveries of Y, La, Ce, and Dy increased significantly to 95%, 93%, 92%, and 92%, respectively, with the use of $H_2SO_4$. The higher recovery of REEs using $H_2SO_4$ as the lixiviant can be attributed to the higher concentration of hydrogen ions ($H^+$) available in the $H_2SO_4$ solution compared to using the same concentrations of $HNO_3$ and HCl. The higher concentration of $H^+$ facilitated the solubility of REEs from the GL (Larsson, Ekberg, and Ødegaard-Jensen 2013; Zielinski et al. 2020). In addition, it was reported that sulfate ions can form more stable complexes with REEs than chloride ions, promoting the dissolution of REEs from ion-adsorption clays (Moldoveanu and Papangelakis 2012). Therefore, it can be inferred that the strong complexing ability of REEs and sulfate ions also promoted the REE dissolution from GL when using $H_2SO_4$ as a lixiviant.

As can be seen from Figure 2.4, using $H_2SO_4$ as the lixiviant not only enhanced the recovery of REEs but also led to an increase in P recovery. This phenomenon can be ascribed to the fact that the occurrence of REEs in the GL was in the complexation with a portion of P in the GL. Therefore, during the leaching process, the complexes of REEs and P were disrupted by $H_2SO_4$, thus leading to the enhanced recovery of REEs and P. It is worth mentioning that using $H_2SO_4$ is more economically viable than using $HNO_3$ and HCl due to the low average price

(Yang and Honaker 2020). Therefore, $H_2SO_4$ was selected as the preferred lixiviant for the recovery of REEs from the GL.

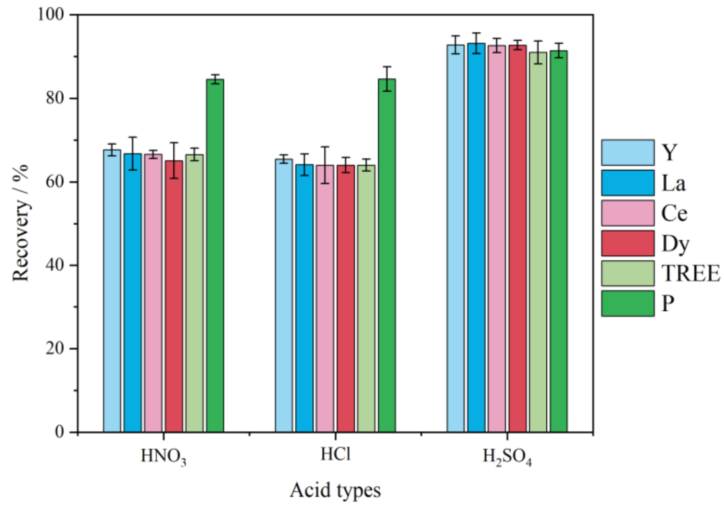


Figure 2.4 Effect of acid types on the elemental recovery from the GL.

#### 2.3.2.2 Effect of solid concentration

The solid concentration represents the stoichiometric ratio of reactants, which directly affects the reaction equilibrium (Dixon and Hendrix 1993). The effect of solid concentration (1 wt.%, 2 wt.%, 5 wt.%, and 10 wt.%) on the recovery of REEs and P from GL was investigated using a fixed 0.5 mol/L $H_2SO_4$. Figure 2.5 shows that the maximum recovery of REEs (around 99%) is obtained at a solid concentration of 1 wt.%. Slight decreases in REE recovery were observed as the solid concentration increased from 1 wt.% to 5 wt.%. When further enhanced solid concentration from 5 wt.% to 10 wt.%, the recovery decreased further to 90%, 89%, 89%, and 88% for Y, La, Ce, and Dy, respectively. A low solid concentration is favorable for the extraction of REEs from the GL since increasing the volume of the leaching solution can increase the efficiency of mass transfer, thus leading to an increase in REE recovery (Chen et al. 2015). In addition, as the solid concentration increased from 1 wt.% to 10 wt.%, the recovery of

P decreased from 99% to 89%. The simultaneous decrease in the recovery of REEs and P can also be attributed to the reason mentioned in section 3.2.1. Based on the leaching results, the most suitable solid concentration was selected to be 5 wt.%.

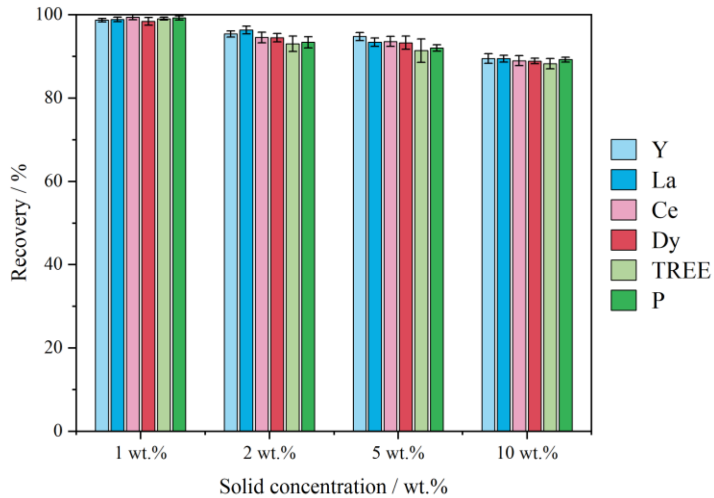


Figure 2.5 Effect of solid concentration on the elemental recovery from the GL.

### 2.3.2.3 Effect of acid concentration

It is well known that acid concentration is one of the most influential factors in REE leaching experiments (Mokoena, Mokhahlane, and Clarke 2022). Increased acid concentration represents more $H^+$ can react with REE-bearing minerals, thus resulting in higher REE recovery (Zeng et al. 2021). The effect of $H_2SO_4$ concentration (0.1 mol/L, 0.5 mol/L, 1 mol/L, and 2 mol/L) on the leaching recovery of REEs and P was investigated at a fixed solid concentration of 5 wt.%. As can be seen from Figure 2.6, around 85% of REEs can be recovered using 0.1 mol/L $H_2SO_4$. When further increasing $H_2SO_4$ concentration from 0.1 mol/L to 0.5 mol/L, the recovery of Y, La, Ce, and Dy increased to 96%, 93%, 92%, and 93%, respectively. The further increase of $H_2SO_4$ concentration from 0.5 mol/L to 2 mol/L led to a minor increase in the REE recovery. The final pH values of the leaching solutions were 1.3, 0.8, 0.7, and 0.6, respectively. An increase in the acid concentration leads to a decrease in the pH of the solution, and a low pH value of the leaching solution is favorable for metal leaching (Lie and Liu 2021). Therefore, the recovery of REEs was increased with the increase of acid concentration and the decrease of pH of the leaching solutions.

There was still a proportion (around 5%) of difficult-to-leach REE-bearing compounds in the GL when using 2 mol/L $H_2SO_4$ as the lixiviant at a solid concentration of 5 wt.% (Figure 2.6). This phenomenon might be because with the increase of acid concentration from 0.5 mol/L to 2 mol/L, more sulfate ions released into the leachate combined with $Ca^{2+}$, leading to the formation of insoluble $CaSO_4$ (gypsum). Gypsum precipitation might coat the surface of the REE-bearing GL, resulting in decreases in the surface area and pore size of particles (Zhang and Noble 2020a). As a result, the remaining REEs in the GL were difficult to be leached. The recovery of P increased from 89% to 93% with the increase of acid concentration from 0.1 mol/L to 0.5 mol/L, while there was a negligible increase in P recovery when increasing the acid concentration from 0.5 mol/L to 2 mol/L. In addition, around 3% of P cannot be recovered using 2 mol/L $H_2SO_4$. This phenomenon was due to the reason that REEs were in the form of the complexation with P, thus the leaching of P exhibited a leaching pattern similar to that of REEs. Overall, 0.5 mol/L $H_2SO_4$ was selected as an optimal acid concentration for recovering REEs from the GL.

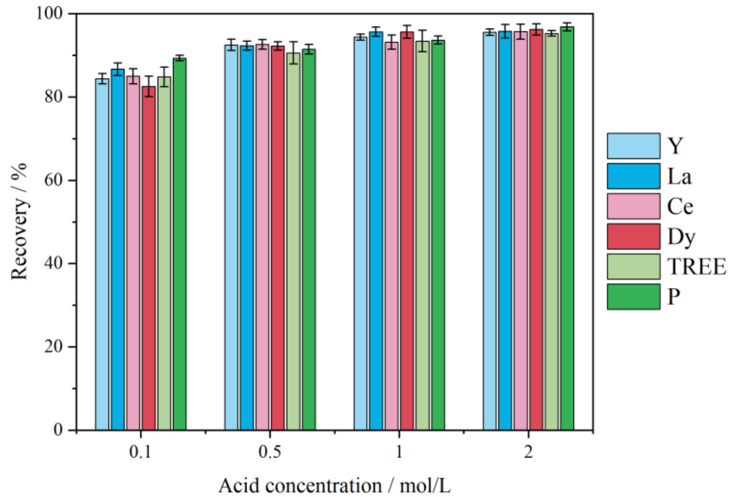


Figure 2.6 Effect of acid concentration on the elemental recovery from the GL.

### 2.3.3 Hydrochar characterization

#### 2.3.3.1 Structural properties of the hydrochar

The optimum conditions for recovering REEs from the GL were determined after optimizing the acid type, solid concentration, and acid concentration. To make a comprehensive utilization of GL, MHTC was employed to convert the leaching residue into hydrochar, which is an exceptionally valuable product with a wide range of applications (Nizamuddin, Qureshi, Baloch, Siddiqui, Takkalkar, Mubarak, Deepa K. Dumbre, et al. 2019; Shao et al. 2020). As can be seen from Figure 2.7, compared with the leaching residue of GL, the color of hydrochar samples became darker with the increase in MHTC temperature, indicating that the GL residue was gradually carbonized (Cai et al. 2016). The SEM images illustrate the morphological variations of the hydrochar obtained from the GL residue via MHTC at various temperatures. Firstly, as can be seen in Figure 2.8(a), the surface of the raw GL residue was smooth and compact. The degree of surface roughness increased gradually as the reaction temperature increased from 120 ºC to 140 ºC (as shown in Figure 2.8(b) and (c)). This can be attributed to the decomposition of hemicellulose, depolymerization of cellulose, and partial degradation of lignin

(Cai et al. 2016; Kambo and Dutta 2015b; Sevilla and Fuertes 2009). When further increasing the temperature from 140 ºC to 160 ºC, a few microspheres can be clearly discerned in the area of the red rectangle in Figure 2.8(d). With the temperature increased from 160 ºC to 180 ºC, numerous sphere-like microparticles were produced as shown in the red rectangles of Figure 2.8(e).

Notably, the surface of the hydrochar exhibited distinct pores (red circle in Figure 2.8(d)) at the temperature of 160 ºC. Moreover, the morphology of GL residue was almost completely disrupted at the reaction temperature of 180 ºC, revealing the presence of solely pore structures without any fibrous strands, as depicted in the red circles in Figure 2.8(f). The formation of microspheres and the presence of pores indicated that the GL residue underwent the decomposition transformation during MHTC. The process of microsphere formation involved the decomposition of complex macromolecules present in the GL residue, including carbohydrates, proteins, and lipids (Wang et al. 2018). As these macromolecules underwent decomposition, the resulting breakdown products precipitated and gradually aggregated, eventually forming spherical structures (Kannan, Gariepy, and Raghavan 2017). In addition, most hemicellulose contained in the GL was violently decomposed at high temperatures during MHTC process, leading to the formation of pores on the surface of hydrochar (Nizamuddin et al. 2018). Also, according to (Marx, Chiyanzu, and Piyo 2014), the walls between adjacent pores are destroyed at high temperatures, causing enlargement of the pores, which can be clearly observed in Figure 2.8(f). The porous structure of hydrochar obtained at high temperatures suggests that the hydrochar can be used for sequestration and adsorption purposes (Kannan et al. 2017).

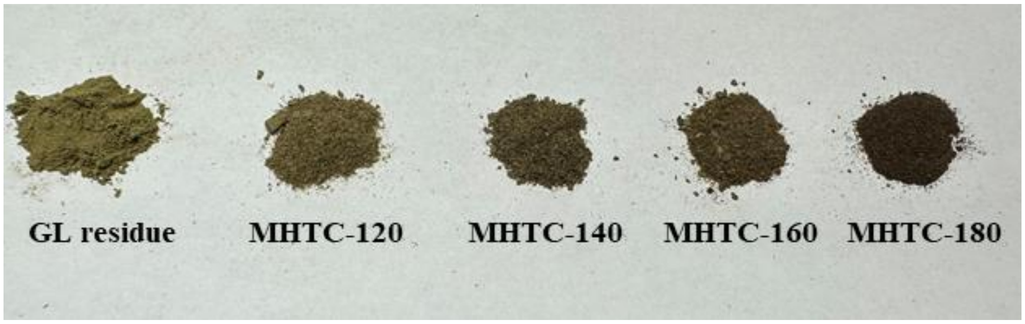


Figure 2.7 Hydrochar obtained at different reaction temperature during MHTC.

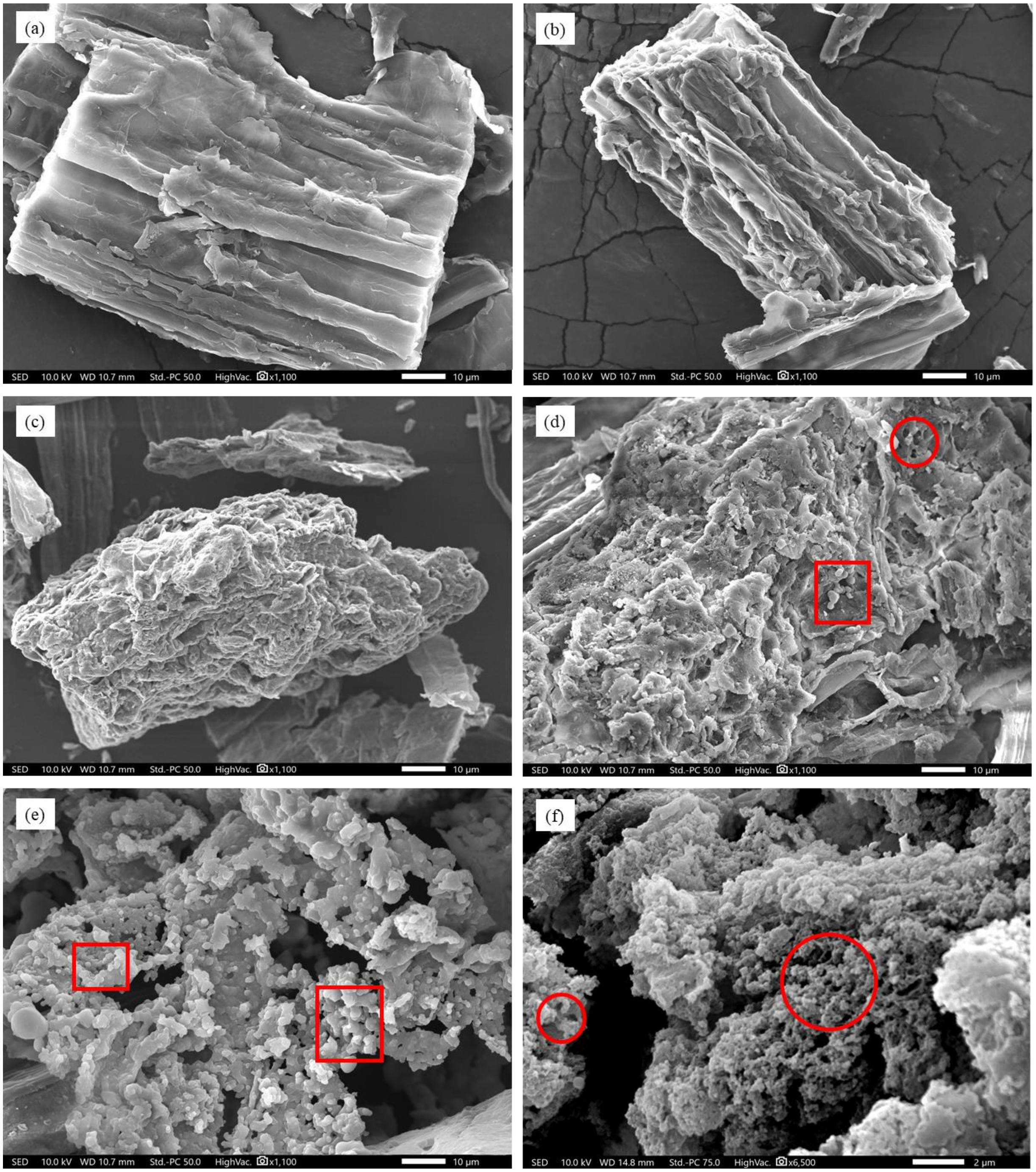


Figure 2.8 SEM images of GL residue and hydrochar obtained at different reaction temperatures: (a): GL residue, (b) MHTC-120, (c) MHTC-140, (d) MHTC-160, (e)-(f) MHTC-180.

The porous textural characteristics were assessed by the nitrogen physisorption method. As Table 2.3 shows, the surface area of hydrochar increased slightly with the increase in reaction temperature from 120 ºC to 140 ºC. When further increased the temperature to 180 ºC, the surface area increased significantly from 2.345 $m^2/g$ to 9.428 $m^2/g$. The increased surface roughness and the formation of microspheres during MHTC led to an increase in the surface area of hydrochar. The increase in hydrochar porosity was caused by the growth of existing pores and the formation of new micropores due to the decomposition of cellulose and hemicellulose at higher temperatures (Nizamuddin et al. 2018). High surface area and pore volume are correlated with enhanced sorption ability and are desired traits for the char used for the remediation of soil or water contamination (Bahcivanji et al. 2020).

Table 2.3 Textural parameters for GL residue and hydrochar obtained at 120 ºC, 140 ºC, 160 ºC, and 180 ºC.

| | $S_{BET}$ / $m^2/g$ | $V_t$ / $cm^3/g$ | Average pore diameter / nm |
|---|---|---|---|
| GL residue | 0.052 | 0.004 | 1.519 |
| MHTC-120 | 1.625 | 0.009 | 1.528 |
| MHTC-140 | 2.345 | 0.016 | 1.578 |
| MHTC-160 | 5.615 | 0.033 | 1.582 |
| MHTC-180 | 9.428 | 0.040 | 1.908 |

**2.3.3.2 Chemical characterization**

Elemental compositions of the GL residue and hydrochar, and yields of the hydrochar are summarized in Table 2.4. The maximum hydrochar yield was obtained at 120 ºC. When increasing the reaction temperature from 120 ºC to 180 ºC, the hydrochar yield decreased significantly from 70.5% to 54.2%. This phenomenon was due to the greater primary decomposition or secondary decomposition of the GL residue occurring at higher temperatures during MHTC (Cheng, Winter, and Stipanovic 2012; Demirbaş 2000; Fisher et al. 2002).

The results shown in Table 2.4 also indicate that the elemental composition of hydrochar varies due to the various degrees of carbonization at different reaction temperatures. With the increase of reaction temperature from 120 ºC to 180 ºC, the carbon content increased from 44.28% to 49.67%, while the content of hydrogen and oxygen decreased from 40.97% and 5.52% to 38.19% and 5.45%, respectively. In addition, the ratios of O/C and H/C decreased from 0.69 and 1.50 to 0.58 and 1.32, respectively. The variations in the elemental composition of GL residue and hydrochar were analyzed via van Krevelen diagram (Van Krevelen 1950). The three arrows in Figure 2.9 represent the process of dehydration, decarboxylation, and demethylation (Xiao et al. 2012). The van Krevelen diagram clearly shows that the alternations of H/C and O/C atomic ratios from GL residue to hydrochar followed the paths of dehydration and decarboxylation, while the demethylation pathway can be negligible. A similar phenomenon was observed during the hydrothermal carbonization process of cellulose and other kinds of lignocellulosic biomass (Gao, Remón, and Matharu 2021; Shao et al. 2021). Therefore, higher temperatures promoted dehydration and decarboxylation reactions of the GL residue, resulting in decreased H/C and O/C ratios.

Table 2.4 Elemental analysis and yield of GL residue and hydrochar.

| Sample | Yield (%) | Elemental analysis (%) | | | | |
|---|---|---|---|---|---|---|
| | | C | H | O | O/C[a] | H/C[a] |
| GL residue | - | 44.28 | 5.52 | 40.97 | 0.69 | 1.50 |
| MHTC-120 | 70.5 | 44.42 | 5.50 | 40.81 | 0.69 | 1.49 |
| MHTC-140 | 62.6 | 44.81 | 5.48 | 40.36 | 0.68 | 1.47 |
| MHTC-160 | 57.8 | 46.43 | 5.46 | 39.60 | 0.64 | 1.41 |
| MHTC-180 | 54.2 | 49.67 | 5.45 | 38.19 | 0.58 | 1.32 |

[a] O/C and H/C are given in molar ratio.

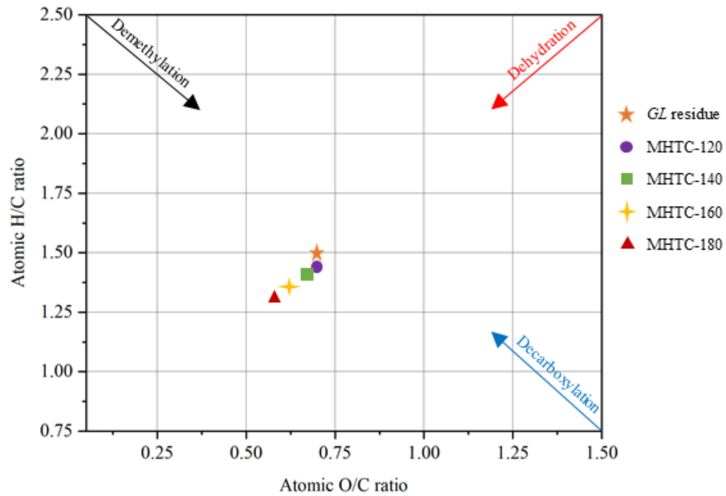


Figure 2.9 Atomic H/C versus O/C ratios (van Krevelen diagram) of GL residue and hydrochar.

The proximate analysis, HHV, ERE, and energy densification are summarized in Table 2.5. It can be found from Table 2.5 that the GL residue contained 14.78% of FC and 76.63% of VM. After being treated by MHTC at 180 ºC, the FC content of hydrochar increased to 37.99%, while the VM amount decreased to 55.97%. This phenomenon was caused by the chemical dehydration and decarboxylation reactions during MHTC (Funke and Ziegler 2010; Heilmann et al. 2011; Hoekman, Broch, and Robbins 2011; Kim et al. 2014). In addition, the ash content increased significantly due to the loss of VM (Kim et al. 2014). The HHV increased from 18.11 MJ/kg to 19.49 MJ/kg with the increase of the reaction temperature from 120 ºC to 180 ºC. The increase in HHV confirmed the high efficiency of MHTC in converting the GL residue into a solid fuel (Lee et al. 2018). A higher MHTC reaction temperature demonstrated a better energy potential of the produced hydrochar in terms of HHV value. However, ERE, which is determined by energy densification and hydrochar yield, led to a different path in determining the optimum MHTC reaction temperature (Lee and Park 2021). Energy densification increased slightly with the increase in the reaction temperature during MHTC, suggesting enhancements in the viability of utilizing the treated GL residue for fuel applications (Mäkelä, Benavente, and Fullana 2015).

In contrast to energy densification, hydrochar yield decreased significantly as temperature increased, with the lowest yield of 54.2% being obtained at the reaction temperature of 180 ºC. Therefore, ERE was significantly influenced by the decrease in hydrochar yield (Table 2.5). Considering the HHV and ERE of hydrochar, a temperature range of 160 ºC to 180 ºC was optimal for converting the GL residue into value-added solid fuel via MHTC. In addition, the relatively high ERE values (around 60%-70%) suggested that MHTC is an effective way to upgrade the GL residue into valuable hydrochar (Yang et al. 2016).

Table 2.5 Proximate analysis, HHV, ERE, and energy densification of GL residue and hydrochar.

| Sample | Proximate analysis | | | | HHV (MJ/kg) | ERE (%) | Energy densification |
|---|---|---|---|---|---|---|---|
| | M | VM | FC | Ash | | | |
| GL residue | 5.90 | 76.63 | 14.78 | 2.69 | 18.09 | - | - |
| MHTC-120 | 5.62 | 75.75 | 15.62 | 3.01 | 18.11 | 70.59 | 1.00 |
| MHTC-140 | 5.19 | 73.30 | 17.99 | 3.52 | 18.19 | 62.94 | 1.01 |
| MHTC-160 | 3.90 | 67.37 | 24.76 | 3.97 | 18.61 | 59.49 | 1.03 |
| MHTC-180 | 0.62 | 55.97 | 37.99 | 5.42 | 19.49 | 58.41 | 1.08 |

Note: M is moisture, VM is volatile matter, FC is fixed carbon, HHV is high heating value, and ERE is energy recovery efficiency.

## 2.4 Conclusion

In the present study, grass was found to be a hyperaccumulator that can accumulate REEs from feeding solution with a TREE content of 510.5 mg/kg. The EPMA analysis showed that REEs in the GL were in complexation with P. The effects of acid types, solid concentration, and acid concentration on the REE recovery from GL were investigated. High recoveries of Y, La, Ce, and Dy, reaching 96%, 93%, 92%, and 93%, respectively, were achieved by employing 0.5 mol/L $H_2SO_4$ as the lixiviant and maintaining a solid concentration of 5 wt.%. In addition, the recovery of P showed a similar trend as the recovery of REEs due to the complexation of REEs with P in the GL.

MHTC was used to convert GL residue obtained after REE extraction into hydrochar to expand the utilization of the GL biomass. The effect of reaction temperature during MHTC on hydrochar characteristics was investigated. SEM analysis showed that more microspheres and pores appeared on the surface of hydrochar with the increase in temperatures. The porous structure of hydrochar obtained at high temperatures suggested the application of sequestration and adsorption. Considering the values of HHV and ERE, MHTC reaction temperatures between 160 ºC to 180 ºC were suitable for converting GL residue to value-added solid fuel. The analysis of hydrochar characteristics revealed that MHTC is an effective way to convert GL residue into hydrochar, which can be used as solid fuels and adsorbents.

# Chapter 3 REE Recovery and Hydrochar Production from Grass Leaves by Microwave-Assisted Hydrothermal Carbonization

**Abstract**

In addition to utilizing conventional hydrometallurgy for REE recovery and employing MHTC to convert leaching residue into hydrochar, in the MHTC process, REEs were transferred into the aqueous medium, while hydrochar was produced. In this study, the effects of acid type (HCl, $H_2SO_4$, and $HNO_3$) and acid concentration (0.01 mol/L-0.2 mol/L) on REE extraction from GL during MHTC were investigated. The structural properties and thermal decomposition behavior of both the GL and the hydrochar produced from the MHTC process were characterized. It was found that at the same concentration, $H_2SO_4$ yielded the highest REE extraction efficiency due to the greater availability of hydrogen ions. Notably, the utilization of 0.2 mol/L $H_2SO_4$ led to the extraction of nearly 100% of REEs from the GL into the resulting biocrudes. Concurrently, this also caused the degradation of amorphous hemicellulose and crystalline cellulose present in the GL, thereby enhancing the thermal stability of the resulting hydrochar. The physiochemical properties of the hydrochar were also influenced by acid type and acid concentration. The increase in acid concentration significantly contributed to the reduction in the volatile matter and ash content of the hydrochar. Using 0.2 mol/L $H_2SO_4$ as the reaction medium, MHTC resulted in a hydrochar with enhanced high heating value and energy densification. These results suggest that MHTC in the presence of an appropriate concentration of $H_2SO_4$ is an effective way to extract REEs and produce hydrochar from the GL.

## 3.1 Introduction

Thermochemical treatments, including pyrolysis and hydrothermal processing, are increasingly garnering attention for the treatment of hyperaccumulators, owing to their notable efficiency, economic viability, and environmentally friendly characteristics (Chai, Chen, et al.

2022b; Cui, Zhang, Wang, Pan, Lin, Khan, Yan, Li, He, and Yang 2021; Li, Ji, and Zhang 2023; Yuan et al. 2011b). Specifically, hydrothermal carbonization has been most widely researched due to its mild reaction temperatures (160-270 ºC) and effective capability to convert hyperaccumulators into a valuable solid product, hydrochar, which holds great promise in various applications, including energy production, carbon sequestration, soil remediation, and pollutant adsorption (Shao et al. 2019; Tag et al. 2018; Zhang et al. 2019). A high amount of REEs in the hydrochar resulting from the hydrothermal carbonization (HTC) of REE hyperaccumulators has posed a significant obstacle to its potential applications. This is primarily because the release of REEs from the use of hydrochar likely causes environmental hazards (Li, Ji, et al. 2023; J. Zhang et al. 2022). Moreover, extracting REEs from the liquid phase, such as biocrudes, is more practical compared to the solid phase, like hydrochar. This is because REEs in hydrochar still require an additional step of leaching to transfer them into a liquid phase for subsequent separation and purification using hydrometallurgical approaches (Brewer, Florek, and Kleitz 2022). Therefore, based on the above discussion, it is more reasonable to transfer REEs from hyperaccumulators into biocrudes for REE recovery and produce value-added and purified hydrochar.

Zhang et al. found that with the addition of HCl during HTC, 95% of Cd and 89% of Zn were transferred into biocrudes at 210 ºC. The resulting hydrochar demonstrated an increased Cu adsorption capacity and an enhanced energy density, making it suitable for use as solid fuel (J. Zhang et al. 2022). It was found by Carrier et al. that several elements, such as Al, Fe, P, Zn, and Ca, were retained in the hydrochar with the increase in temperature from 300 ºC to 400 ºC, while As and S were transferred into biocrudes under the subcritical and supercritical water conditions of hydrothermal conversion (Carrier et al. 2011). In addition, Zhu et al. found that Pb, K, Ca, Na, and Mg can be released into biocrudes by adding HCl at 240 ºC during the hydrothermal liquefaction (HTL) processing of *Rhus chinensis* (Zhu et al. 2019). Regarding the production of value-added hydrochar, despite the fact that elevated temperatures during HTC result in a decrease in hydrochar yield, many studies have found that the hydrochar produced under these conditions possesses a high energy densification, making it a good source of solid fuel (Wang et al. 2018). Nizamuddin et al. found that the hydrochar yield exhibited a decline, decreasing from approximately 60% at 180 ºC to 47% at 260 ºC as the temperature increased, whereas the high heating value (HHV) of the hydrochar enhanced from 16.3 MJ/kg to 26.7 MJ/kg (Nizamuddin et al. 2017). Compared with temperature, residence time exerted less impact on hydrochar yield during HTC (Li, Ji, et al. 2023). Overall, to facilitate the transfer of REEs into biocrudes and obtain value-added hydrochar, high reaction temperatures and the addition of acids are required during HTC.

Compared with HTC, microwave-assisted hydrothermal carbonization (MHTC) emerges as a more promising method due to its lower energy consumption and rapid volumetric heating (Afolabi and Sohail 2017). Unfortunately, there are no studies focusing on the transfer of REEs from hyperaccumulators into biocrudes for REE recovery and the production of value-added hydrochar using MHTC. In view of all the considerations, the use of an acidic reaction medium during high-temperature MHTC has the potential to transfer REEs from hyperaccumulators into biocrudes and produce value-added hydrochar. In the process of MHTC, compared to biocrudes and hydrochar, the yield of biogas is considered negligible (Deng et al. 2020). MHTC is a process primarily aiming at converting biomass into hydrochar (Wang et al. 2022). Even though microwaves provide rapid and uniform heating, which efficiently promotes the carbonization process, the moderate temperature conditions are not optimal for the production of biogas (Sun, Wang, and Yue 2016; Westerholm et al. 2018). Therefore, it is unnecessary to address the management of the negligible yield of biogas generated during the MHTC process.

In this chapter, MHTC experiments of grass leaves (GL) were performed with the addition of different acids (HCl, $H_2SO_4$, and $HNO_3$) to identify the optimal acid yielding the maximum recovery of REEs into biocrudes. The recovery process was further refined by optimizing the selected acid through adjustments in acid concentration (0.01 mol/L, 0.05 mol/L, 0.1 mol/L, and 0.2 mol/L). XRD and TGA analyses were performed to characterize the structural changes and thermal decomposition behavior of the GL and the hydrochar produced from the MHTC process. In addition, the hydrochar and biocrudes were comprehensively characterized with the use of TGA and GC-MS, respectively. The outcomes of this chapter will contribute valuable insights to the advancement of sustainable techniques for recovering REEs from hyperaccumulators.

## 3.2 Materials and methods

### 3.2.1 Chemicals and reagents

The chemicals used in this chapter include nitric acid ($HNO_3$, 67 wt.% to 70 wt.%), hydrochloric acid (HCl, 37 wt.%), sulfuric acid ($H_2SO_4$, 93 wt.% to 98 wt.%). All the chemicals were of trace metal grade and purchased from Thermo Fisher Scientific, USA. Type I deionized water with a resistivity of 18.2 MΩ·cm at 25 °C was prepared using the Direct-Q Water Purification System (Millipore, USA), and used throughout this study.

### 3.2.2 Materials

Grass leaves (GL) were harvested from grass grown by the author. The GL was dried in an oven at 80 ºC for 24 h. The resulting dry sample was then ground to a particle size of less than 297 µm and stored as the feed for MHTC tests.

### 3.2.3 Microwave-assisted hydrothermal carbonization

MHTC experiments were conducted in a microwave reactor (Multiwave GO Plus, Anton Paar GmbH, Austria) with a magnetron frequency of 2450 MHz. 0.5 g of the GL and 10 mL of a loading solvent were added into a 50-mL reaction vessel (HVT50, Anton Paar, Austria). The MHTC experiments were conducted with different acids (HCl, $H_2SO_4$, and $HNO_3$) at varying acid concentrations (0.01 mol/L, 0.05 mol/L, 0.1 mol/L, and 0.5 mol/L) at a fixed temperature of 180 ºC, using a heating rate of 10 ºC/min. After retaining at 180 ºC for 60 min, the vessels were cooled down naturally to room temperature. During the MHTC process, the increasing reaction temperatures led to the production of more value-added hydrochar, which can be used as fuel (Li, Ji, et al. 2023; Ul Saqib, Sarmah, and Baroutian 2019). Considering that the microwave reactor's maximum reaction temperature is 180 ºC, this temperature was selected as the preferred operating condition in this research. Additionally, Nizamuddin et al. found that compared to the reaction temperature, other parameters, such as residence time and solid concentration, exerted a negligible influence on the alternations of the chemical composition of the hydrochar (Nizamuddin et al. 2017). Therefore, 60 min reaction time and 5 wt.% solid concentration were selected (Ding et al. 2021; Gao et al. 2018; Nizamuddin, Qureshi, Baloch, Siddiqui, Takkalkar, Mubarak, Deepa K. Dumbre, et al. 2019; Shao et al. 2019; Zhuang et al. 2020). In general, in order to produce value-added hydrochar, MHTC experiments were conducted at a maintained temperature of 180 ºC with 5wt.% solid concentration for 60 min. Subsequently, the suspension was collected and centrifuged at 5000 rpm for 5 min. The solid residue (hydrochar) was rinsed thoroughly with deionized water, dried at 80 ºC for 48 hours, weighed, and collected for further analysis. The liquid product, biocrudes, was diluted 100 times with a solution containing 5% (v/v) $HNO_3$. Elemental concentrations of the diluted solution were analyzed using an inductively coupled plasma emission mass spectrometer (ICP-MS, Thermo Electron iCAP-RQ, Thermo Scientific, USA). The liquid product was also collected and stored for further analysis. Each run was performed three times. The average results are reported, with experimental errors represented by error bars.

### 3.2.4 Elemental concentration analysis

To measure the elemental composition of the GL and hydrochar, 0.2 g of solid was mixed with 12 mL aqua regia, and then placed in a 50 mL digestion vessel (HVT50, Anton Paar, Austria). The vessel was then placed in a microwave digestor (Multiwave GO Plus, Anton Paar, Austria) and subjected to microwave digestion with a heating rate of 18.5 ºC/min. The digestion was carried out at 185 ºC with a residence time of 40 minutes. After digestion, the vessel was allowed to cool completely, and then the digestion solution was collected and centrifuged. The resultant supernatant was then diluted 100 times with 5% (v/v) $HNO_3$ for the measurement of elemental concentrations using ICP-MS. ICP-MS analysis data was used to calculate the elemental composition of the GL and hydrochar. Elemental concentrations of the GL are presented in Table 3.1. The GL contained 510.5 mg/kg of total REEs, suggesting a good feedstock for metal extraction tests.

Table 3.1 Elemental concentrations (mg/kg) of GL.

| K | Ca | P | Mg | Na | Fe | Al | Si | Mn | Zn |
|---|---|---|---|---|---|---|---|---|---|
| 48730.2 | 12360.5 | 7725.4 | 3628.8 | 544.5 | 255.7 | 266.2 | 182.0 | 73.7 | 45.6 |
| Sr | Ba | Ti | TREEs | LREEs | HREEs | Y | La | Ce | Dy |
| 20.1 | 18.8 | 10.3 | 510.5 | 247.1 | 263.1 | 125.4 | 119.9 | 122.2 | 135.9 |

Note: TREEs, LREEs, and HREEs represent total, light (La, Ce, Pr, Nd, and Sm), and heavy (Y, Eu, Gd, Tb, Dy, Ho, Er, Tm, Yb, and Lu) rare earth elements, respectively.

The fraction of REEs in the feed GL that was transferred into the biocrudes during the MHTC process was defined as REE recovery (*R*, %), which was calculated using Equation (3.1).

$$R = \frac{C_L \times 0.01}{C_L \times 0.01 + C_S \times m_S} \times 100 \quad (3.1)$$

where $C_S$ and $C_L$ represent REE concentrations in the hydrochar (mg/kg) and biocrudes (mg/L), respectively; $m_s$ (kg) represents the mass of the hydrochar, and 0.01 (L) is the volume of biocrudes.

### 3.2.5 Thermogravimetric analysis

The thermogravimetric (TG) behaviors of the GL and hydrochar were analyzed using a thermogravimetric analyzer (TGA 5500, TA Instruments CO., USA). Each sample (~ 5 mg) was heated from room temperature to 950 ºC at 10 ºC/min under a continuous $N_2$ flow of 50 mL/min.

### 3.2.6 Hydrochar characterization

The proximate analysis of the GL and hydrochar was conducted in accordance with ASTM methods (ASTM 1762-84 and 3173-87). Parikh developed correlations derived from the proximate analysis of biomass, to calculate the elemental composition. These correlations were derived from 200 data points and validated further with additional 50 data points. Parikh formula provided a useful tool to calculate elemental components of biomass from simple proximate analysis (Parikh et al. 2007). The correlations were found useful in performance modeling, combustion, gasification, and pyrolysis processes (Channiwala and Parikh 2002; Evcil et al. 2020b; Muraina, Odusote, and Adeleke 2017). Therefore, the percentages of key elements (C, H, and O) were calculated using the Parikh formula (Equations (3.2)~(3.4)).

$$C = 0.637FC + 0.455VM \tag{3.2}$$

$$H = 0.052FC + 0.062VM \tag{3.3}$$

$$O = 0.304FC + 0.476VM \tag{3.4}$$

where FC and VM represent volatile matter (%) and fixed carbon (%) present in the sample, respectively.

The high heating value (HHV) (MJ/kg) was calculated based on Jenkins's formula (Equation (3.5)) (Channiwala and Parikh 2002; Ebeling and Jenkins 1985).

$$HHV = -0.763 + 0.301C + 0.525H + 0.064O \tag{3.5}$$

where C, H, and O represent the carbon, hydrogen, and oxygen contents of the dry material, respectively.

The hydrochar yield (*Hy*, %) and energy densification (*Ed*) were calculated using Equations (3.6) and (3.7), respectively (Kim et al. 2014).

$$Hy\ (\%) = \frac{M_h}{M_{GL}} \tag{3.6}$$

$$Ed = \frac{HHV_h}{HHV_{GL}} \tag{3.7}$$

where, $M_h$ is the hydrochar weight (g), $M_{GLR}$ is the mass of the GL (g), $HHV_h$ is the high heating value of the hydrochar (MJ/kg), and $HHV_{GLR}$ is the high heating value of the GL(MJ/kg).

The microcrystal structure analysis of the samples was performed by X-ray diffraction (XRD D8 ADVANCE, Bruker, Germany) using Cu target with kα radiation. XRD spectra were obtained at 40 kV voltage and 40 mA current, in a 2θ scanning range of 10º to 70º with a scan speed of 2º per minute.

### 3.2.7 Biocrudes characterization

The chemical composition of biocrudes was analyzed using gas chromatography/mass spectrometry (GC-MS; Agilent Technologies, Santa Clara, CA). GC-MS analysis was conducted using an Agilent 7890 GC/5975 MS system equipped with an HP-5 MS capillary column (30m × 25mm × 0.25μm). High purity helium served as the carrier gas at a flow rate of 1 mL/min, with a split ratio of 50:1. The initial temperature was established at 28 ºC for 3 minutes, followed by a ramp to 180 ºC at a rate of 5 ºC/min, and further increased to 280 ºC at 10 ºC/min for 10 minutes. Compound identification in biocrudes was performed using the NIST 08 library.

## 3.3 Results and discussion

### 3.3.1 REE recovery during MHTC

#### 3.3.1.1 Effect of acid types

The reaction medium (i.e., loading solvent) is of great importance to metal fate during hydrothermal processing (J. Zhang et al. 2022). Particularly, it was found that acid media favored the removal of heavy metals from the resulting hydrochar into the liquid phase (Cui, Zhang, Wang, Pan, Lin, Khan, Yan, Li, He, and Yang 2021). Therefore, the effect of acid types (HCl, $H_2SO_4$, and $HNO_3$) on REE recovery during MHTC was investigated using a fixed acid concentration of 0.05 mol/L. As depicted in Figure 3.1, the addition of HCl and $HNO_3$ had a similar impact on REE recovery. However, the addition of $H_2SO_4$ had the most significant positive influence on the removal of REEs from the solid phase. Around 65%, 66%, 61%, and 63% of Y, La, Ce, and Dy were released into the biocrudes, respectively, and the recovery of total REEs (TREEs) reached 63%. The addition of $H_2SO_4$ increased the recovery of REEs by approximately 15 absolute percentage points in comparison to using HCl and $HNO_3$. The higher REE recoveries achieved by using $H_2SO_4$ as the reaction medium can be attributed to the higher concentration of hydrogen ions ($H^+$) available in the $H_2SO_4$ solution compared to using the same concentrations of HCl and $HNO_3$ (Larsson et al. 2013; Zielinski et al. 2020). The presence of $H^+$ hinders the formation of metal-containing precipitates and/or surface adsorbed forms that could adhere to hydrochar. Instead, it facilitates the release of metals into the liquid phase in the form of metal cations and/or metal-sulfate complexes (Cui, Zhang, Wang, Pan, Lin, Khan, Yan, Li, He, and Yang 2021; Wei et al. 2021). Therefore, a higher concentration of $H^+$ facilitates the release of REEs from the GL into biocrudes. Zhang et al. and Zhu et al. also found that around 90% of Cd and Zn as well as over 70% of Pb were removed from hydrochar with the addition of HCl at 240 ºC during hydrothermal processing (J. Zhang et al. 2022; Zhu et al. 2019).

The influence of acid types on the hydrochar yield is shown in Figure 3.2. The yields of hydrochar obtained by adding HCl, $H_2SO_4$, and $HNO_3$ were 38%, 32%, and 37%, respectively. As reported by Rabemanolontsoa et al., inorganic acids can be used as catalysts for the hydrolysis of lignocellulose to yield sugars such as glucose. In addition, dilute acid hydrolysis at high temperatures resulted in extensive degradation of amorphous hemicelluloses (Rabemanolontsoa and Saka 2016). Therefore, in this study, compared to HCl and $HNO_3$, a higher concentration of available $H^+$ present in the $H_2SO_4$ solution promoted the degradation of the GL during MHTC process, leading to the lowest yield of hydrochar during MHTC.

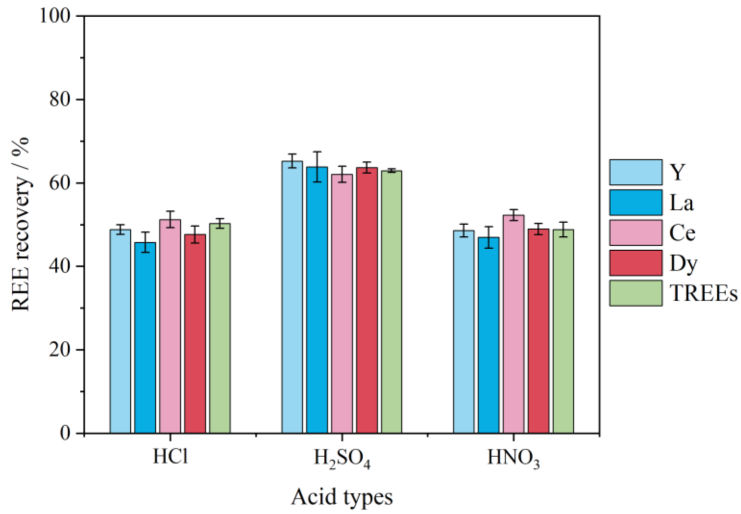


Figure 3.1 Effect of acid types on REE recovery from the GL into biocrudes.

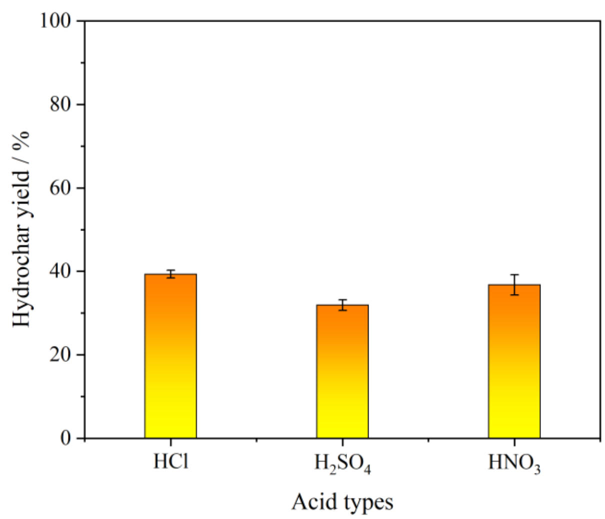


Figure 3.2 Effect of acid types on hydrochar yield from the GL.

The effect of acid type on the recovery of major (>1000 mg/kg) and trace (10-1000 mg/kg) elements from the GL into biocrudes was also investigated. As shown in Figure 3.3, almost 100% of K is recovered with the addition of all three acids. It was reported by Liu et al. that K in biomass was typically found in the form of ionic $K^+$ and exhibited high solubility in water. Additionally, it may form relatively weak complexes with organic acids. Therefore, K was easy to extract from the GL into biocrudes (Liu et al., 2021). Si exhibited opposite leaching patterns when compared to REEs. Approximately 82% of Si was released into biocrudes with the addition of $H_2SO_4$, while more Si was leached in the systems of HCl-mediated and $HNO_3$-mediated MHTC. It was reported that the addition of $H_2SO_4$ led to the formation of relatively insoluble silica (silica gel) (Equation (3.8)), thus reducing the leachability of Si from the GL (Vafaei and Allahverdi 2017).

$$H_2SO_4 + SiO_2 \rightarrow SiO_2 \cdot H_2SO_4 \tag{3.8}$$

In addition to K and Si, the remaining major and trace elements in the GL showed leaching patterns similar to REEs. For instance, 96% and 85% of Mg and Ca, elements riched in plants (Chour et al. 2020), were recovered into biocrudes when adding $H_2SO_4$. However, with the addition of HCl and $HNO_3$, the recoveries of Mg reached 91% and 93%, and the recoveries of Ca attained 60% and 75%, respectively. Regarding the nutrient element P, 93% of this element was extracted from the GL in the $H_2SO_4$-mediated system, while the recovery decreased to 81% and 84%, respectively, with the addition of HCl and $HNO_3$ during MHTC. As mentioned above, $H_2SO_4$ is a strong diprotic acid, which provides more $H^+$ per mole compared to HCl and $HNO_3$ (Ciszkowska, Stojek, and Osteryong 1995). Therefore, the increased acidity facilitated the breakdown of the GL components and the release of elements into biocrudes.

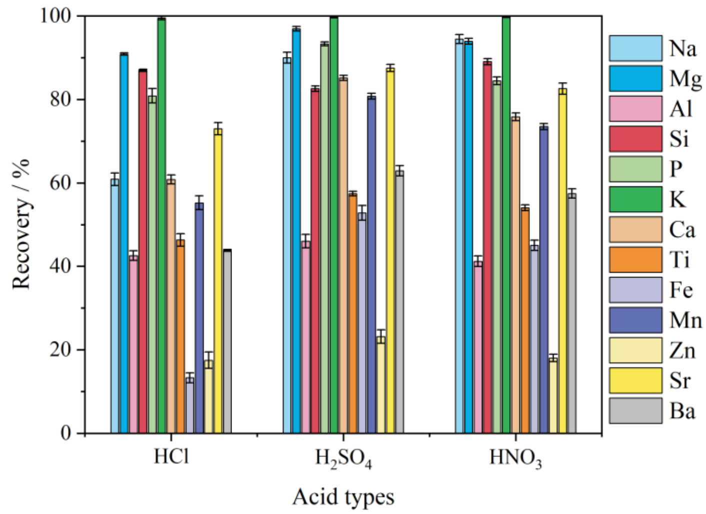


Figure 3.3 Effect of acid types on the recovery of major and trace elements from the GL into biocrudes.

The XRD patterns of the GL and the hydrochar resulting from MHTC with different acids are shown in Figure 3.4, which can be used to understand the structural changes of the GL during the MHTC process. Three broad peaks found at 2θ values of 15.5º, 22.5º, and 34.4º indicated the coexistence of the amorphous (hemicellulose, extractives, lignin, and amorphous cellulose) and crystalline (crystalline cellulose) structures in the GL and hydrochar (Guo et al. 2015). The diffraction peaks of hydrochar at these three positions were sharper than those of the GL, indicating that a portion of the amorphous components were removed during the acid-mediated MHTC process. In particular, the hydrochar produced from the $H_2SO_4$-mediated MHTC system presented the highest peak intensities, indicating that more amorphous structures were detached. As mentioned before, the decomposition of amorphous components during microwave treatment resulted in a decrease in hydrochar yield (Kang et al. 2019). Therefore, the addition of $H_2SO_4$ led to the removal of more amorphous structures in the GL and the lowest yield of hydrochar.

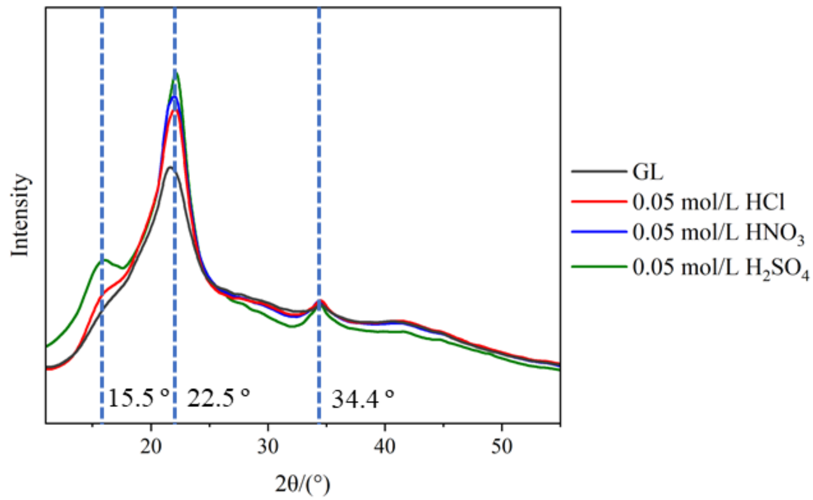


Figure 3.4 XRD patterns of the GL and hydrochar.

TG and differential thermogravimetric (DTG) analyses were performed to study the thermal decomposition behaviors of the GL and the produced hydrochar (Kang et al. 2019). It can be seen from Figure 3.5(a) that the TGA curves can be divided into three stages. The first stage (25 ºC-200 ºC) was characterized by slow weight loss, which can be attributed to the loss of moisture and the release of light volatiles (Parshetti, Hoekman, and Balasubramanian 2013). The second stage was in the temperature range from 200 ºC to 400 ºC. The sudden decrease in weight loss from around 95% to 35% was mainly due to the decomposition of hemicellulose and cellulose. After 400 ºC, the third stage took place and showed a gradual decrease. This phenomenon might be due to the slower thermal decomposition of lignin occurring after 400 ºC (Elaigwu and Greenway 2016; Nizamuddin et al. 2017). With the increase in temperature from 200 ºC to 950 ºC, the weight loss of the GL was 93%, while the weight loss of hydrochar was lower than the GL by 10 absolute percentage points, which indicated that the produced hydrochar possessed higher thermal stability compared to the GL.

As indicated in Figure 3.5(b), the intensive decomposition of the GL occurred at the temperature of 300 ºC, while in terms of the hydrochar, the intensive decomposition occurred at 370 ºC. The occurrence of intensive decomposition of the GL at the lower temperature was principally due to the degradation of hemicellulose. On the other hand, the occurrence of intensive decomposition of the hydrochar at the higher temperature was mainly attributed to the decomposition of cellulose. This phenomenon can be explained by the fact that cellulose needs higher temperatures for hydrolysis compared to hemicellulose (Finkelstein 2000). Generally, the contrast-intensive decomposition temperatures indicated that the MHTC process promoted the decomposition of amorphous hemicellulose in the GL, and as such, the main component contained in hydrochar became cellulose. In addition, Figure 3.5(b) also illustrates that the highest weight loss rate of hydrochar produced by adding $H_2SO_4$ is lower than by adding HCl and $HNO_3$, which indicates that hydrochar produced in the $H_2SO_4$-mediated MHTC system had improved stability and quality (Ding et al. 2022).

In summary, $H_2SO_4$ was identified as the preferred acid, with the aim of maximizing the recovery of REEs from the GL into biocrudes and obtaining value-added hydrochar with high thermal stability and other advantageous properties (see Section 3.2).

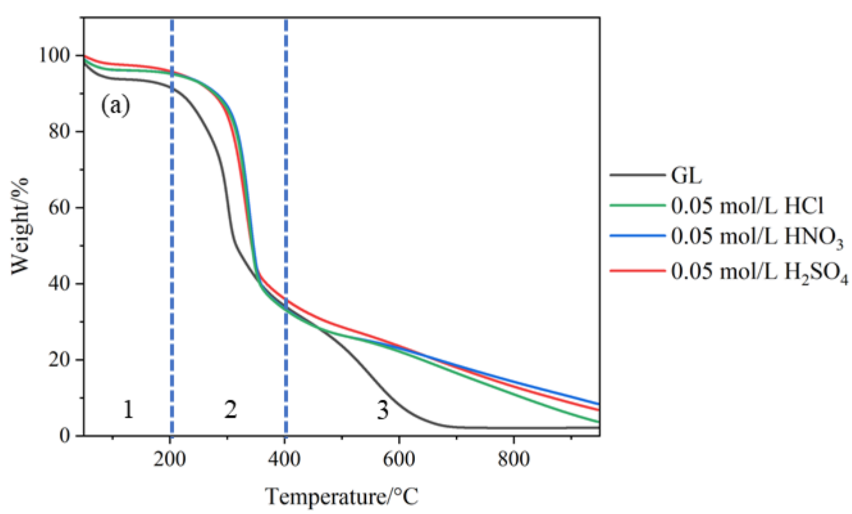

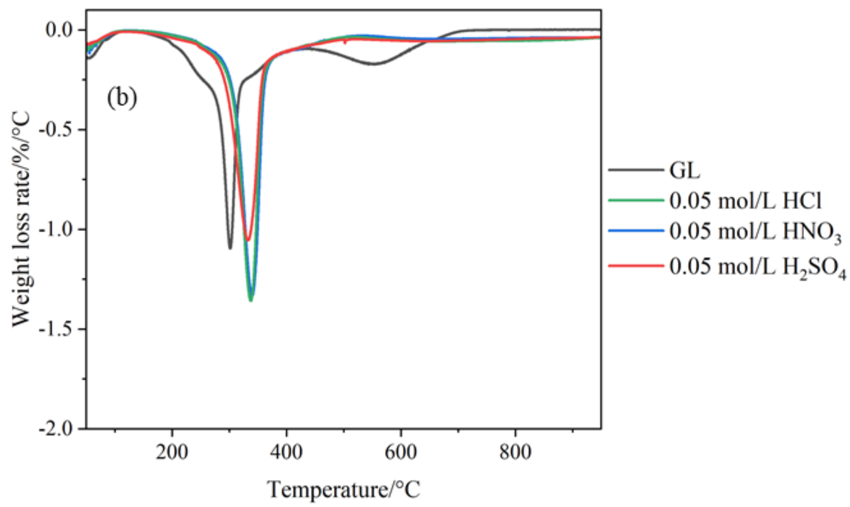


Figure 3.5 TG (a) and DTG (b) curves of the GL and hydrochar.

### 3.3.1.2 Effect of $H_2SO_4$ concentration

As reported in the literature, acid concentration played a significant role in REE recovery from various sources (Jally et al. 2021b; Ji and Zhang 2021; Li, Ji, et al. 2023; Mwewa et al. 2022). This phenomenon was because acid concentration exerted an influence on the pH of the solution, and a specific pH range was crucial for controlling the solubility of REEs (Cao et al. 2001). The effect of $H_2SO_4$ concentration (0.01 mol/L, 0.05 mol/L, 0.1 mol/L, and 0.2 mol/L) on REE recovery from the GL during the MHTC process was investigated. As can be seen from Figure 3.6, the recovery of REEs increases by around 10% with the increase in $H_2SO_4$ concentration from 0.01 mol/L to 0.05 mol/L. When further increased $H_2SO_4$ concentration from 0.05 mol/L to 0.1 mol/L, the recovery increased significantly to 94%, 93%, 94%, and 94% for Y, La, Ce, and Dy, respectively. A slight increase was observed in REE recovery with the enhancement in $H_2SO_4$ concentration from 0.1 mol/L to 0.2 mol/L, and almost 100% of REEs were released from the GL into biocrudes with the addition of 0.2 mol/L $H_2SO_4$. The final pH values of the biocrudes produced under the four different acid concentrations were 4.8, 2.8, 2.1, and 1.8, respectively. It was found by Borra et al. that low pH values were beneficial for REE leaching (Borra et al. 2015). In addition, strong acids were found to effectively promote the dissolution of lignin and the release of REEs from it (Song et al. 2023).

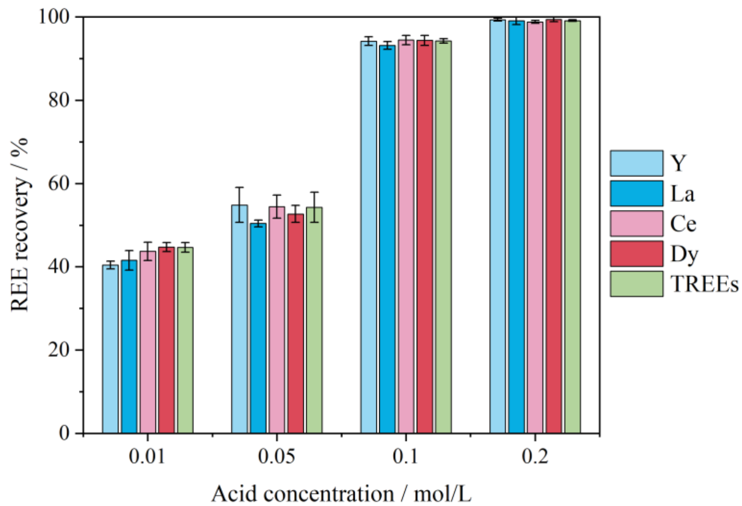


Figure 3.6 Effect of acid concentration on REE recovery from the GL into biocrudes.

The hydrochar yields with different concentrations of $H_2SO_4$ are shown in Figure 3.7. With the increase in $H_2SO_4$ concentration from 0.01 mol/L to 0.1 mol/L, the yield of produced hydrochar decreased gradually from 37% to 26%. However, a hydrochar yield of only 11% was obtained with the addition of 0.2 mol/L $H_2SO_4$. As mentioned before, processing biomass in an acidic medium at high temperatures led to the degradation of lignocellulose, and thus, the yield of hydrochar was reduced. Lu et al. performed hydrothermal carbonization (HTC) of cellulose in the presence of HCl, $H_2SO_4$, NaOH, $Ca(OH)_2$, and acetic acid. It was found that hydrochar yield was not significantly affected by any of these acids and bases (Lu, Flora, and Berge 2014). However, in this study, the concentration of $H_2SO_4$ exhibited a noticeable impact on the yield of hydrochar, especially with the addition of 0.2 mol/L $H_2SO_4$, the hydrochar yield decreased sharply. The possible explanation is that compared to HTC, microwave heating used in MHTC further increased the degradation of biomass due to its advantages of rapid and selective heating (Hibbert, Welham, and Zein 2019; Li et al. 2019). Furthermore, a strong acid used as a catalyst can promote the degradation of some difficult-to-degrade components in biomass, such as lignin (Song et al. 2023).

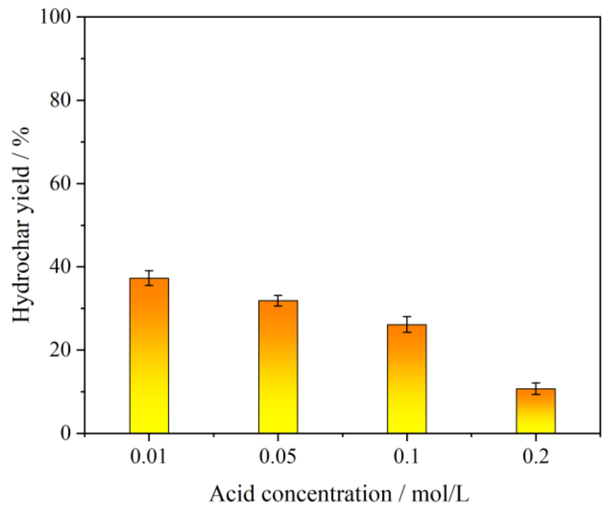


Figure 3.7 Effect of acid concentration on hydrochar yield from the GL.

In addition to REEs, the effect of $H_2SO_4$ concentration on the recovery of other elements was also investigated. It can be seen from Figure 3.8 that all K was recovered from the GL into biocrudes, regardless of the acid concentration used due to the reason mentioned in Section 3.1.1. When increasing the $H_2SO_4$ concentration from 0.01 mol/L to 0.2 mol/L, the recovery of Si decreased from 94% to 28%. At lower pH values, Si may precipitate as insoluble silicate compounds or form silica gel, making it less soluble (Mai and Militz 2004). With the increase in $H_2SO_4$ concentration, the pH of the solution decreased, leading to a decrease in Si recovery. In addition, microwave heating accelerates chemical reactions by providing rapid and efficient energy transfer to the reaction system (Larhed, Moberg, and Hallberg 2002). Therefore, with a higher $H_2SO_4$ concentration during MHTC, the precipitation of Si became more aggressive, resulting in a significant decrease in Si recovery. The recoveries of other major and trace elements in the GL showed similar patterns with the increase in $H_2SO_4$ concentration. The recoveries of these elements initially increased as the acid concentration was raised from 0.01

mol/L to 0.1 mol/L, but subsequently, decreased as the acid concentration was further raised from 0.1 mol/L to 0.2 mol/L. Increasing the acidity of the solutions dissolved minerals and ores more effectively, thus resulting in higher element recovery (Hidayah and Abidin 2018). Therefore, the recovery of these elements increased with the increase in acid concentration from 0.01 mol/L to 0.1 mol/L. However, when further increased from 0.1 mol/L to 0.2 mol/L, the formation of insoluble silicate compounds or silica gel trapped other elements and reduced their recoveries from the GL (Alkan et al. 2018).

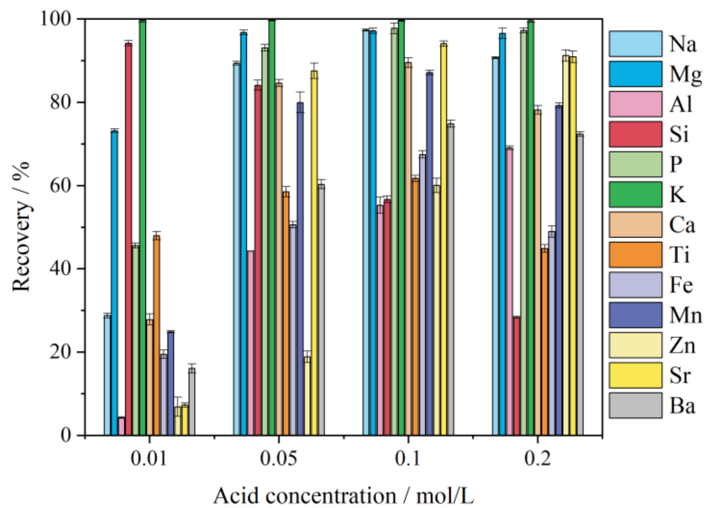


Figure 3.8 Effect of acid concentration on the element recovery from the GL into biocrudes.

The XRD patterns of hydrochar are shown in Figure 3.9. It was found that the intensities of three broad peaks representing the amorphous and crystalline structures increased initially with the increase in $H_2SO_4$ concentration from 0.01 mol/L to 0.1 mol/L. However, the intensities of these peaks decreased significantly as the acid concentration was further increased to 0.2 mol/L. The increase in the intensity of these three peaks implied the removal of amorphous structures in the GL. With the addition of 0.2 mol/L $H_2SO_4$, the crystalline cellulose was degraded and converted, subsequently leading to the formation of amorphous products (Chen et al. 2018). Therefore, the intensities of the three peaks reduced again when the acid concentration increased to and above 1 mol/L.

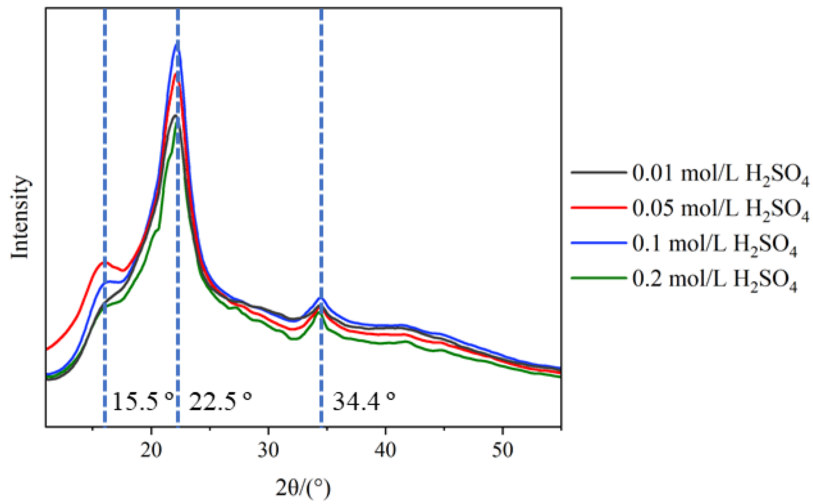


Figure 3.9 XRD patterns of the hydrochar.

Figure 3.10 depicts the TG and DTG curves of the hydrochar. As can be seen from Figure 3.10(a), the weight loss of hydrochar produced with the addition of 0.2 mol/L $H_2SO_4$ is around 77%, which is lower than the hydrochar produced by adding 0.01 mol/L, 0.05 mol/L, and 0.1 mol/L $H_2SO_4$ by around 12 absolute percentage points. These results signified a significant improvement in the thermal stability of hydrochar with the addition of 0.2 mol/L $H_2SO_4$. This observation holds promise for the development of hydrochar products from the GL, particularly for fuel applications (Naderi and Vesali-naseh 2021).

Figure 3.10(b) illustrates that the intensive decomposition of the hydrochar produced with the addition of 0.01 mol/L, 0.05 mol/L, and 0.1 mol/L $H_2SO_4$ occurs at around 375 ºC. In terms of the hydrochar produced by adding 0.2 mol/L $H_2SO_4$, the intensive decomposition took place at a lower temperature (225 ºC). This observation suggested that hydrochar derived with the addition of 0.2 mol/L $H_2SO_4$ was primarily composed of structures that are more easily decomposed. As mentioned above, the presence of 0.2 mol/L $H_2SO_4$ led to the degradation and alteration of the crystalline cellulose present in the GL, resulting in the generation of amorphous products. The amorphous products are more easily degraded than crystalline cellulose, thus leading to a lower temperature required for intensive decomposition.

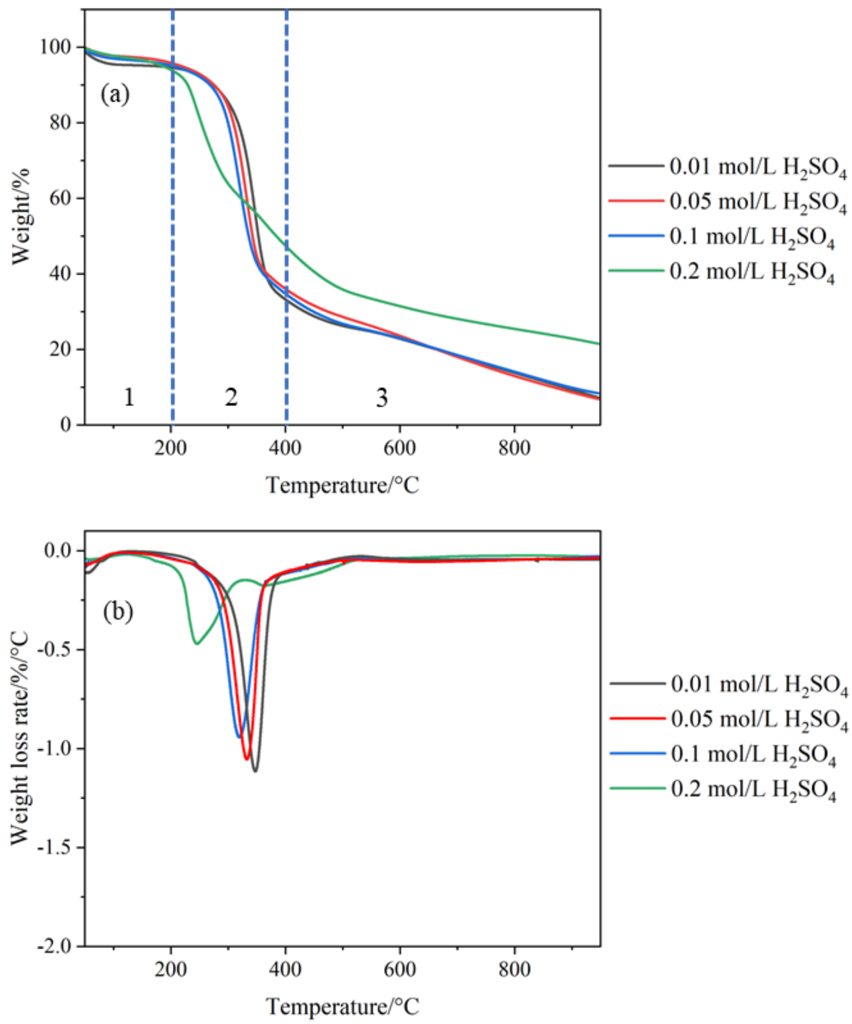


Figure 3.10 TG (a) and DTG (b) curves of the hydrochar.

In general, the increase in $H_2SO_4$ concentration leads to an increase in REE recovery from the GL, while hydrochar yield decreased with the increased $H_2SO_4$ concentration due to the degradation of lignocellulose. The crystalline structure of the hydrochar increased initially with the increase in $H_2SO_4$ concentration from 0.01 mol/L to 0.1 mol/L. However, with the addition of 0.2 mol/L $H_2SO_4$, the crystalline structure was degraded, as evidenced by the decreased intensities of the peaks, indicating that the amorphous products were formed in 0.2 mol/L $H_2SO_4$-mediated MHTC system. TG and DTG curves (Figure 3.10) indicate that a significant improvement in the thermal stability of hydrochar was obtained with the addition of 0.2 mol/L $H_2SO_4$. The hydrochar with increased thermal stability is more promising for fuel applications. In conclusion, considering maximizing the recovery of REEs and producing value-added hydrochar from the GL, 0.2 mol/L $H_2SO_4$ was chosen as the optimal condition.

### 3.3.2 Hydrochar characterization

The basic physicochemical properties of the GL and hydrochar derived from the GL under various MHTC conditions are shown in Table 3.2. Hydrochar produced with the addition of acids had lower VM values than the GL, which can be explained that the acid-induced decomposition of the GL produces volatile organic compounds, such as furfural, which then give rise to the formation of pseudo-lignin on the surface of the hydrochar (Ma et al. 2023). When increasing the acid concentration from 0.01 mol/L to 0.2 mol/L, the VM of hydrochar decreased from 74.49% to 56.37%. This was because, with the increase in acid concentration, the decomposition of the GL became more effective, resulting in the formation of more pseudo lignin and low VM contents.

Compared to the GL, the addition of various acids led to a decrease in the ash content of derived hydrochar (J. Zhang et al. 2022). An acidic environment promoted the conversion of alkali and alkaline earth metals into soluble compounds, resulting in a decrease in the ash content of derived hydrochar (Lei, Kannan, and Raghavan 2021). Hydrochar with reduced ash content is desirable to be used in soil amendment and as an energy fuel (Kambo and Dutta 2015a). A slight fluctuation was observed in the ash content of hydrochar produced from MHTC of the GL with the addition of different acids. With an increase in $H_2SO_4$ concentration from 0.01 mol/L to 0.2 mol/L, the ash content decreased from 5.58% to 2.10%. It can be inferred that in comparison with acid types, acid concentration played a more significant role in changing the ash content of the derived hydrochar.

The hydrochar produced with the addition of various acids at a concentration of 0.05 mol/L exhibited C contents ranging from 44.84% to 47.69%, exceeding the C content found in the GL. In addition, the C content increased gradually from 43.42% to 50.82% when increasing the $H_2SO_4$ concentration from 0.01 mol/L to 0.2 mol/L. In terms of the contents of H and O, a minor variation was observed with adding various acids and changing $H_2SO_4$ concentrations. The H/C and O/C ratios are used to describe the internal chemical transformations occurring during the MHTC process of the GL (Liu, Ma, and Chen 2018). The H/C of hydrochar showed minor differences when adding acids and elevating acid concentrations during the MHTC process, indicating that the addition of acids and increased acid concentrations exerted negligible influences on the formation of aromatic structures in hydrochar (Wilk et al. 2020). However, the O/C of hydrochar decreased to 0.84-0.89 with the addition of acids at a concentration of 0.05 mol/L, and it further decreased significantly to 0.78 with the addition of 0.2 mol/L $H_2SO_4$. A low O/C ratio represents a high carbonization degree and the existence of less polar functional groups (Wiedner et al. 2013). Therefore, it can be inferred that hydrochar with a high carbonization degree and less polar functional groups can be produced from MHTC of the GL with the addition of acids and increased acid concentrations, and this type of hydrochar was anticipated to exhibit greater environmental stability (Liu et al. 2018).

Table 3.2 Physicochemical properties of the GL and hydrochar.

| | Proximate analysis (%) | | | | HHV (MJ/kg) | Elemental analysis (%) | | | H/C | O/C | Yield (%) | Energy Densification |
|---|---|---|---|---|---|---|---|---|---|---|---|---|
| | M | VM | FC | Ash | | C | H | O | | | | |
| GL | 5.90 | 75.63 | 11.78 | 6.69 | 17.07 | 41.63 | 5.30 | 39.32 | 0.13 | 0.94 | | |
| G-HCl | 3.83 | 70.44 | 20.71 | 5.01 | 18.25 | 45.08 | 5.50 | 39.97 | 0.12 | 0.89 | 38.32 | 1.07 |
| G-$HNO_3$ | 3.73 | 71.52 | 19.58 | 5.17 | 18.19 | 44.84 | 5.50 | 40.08 | 0.12 | 0.89 | 31.12 | 1.07 |

| | | | | | | | | | | | | |
|---|---|---|---|---|---|---|---|---|---|---|---|---|
| G-$H_2SO_4$ | 2.40 | 64.67 | 28.87 | 4.07 | 19.11 | 47.69 | 5.62 | 40.05 | 0.12 | 0.84 | 31.84 | 1.12 |
| G-0.01 mol/L $H_2SO_4$ | 4.67 | 74.49 | 15.26 | 5.58 | 17.72 | 43.42 | 5.43 | 40.00 | 0.12 | 0.92 | 35.74 | 1.04 |
| G-0.05 mol/L $H_2SO_4$ | 2.40 | 64.67 | 28.87 | 4.07 | 19.11 | 47.69 | 5.62 | 40.05 | 0.12 | 0.84 | 31.84 | 1.12 |
| G-0.1 mol/L $H_2SO_4$ | 2.16 | 63.94 | 30.37 | 3.53 | 19.34 | 48.36 | 5.66 | 40.23 | 0.12 | 0.83 | 27.80 | 1.13 |
| G-0.2 mol/L $H_2SO_4$ | 2.02 | 56.37 | 39.50 | 2.10 | 20.09 | 50.82 | 5.73 | 39.82 | 0.11 | 0.78 | 10.30 | 1.18 |

Note: M is moisture, VM is volatile matter, FC is fixed carbon, and HHV is high heating value.

HHV is a significant characteristic of hydrochar, representing the amount of heat released from fuel combustion (Su et al. 2021). It can be seen from Table 3.2 that the HHV increases from 17.07 MJ/kg (GL) to 18.25-19.11 MJ/kg (hydrochar produced with the addition of acids). Moreover, the HHV enhanced significantly from 17.72 MJ/kg to 20.09 MJ/kg with the increase in acid concentration from 0.01 mol/L to 0.2 mol/L. The HHV of hydrochar obtained by adding 0.2 mol/L $H_2SO_4$ was higher than conventional lignite (15-20 MJ/kg) (Kim et al. 2014). Based on Equation (3.7), the energy densification shows the same trend as the HHV of hydrochar. The highest energy densification of hydrochar can be achieved under the condition of adding 0.2 mol/L $H_2SO_4$ during the MHTC process. This implied that the increase in acid concentration can greatly enhance the energy densification of hydrochar, which increased the viability of utilizing the produced hydrochar for fuel applications (Mäkelä et al. 2015).

### 3.3.3 GC-MS analysis of biocrudes

GC-MS analysis was performed to investigate the composition of biocrudes produced from MHTC of the GL with the addition of 0.2 mol/L $H_2SO_4$. In Figure 3.11, the x-axis represents the retention time, and the y-axis denotes the relative total peak area for each component (Tu et al. 2021). The major components (>1% relative total peak area) in the biocrudes were labeled with serial number ①~⑧ (Chen et al. 2014). As can be seen from Figure

3.11, the alicyclic compound, furfural, occupies the largest proportion (14.67%) of the biocrudes. Furfural primarily originates from the hydrolysis of cellulose and hemicellulose, leading to the breakdown of sugars and their derivatives (Tang et al. 2017). It can be inferred that instead of lignin, the GL was mainly composed of hemicellulose and cellulose. In addition, the proportion of 5-methyl-2-furancarboxaldehyde in the biocrudes was 4.14%. It was found by Tu et al. that the acid-catalyzed hydrolysis facilitated the transformation of cellulose into furfural and 5-methyl-2-furancarboxaldehyde, rather than inducing cracking to produce smaller molecules like 1-hydroxy-2-propanone (Tu et al. 2021). Therefore, furfural and 5-methyl-2-furancarboxaldehyde were the main components in biocrudes produced from MHTC of the GL with adding 0.2 mol/L $H_2SO_4$. In addition, it was found that octaethylene glycol monododecyl ether, constituting 13.42% of the total, emerged as a significant constituent in biocrudes.

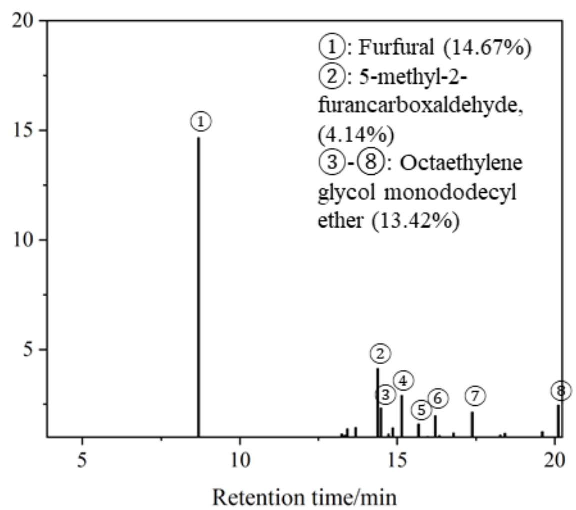


Figure 3.11 The component of biocrudes from MHTC of the GL with the addition of 0.2 mol/L $H_2SO_4$.

In order to analyze the MHTC paths of the GL with the addition of 0.2 mol/L $H_2SO_4$, the reaction mechanisms of two main components (hemicellulose and cellulose) in the GL are investigated in Figure 3.12. During MHTC, the glycosidic bonds in hemicellulose were initially broken, leading to the release of xylose. Xylose underwent further reactions in acidic conditions, thus promoting the production of furfural eventually. Cellulose underwent initial conversion to glucose, which was subsequently transformed into 5-methyl-2-furancarboxaldehyde through acid-catalyzed dehydration reactions (Xiang et al. 2003). Finally, 5-methyl-2-furancarboxaldehyde was converted to furfural.

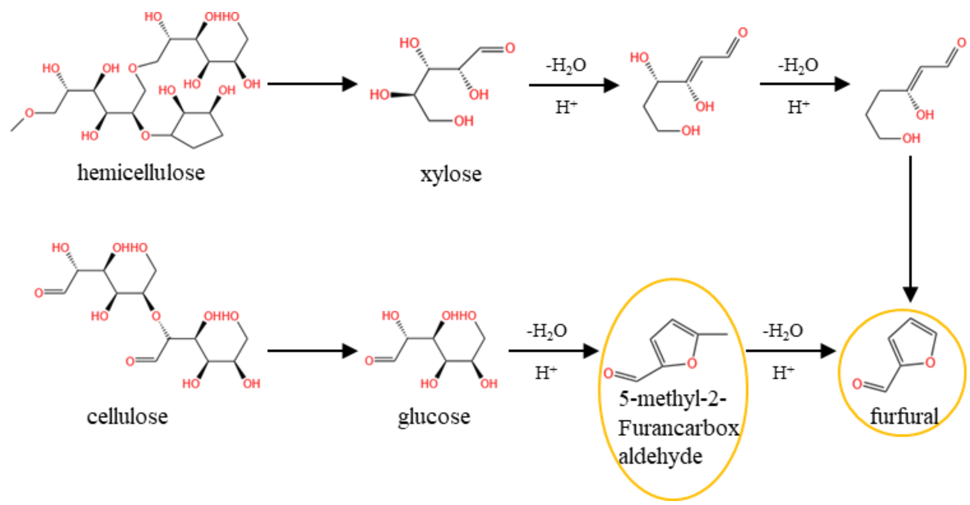


Figure 3.12 Reaction mechanisms for MHTC of the GL with the addition of 0.2 mol/L $H_2SO_4$.

### 3.4 Conclusion

MHTC experiments with different acid types (HCl, $H_2SO_4$, and $HNO_3$) and acid concentrations (0.01 mol/L, 0.05 mol/L, 0.1 mol/L, and 0.2 mol/L) were performed to achieve the maximum recovery of REEs and the production of value-added hydrochar from the GL. The addition of various acids and the increase in acid concentration favored the release of REEs into biocrudes. Almost 100% of REEs were recovered using 0.2 mol/L $H_2SO_4$ as the reaction medium during MHTC. Most of the elements in the GL showed recovery patterns similar to REEs. XRD and TGA analyses showed that the amorphous structures in the GL were degraded with the addition of acid, and partial crystalline cellulose was decomposed into amorphous products with the addition of 0.2 mol/L $H_2SO_4$. In addition, the hydrochar produced by adding 0.2 mol/L $H_2SO_4$ has high thermal stability, carbonization degree, HHV, and energy densification, showing great potential for energy production. The main components in biocrudes derived with the addition of 0.2 mol/L $H_2SO_4$ were furfural and 5-methyl-2-furancarboxaldehyde, the derivatives from hemicellulose and cellulose. Therefore, adding 0.2 mol/L $H_2SO_4$ during MHTC is an effective way to recover REEs from the GL and obtain value-added hydrochar. These results confirmed that REEs present in hyperaccumulators can be transferred into biocrudes during MHTC in an acid-mediate system. Studies on the separation and purification of REEs from the biocrudes will be investigated in the future. A flowsheet for the processing of REE-contained biocrudes with the applications of solvent extraction, scrubbing, and precipitation stripping will be considered to be proposed to produce high purity REE products.

# Chapter 4 Process Development for Rare Earth Elements Recovery and Struvite Production from Biocrudes


## Abstract

A process that combines solvent extraction and struvite precipitation was first developed to address this challenge. In the extraction step, 95.6% of REEs were extracted using 0.05 mol/L di(2-ethylhexyl)phosphoric acid (D2EHPA) with an aqueous to organic (A/O) ratio of 1:1 at pH 3.0. However, 75.1% of Al, 81.2% of Ca, 54.5% of Fe, 61.5% of Mn, and 81.3% of Zn were co-extracted into the organic phase with the REEs. To solve this issue, a subsequent scrubbing step using deionized water was applied, with the removal of over 98% of these impurities, while incurring negligible loss of REEs. After the scrubbing step, over 97% of REEs were ultimately stripped out from the organic phase as REE oxalates using 0.01 mol/L oxalic acid as the stripping agent. Furthermore, phosphorous (P) was found to be retained in the raffinate after the solvent extraction process. 94.4% of the P was recovered by forming struvite precipitate at pH 9.0 and a Mg/P molar ratio of 1.5. In general, high purity and value-added REE products and struvite precipitate were eventually achieved from biocrudes in environmentally friendly and economically viable ways.


## 4.1 Introduction

After the phytomining process, the treatment of REE hyperaccumulators continues to pose a significant challenge. Given the value of REEs in advanced technologies, some studies have focused on recovering REEs from hyperaccumulators (Jally et al. 2021b; Laubie et al. 2018; Li and Zhang 2024). Conventional approaches employ hydrometallurgical techniques to directly extract REEs from hyperaccumulators or indirectly from the incineration ash, suffering from the disadvantages of being cost-prohibitive and environmentally unfriendly (Ashraf et al. 2022; Chour et al. 2018; Jally et al. 2021a; Laubie et al. 2018). Li and Zhang found that during microwave-assisted hydrothermal carbonization (MHTC), nearly 100% of REEs were extracted from an REE hyperaccumulator into biocrudes (liquid product) using 0.2 mol/L $H_2SO_4$ (Li and Zhang 2024). Additionally, the produced hydrochar (solid product) with high thermal stability and higher heating value (HHV) shows great potential for energy production. While hydrochar obtained after MHTC has the potential to be used as a fuel source, biocrudes necessitates additional refinement. Therefore, more attention is worth paying to the further processing of biocrudes.

In addition to REEs, Li and Zhang found that the biocrudes obtained from the MHTC treatment of REE hyperaccumulators in acidic media contains other elements, such as Mg, Al, Ca, Fe, Mn, Zn, P, etc (Li and Zhang 2024). Solvent extraction is commonly employed for the generation of mixed rare earth solutions or the separation of individual REEs (Xie et al. 2014). Organic extractants have been extensively utilized in the solvent extraction processes of REEs. Almost 99.9% of REEs were extracted from actual monazite leachate using di(2-ethylhexyl)phosphoric acid (D2EHPA) (Wu et al. 2018). Over 99% of REEs were recovered from ion-adsorption REE ores by stepwise extraction using 2-ethylhexyl phosphonic acid mono-2-ethylhexyl ester (HEHEHP) and bis(2-ethylhexyl) phosphate (HDEHP) as the organic extractants (Huang et al. 2017). La, Ce, and Y were extracted from waste electrical and electronic equipment at high efficiencies using a mixture neodecanoic acid (Versatic 10) and tributyl phosphate (TBP) at pH 7.0 (Talebi et al. 2018). Co and Sm chlorides dissolved in water were extracted by tricaprylylmethylammonium chloride (Aliquat 336) diluted in toluene (Z. Li et al. 2018).

In addition to REEs, the recovery of nutrient elements from biocrudes is worth exploring due to the value of nutrient elements in plant growth and the negative influence of improper disposal of nutrient-rich biocrudes on the environment (Martinez-Fernandez and Chen 2017; Njira and Nabwami 2015). Struvite precipitation has been widely investigated in phosphorous (P) recovery from wastewater, preventing the water from becoming eutrophic (Kumar and Pal 2015).

Furthermore, owing to its low solubility, struvite is regarded as an optimal candidate for slow-release fertilization (Rech et al. 2018; Talboys et al. 2016). A number of studies investigated the potential influencing factors on the struvite crystallization process, aiming to understand their impact on P recovery efficiency and product purity. Over 90% of P was recovered from an anaerobically digested chicken slurry with a molar ratio of 1:1:1 for Mg: N: P at a pH range of 9.5 to 10.5, resulting in a high-purity struvite precipitate (Muhmood et al. 2018). High P recovery and over 90% of struvite precipitation efficiency were obtained from urine systems with the addition of $MgCl_2$ or seawater as Mg sources (Aguado et al. 2019). 70% of P was recovered from wastewater, and pure struvite was produced (Sciarria et al. 2023). Over 98% of P was recovered as struvite from the black water using active serpentine (Li et al. 2022). Prior studies mainly focused on the fate of elements during hydrothermal treatment, while few studies emphasized the subsequent recovery of these elements (Chai, Bai, et al. 2022; Conti et al. 2018; Cui, Zhang, Wang, Pan, Lin, Khan, Yan, Li, He, and Yang 2021; Lu et al. 2017). Therefore, in this study, a process that combines solvent extraction and struvite precipitation with the aim of recovering valuable elements from biocrudes was first developed to address this difficulty.

In this study, a process flowsheet for the recovery of valuable elements from biocrudes was elaborated from both environmentally friendly and economically viable perspectives. Biocrudes produced from treating a REE hyperaccumulator in an acid-mediated MHTC system was collected and used as the feedstock. The separation and purification of REEs from the biocrudes was accomplished via a solvent extraction process that encompassed stages of extraction, scrubbing, and precipitation stripping, with each phase undergoing parametric optimization to enhance operational efficiency. REEs in biocrudes were finally recovered as high purity REE products, which had a wide application in advanced technologies. P contained in the biocrudes was precipitated as struvite after the extraction step of REEs. The struvite precipitation experiments were performed through adjustments of pH and Mg/P molar ratio to identify optimum conditions aiming at maximizing P recovery. P was recovered by forming struvite precipitate employed as a slow-release fertilizer. This study offered insights into the treatment of biocrudes in practice and economically.

## 4.2 Materials and methods

### 4.2.1 Materials and reagents

Grass leaves (GL) utilized in this study were cultivated and harvested by the authors, following a methodology detailed in (Li, Ji, and Zhang 2024). 1 g of the GL and 20 mL of 0.2 mol/L $H_2SO_4$ were mixed in the vessel, and then inserted into the rotor of the microwave reactor (Multiwave GO Plus, Anton Paar GmbH, Austria), where the temperature was ramped up to 180°C at 10 ºC/min heating rate and sustained for 60 min. The resultant suspension was centrifuged at 5000 rpm for 5 min to separate the liquid fraction, termed biocrudes, which was preserved for subsequent experimental analysis. Detailed information concerning this experiment was published (Li and Zhang 2024). Biocrudes was diluted in a 100-fold volume of 5% (v/v) $HNO_3$ solution for the analysis of elemental concentration, conducted by an inductively coupled plasma emission mass spectrometer (ICP-MS, Thermo Electron iCAP-RQ, Thermo Scientific, USA).

Chemicals used in this chapter involve hydrochloric acid (HCl, 37 wt.%), 50% w/w sodium hydroxide (NaOH, ≥ 97 wt.%), anhydrous magnesium chloride ($MgCl_2$, ≥98%), odorless kerosene, and oxalic acid. Di(2-ethylhexyl)phosphoric acid (D2EHPA) was utilized as received without further purification. All chemicals employed in this study were purchased from Thermo Fisher Scientific. Deionized water was used for all solutions.

### 4.2.2 Solvent extraction

#### 4.2.2.1 Extraction Experiments

The purification of REEs from biocrudes was conducted through a series of extraction, stripping, and scrubbing steps (Zhang and Honaker 2020). In the extraction step, the organic phase was prepared by adding D2EHPA into kerosene. The organic phase was thoroughly mixed with 20 mL biocrudes by magnetic stirring at room temperature (21 ± 0.5 ºC) during the extraction process. 37 wt.% HCl and 50% (w/w) NaOH were used as pH regulators. Following each pH adjustment, the mixture was agitated at 28 g for 2 min to obtain a relatively stable pH value. After achieving the desired pH value, the mixture was stirred at 28 g for 20 min to attain equilibrium. Subsequently, the pH value was recorded using a portable pH meter (AP110, Thermo Fisher Scientific, USA) for measurement. The resulting aqueous and organic phases from the extraction step were transferred to a separatory funnel and left for 5 min for phase separation. Elemental concentrations of the separated aqueous phase were measured by ICP-MS. The extraction efficiency (*E*, %) is determined by calculating the ratio of elements transferred to the organic phase relative to their initial quantity in the feed solution. The extraction efficiency (*E*, %) was calculated in accordance with Equation (4.1).

$$E = \frac{[M]_A - [M]_B}{[M]_A} \times 100 \qquad (4.1)$$

where $[M]_A$ (mg/L) and $[M]_B$ (mg/L) denote the elemental concentration in the feed biocrudes and in the raffinate obtained from the extraction test, respectively.

During the extraction process, investigations were conducted to identify optimal conditions for extracting REEs from biocrudes, focusing on varying pH levels (1.0 to 7.0), D2EHPA concentrations (0.01 mol/L to 0.2 mol/L), and aqueous to organic (A/O) ratios (1/5 to 5/1).

#### 4.2.2.2 Scrubbing and Precipitation Stripping Experiments

Subsequent to the extraction step, the organic phase enriched with REEs was subjected to scrubbing tests to eliminate undesirable elements using deionized water at a fixed A/O ratio of 1/1 (W. Zhang et al. 2022). The scrubbing process was under continuous magnetic stirring at 28 g for 30 min. Phase separation after scrubbing was carried out using the same method as employed during the extraction step. Scrubbing efficiency (*S*, %) was calculated according to Equation (4.2).

$$S = \frac{[M]_C}{[M]_A - [M]_B} \times 100 \tag{4.2}$$

where $[M]_C$ (mg/L) denotes metal ion concentration, M, in the aqueous phase after the scrubbing step.

After the scrubbing tests, the organic phase containing REEs was mixed with oxalic acid solutions at concentrations spanning from 0.005 mol/L to 0.1 mol/L to strip REEs from the organic phase by forming REE oxalate precipitate (Jorjani and Shahbazi 2016). During the precipitation stripping experiments, the A/O ratio was maintained at 1/1, and the stirring process was conducted at 28 g for 60 min at a pH value of 2.5. The mixtures were allowed to stand until separation into three distinct layers was observed. The aqueous precipitating solution was diluted by a factor of 100 with a 5% (v/v) $HNO_3$ and sent to ICP-MS for elemental concentration analysis. The REE oxalate precipitate was separated from the other two phases by filtration and rinsed with 2-propanl thoroughly. Elemental concentrations of the precipitate were analyzed following the digestion procedure published by Li *et al.* (Li, Tran, et al. 2023). The REE precipitation ($P_{REE}$, %) efficiency was calculated according to Equation (4.3).

$$P_{REE} = \frac{[M]_A - [M]_B - [M]_C - [M]_D}{[M]_A - [M]_B - [M]_C} \times 100 \tag{4.3}$$

where $[M]_D$ (mg/L) is the metal ion concentration in the aqueous precipitating solution.

The concentration of total organic carbon (TOC) in the raffinate after both extraction and stripping precipitation steps was analyzed by using TOC-L Total Organic Carbon Analyzer (Shimadzu, Kyoto, Japan). The sample was diluted 100 times with 0.1 mol/L HCl for analysis.

### 4.2.3 Struvite ($MgNH_4PO_4{\cdot}6H_2O$) precipitation

Batch experiments of struvite precipitation were implemented to recover P from the raffinate obtained after the extraction step (Sena et al. 2021; Sun, Mohammed, and Liu 2020). 20 mL of the raffinate and added reagents were mixed by magnetic stirring during the precipitation process. Each experiment was conducted in triplicate. $MgCl_2$ prepared at 0.1 mol/L was used as the magnesium source to achieve the required Mg/P molar ratio. After adding $MgCl_2$, the mixture was continuously agitated at 4 g to ensure thorough mixing of the $MgCl_2$ and the raffinate. The pH adjustment was facilitated using 50% (w/w) NaOH. The stirring speed was maintained at 1 g for 35 min after obtaining the desired pH, which was recorded by a portable pH meter (AP110, Thermo Fisher Scientific, USA). The resultant suspension was centrifuged. The obtained precipitate was washed with deionized water, dried at 60 ºC for 48 h, and prepared for additional analysis. The supernatant was diluted by a factor of 100 with 5% (v/v) $HNO_3$ and analyzed for elemental concentrations. The P recovery (*P*, %) by forming struvite precipitate was calculated according to Equation (4.4).

$$P = \frac{[M]_B - [M]_E}{[M]_B} \times 100 \tag{4.4}$$

where $[M]_E$ (mg/L) represents the elemental concentration in the aqueous phase after struvite precipitation.

Each experiment in this study was replicated three times, with the mean outcomes presented and experimental uncertainties indicated by error bars to ensure its efficacy and reproducibility.

The speciation, solubility, and equilibrium of solid and dissolved phases of compounds in an aqueous solution were calculated by Visual MINTEQ (Zhou and Wu 2012). The composition of the raffinate obtained after the extraction process is used as an input to predict potential compounds that could be formed. The activity corrections were facilitated through the Davies method, and the ionic strength was computed by the model. In addition to Mg, the concentrations of P and other elements were selected according to the characteristics of the raffinate. A pH range of 7.0 to 12.0 with increments of 0.2 was selected for the operating condition.

### 4.2.4 Characterization of the struvite precipitate

The morphology of struvite precipitate was characterized using a JSM-IT500 scanning electron microscope (SEM) equipped with a backscattered electron (BSE) detector. Prior to observation, the specimen was affixed to carbon tape and subsequently sputtered with a 7 nm thick palladium/platinum coating via a 208HR sputter coater (Cressington Scientific Instrument, England, UK) to improve electron conductivity for enhanced imaging quality.

X-ray diffraction (XRD) analysis was used to characterize the struvite precipitate, utilizing a Bruker D8 Advance XRD system (Bruker Corporation, USA) outfitted with Cu Kα radiation. The X-ray tube was operated at 40 kV and 40 mA. Data acquisition covered a 2θ range from 10° to 70°, with a scanning velocity of 2° per minute. Peak analysis was conducted using MDI Jade 6.0 software, referencing the PDF-2 database provided by the International Center for Diffraction Data (ICDD).

## 4.3 Results and discussion

### 4.3.1 Biocrudes characterization

Elemental concentrations of the biocrudes are presented in Table 4.1. The concentration of total REEs (TREEs) is 6.44 mg/L with 3.05 mg/L light REEs (LREEs) and 3.39 mg/L heavy REEs (HREEs). Y, La, Ce, and Dy are the only four REEs that are contained in the biocrudes with the concentrations of 1.59 mg/L, 1.53 mg/L, 1.54 mg/L, and 1.78 mg/L, respectively. It was reported by Li and Zhang that the grass was fed with a solution containing each Y, La, Ce, and Dy of 50 mg/L once every two days, and the grass leaves were harvested after 14 days of growth. The grass leaves accumulated 503.4 mg/kg of these four REEs (Li and Zhang 2024). Therefore, only Y, La, Ce, and Dy were transferred from the grass leaves into biocrudes using MHTC process. Additionally, it was also found that biocrudes contained several other metals, such as 114.22 mg/L Mg, 1.32 mg/L Al, 145.23 mg/L Ca, 7.52 mg/L Fe, 2.62 mg/L Mn, and 2.56 mg/L Zn. The concentrations of nutrient elements, including P and K, were 417.78 mg/L and 2223.46

mg/L, respectively. Considering nutrient elements play a crucial role in the growth, development, and stress tolerance of plants, biocrudes possess the capability to serve as a feedstock for nutrient element recovery (Kirkby 2023).

Table 4.1 Elemental concentrations (mg/L) of the biocrudes.

| Mg | Al | Si | P | K | Ca | Ti | Fe | Mn | Cu |
|---|---|---|---|---|---|---|---|---|---|
| 114.22 | 1.32 | 58.27 | 417.48 | 2223.46 | 145.23 | 0.59 | 7.52 | 2.62 | 0.84 |
| Zn | Sr | Ba | TREEs | LREEs | HREEs | Y | La | Ce | Dy |
| 2.56 | 0.43 | 0.19 | 6.44 | 3.05 | 3.39 | 1.59 | 1.53 | 1.54 | 1.78 |

Note: TREEs, LREEs, and HREEs represent total, light (La, Ce, Pr, Nd, and Sm), and heavy (Y, Eu, Gd, Tb, Dy, Ho, Er, Tm, Yb, and Lu) REEs, respectively.

### 4.3.2 Extraction of rare earth elements

Solvent extraction is commonly employed for the generation of mixed rare earth solutions or the separation of individual rare earth elements (Xie et al. 2014). In the process of extraction, parameters including organic extractant types, extractant concentration, A/O ratio, and pH, are crucial to be investigated (Dashti et al. 2021). Among all these factors, pH, extractant concentration, and A/O ratio were explored in the following. In terms of extractant types, many literatures reported that D2EHPA was a prominent organic extractant in the separation of REEs (Gergoric et al. 2017; Khaironie et al. 2014; Kumari et al. 2019; Wu et al. 2018). Therefore, D2EHPA was selected as an organic extractant to recover REEs from biocrudes in this study.

#### 4.3.2.1 Effect of pH

D2EHPA, possessing a cationic nature, facilitates the extraction of REEs through the substitution of hydrogen ions with metal ions (Kumari et al. 2019). The extraction efficiency of REEs using D2EHPA is significantly influenced by the pH of the aqueous phase (Mohammadi et al. 2015). The alternations of pH influence the ionization state of D2EHPA, thus influencing the extraction efficiency of the process (Borai et al. 2016). The effect of pH on the extraction of REEs and metals from biocrudes was investigated using 0.1 mol/L D2EHPA at a fixed A/O ratio of 1/1. As shown in Figure 4.1(a), at a pH value of 1.0, the extraction efficiencies of HREEs, Y and Dy, were 95.9% and 84.4%, respectively. However, the extraction efficiencies of the LREEs, La and Ce, were 4.3% and 5.2%, respectively. D2EHPA shows preferential extraction of HREEs over LREEs (Battsengel et al. 2018). Compared to LREEs, HREEs have a smaller ionic radius and higher charge density, resulting in the formation of more stable complexes with the acidic form of D2EHPA (Wehbie et al. 2017). Therefore, HREEs have greater extraction efficiency compared to LREEs. Wu *et al.* found that 89.4% of HREEs were extracted from wet-process phosphoric acid (WPA) containing REEs under the optimum conditions of 1.0 mol/L D2EHPA at a fixed ratio of 1/1 (Wu et al. 2018). When increasing the pH value from 1.0 to 3.0, the extraction efficiencies of La and Ce enhanced significantly from around 5% to over 95%. The extraction efficiency of Y, La, Ce, and Dy, reached nearly 100%. As the pH value increased, the protonation of D2EHPA decreased, which flavored the formation of extractable REE complexes, thus improving their solubility in the organic phase. With a further increase in pH from 3.0 to 7.0, the extraction efficiencies of REEs remained almost unchanged.

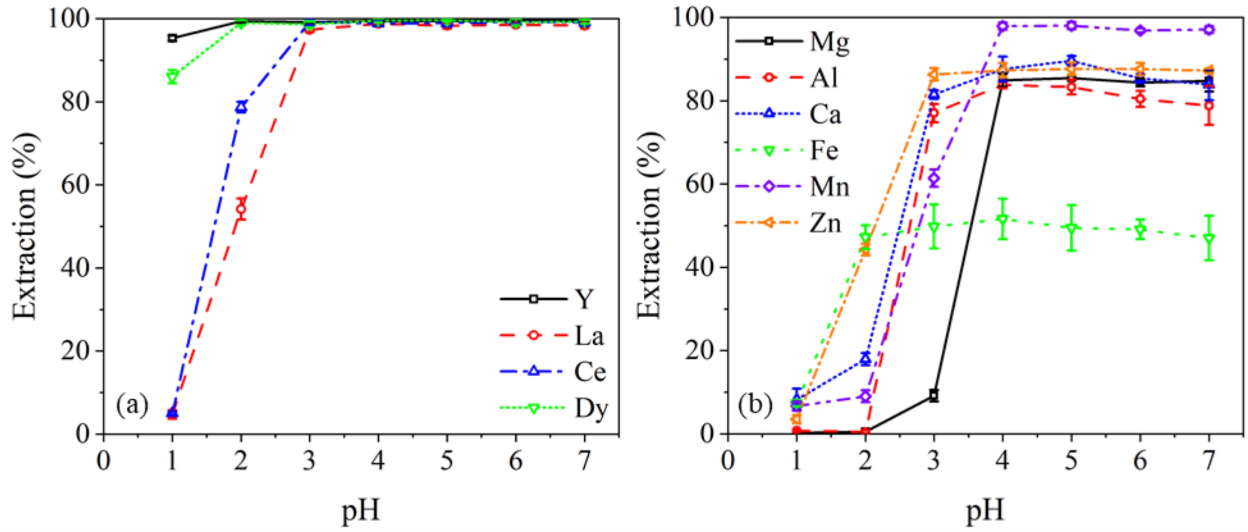


Figure 4.1 Effect of pH on the extraction of REEs (a) and other metals (b).

Figure 4.1(b) illustrates the impact of pH on the extraction of the main metals from the biocrudes, conducted with 0.1 mol/L D2EHPA at an A/O of 1/1. It can be observed that at a pH value of 1.0, the extraction efficiencies of the main metals were below 5%. With the enhancement of pH values from 1.0 to 3.0, there were significant increases in extraction efficiencies of Al, Ca, Fe, Mn, and Zn. There was a negligible increase in Mg extraction in the pH range from 1.0 to 3.0. Compared to other metals, Mg requires a higher pH for the formation of stable and extractable complexes with D2EHPA (Guimarães et al. 2020). Therefore, the extraction efficiency of Mg remained relatively stable with the increase in pH values from 1.0 to 3.0 and increased significantly from 7.6% to 86.3% after enhancing pH from 3.0 to 4.0. Nearly 100% of Zn was recovered from biocrudes at a pH value of 4.0. Organophosphorous extractants, such as D2EHPA and 2-ethylhexyl phosphonic acid mono-2-ethyl hexyl ester (PC88A), were found extensive usage in the extraction of Zn from chloride and sulfate media (Deep and de Carvalho 2008; El Dessouky et al. 2008). In addition, compared to other main metals, the extraction efficiency of Fe was relatively low. The highest extraction efficiency of Fe was 55.8%. Fe(III) can be easily extracted using D2EHPA at a low pH value, but Fe(II) is hardly extracted

(Azizitorghabeh et al. 2017; Li et al. 2015; Majima et al. 1985). Therefore, Fe ions existed as both Fe(III) and Fe(II) in biocrudes.

Overall, based on the aforementioned discussion and considering economic factors, a pH value of 3.0 was selected as the preferred operating condition for maximizing REE extraction from biocrudes. Meanwhile, 75.1% Al, 81.2% Ca, 54.5% Fe, 61.5% Mn, and 85.3% Zn were co-extracted from biocrudes under this condition.

#### 4.3.2.2 Effect of D2EHPA concentration

D2EHPA concentration is crucial in REE extraction process (Battsengel et al. 2018). During the extraction, the complexation capacity of D2EHPA with metal ions, extraction equilibrium, and selectivity are influenced by alternations in D2EHPA concentration, thus affecting the extraction efficiencies of REEs and metals from biocrudes (Kumari et al. 2019; Mohammadi et al. 2015; Ren et al. 2007). Figure 4.2 elucidates the effect of D2EHPA concentrations, spanning from 0.01 mol/L to 0.2 mol/L, on the extraction efficiencies of REEs and main metals from biocrudes. During the extraction process, the pH was maintained at 3.0, and the A/O ratio was consistently held at 1/1. As can be seen from Figure 4.2(a), elevating the D2EHPA concentration from 0.01 mol/L to 0.05 mol/L significantly augmented the extraction efficiencies of La and Ce from 29.6% and 65.6% to 90.2% and 94.8%, respectively. The incremental increase in concentrations from 0.5 mol/L to 2 mol/L had a negligible impact on the extraction efficiencies of La and Ce. However, 96.7% of Y and 88.5% of Dy were extracted when using 0.01 mol/L D2EHPA during the extraction process, and negligible increases were observed with further concentration increments to 0.2 mol/L. As mentioned in Section 3.2.1, compared to LREEs, D2EHPA demonstrates a higher selectivity for extracting HREEs, which explains the lower initial extraction efficiencies of La and Ce as compared to Y and Dy when using 0.01 mol/L D2EHPA. The extraction efficiencies for Y, La, Ce, and Dy exceeded 90% with an increase in D2EHPA concentration to 0.05 mol/L. This improvement is attributed to the higher availability of extractant molecules at elevated D2EHPA concentrations, facilitating greater REE binding and subsequent extraction from biocrudes (Wilson et al. 2014).

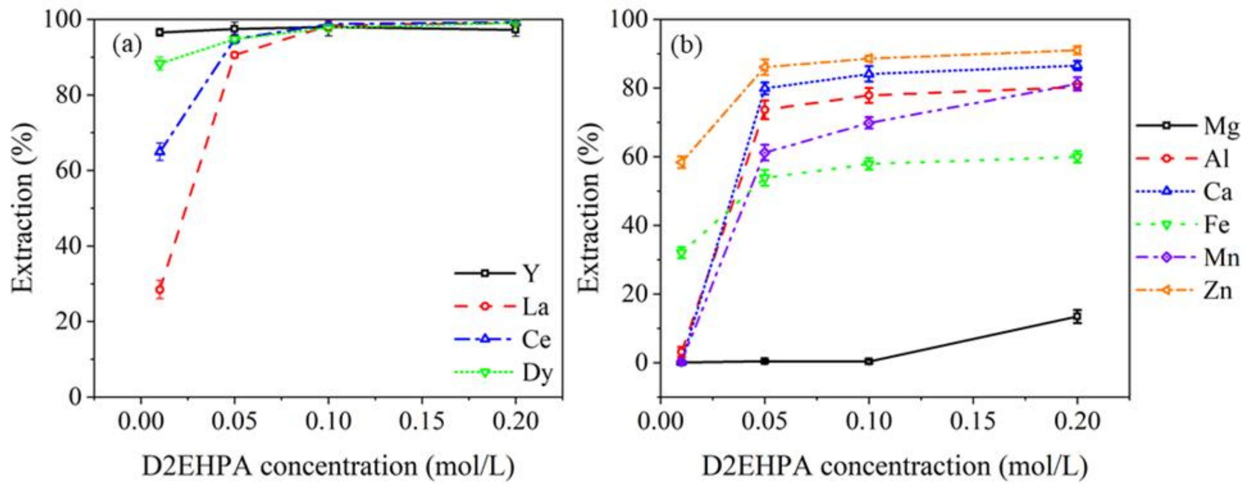


Figure 4.2 Effect of D2EHPA concentration on the extraction of REEs (a) and metals (b).

The D2EHPA concentration also exerts a pivotal influence on the extraction efficiencies of other main metals in biocrudes (Figure 4.2(b)). 33.7% Fe and 58.1% Zn were co-extracted using 0.01 mol/L D2EHPA as the extractant. Few other main metals, including Mg, Al, Ca, and Mn, were co-extracted under this condition. At low concentrations of D2EHPA, the limited availability of extractant molecules resulted in reduced extraction efficiencies of main metals from the biocrudes. With increasing D2EHPA concentration from 0.01 mol/L to 0.05 mol/L, the extraction efficiencies of main metals except for Mg enhanced significantly.

To optimize the extraction of REEs from biocrudes, a D2EHPA concentration of 0.05 mol/L was identified as the optimal operating condition. However, most contaminants, including Al, Ca, Fe, Mn, and Zn, were co-extracted under this condition, which were considered to be separated from REEs using a subsequent scrubbing step (Section 3.3) (Ding et al. 2015).

#### 4.3.2.3 Effect of A/O ratio

Previous research investigated that the A/O ratio was a critical parameter in the extraction process, significantly influencing solvent capacity and extraction equilibrium, and thereby directly affecting the extraction efficiency (Chen et al. 2021; Jung et al. 2008). Figure 4.3 elucidates the impact of A/O ratio on the extraction of REEs and main metals from biocrudes using 0.05 mol/L D2EHPA at a pH 3.0. The increment in the A/O ratio from 1:5 to 1:1 exerted a negligible influence on the extraction efficiencies of REEs (Figure 4.3(a)). As further elevating the A/O ratio to 5:1, there was a remarkable decline in the extraction efficiencies of REEs. With the increase in A/O ratios, fewer extractant molecules are available to bind with REEs, resulting in a decrease in REE extraction efficiency. In addition, an increased A/O ratio implies a decrease in interfacial area and mass transfer between aqueous and organic phases, thus leading to a decrease in REE extraction kinetics and efficiency.

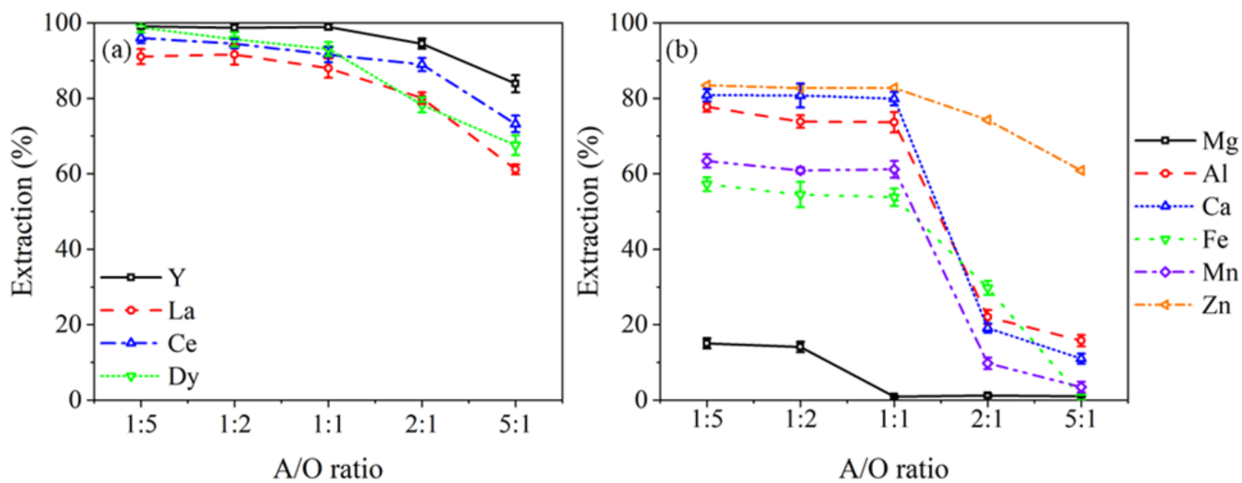


Figure 4.3 Effect of A/O ratio on the extraction of REEs (a) and metals (b).

During extraction process, the impact of A/O ratio on the extraction efficiencies of main metals in biocrudes was also investigated. According to Figure 4.3(b), the extraction efficiencies of Zn, Ca, Al, and Mn show no significant changes as the A/O ratio was adjusted from 1:5 to 1:1.

However, there were sharp decreases in extraction efficiencies of these metals when further increasing the A/O ratio from 1:1 to 2:1. A/O ratio adjustments had a minimal impact on the Mg extraction. The extraction efficiencies of Mg decreased slightly from 13.7% to 1.3% with an increasing A/O ratio from 1:5 to 1:1. In terms of Fe, a gradual decrease in its extraction from 75.2% to 0.6% was observed with an elevation in the A/O ratio from 1:5 to 5:1. Considering the nearly complete extraction of REEs, the A/O ratio of 1/1 was optimal and selected for subsequent experiments.

In conclusion, around 95% of REEs were extracted from biocrudes when using 0.05 mol/L D2EHPA as the extractant with an A/O ratio of 1:1 at pH 3.0. This phenomenon indicated that D2EHPA was also an efficient extractant in recovering REEs from biocrudes, as evidenced by the high recovery of REEs and low consumption of the organic extractant. The assumption of only using D2EHPA as an efficient organic extractant for REE recovery was found to exert minimal influence on REE extraction from biocrudes. In addition, 75.1% of Al, 81.2% of Ca, 54.5% of Fe, 61.5% of Mn, and 81.3% of Zn were co-extracted from biocrudes under this optimized condition. Nearly 100% of Mg remained in the aqueous phase after the extraction process.

### 4.3.3 Impurity removal

After the extraction step, around 95% of REEs were transferred to the organic phase. However, this phase was also loaded with impurities due to the co-extraction. The presence of these impurities, such as trivalent metal ions ($Al^{3+}$ and $Fe^{3+}$), tends to chelate with precipitant in the following precipitation stripping step, leading to an increment in precipitant consumption and a reduction in product purity (Zhang and Honaker 2020; Zhang and Noble 2020b). In addition, in order to obtain high purity REE products, impurities co-extracted with REEs in the organic phase, such as Al, Ca, Fe, Mg, and Zn, were all considered to be removed. Previous studies indicated that impurities in the loaded organic phase could be effectively removed through scrubbing with deionized water (Lv et al. 2023; Zhang et al. 2020). Therefore, deionized water was employed as the scrubbing agent.

The REE-loaded organic phase underwent a scrubbing process using deionized water at an A/O ratio of 1:1. As can be seen from Table 4.2, over 98% of Al, Ca, Fe, Mn, and Zn were effectively removed from the organic phase into the scrubbing raffinate. However, 96.3% of four REEs, including Y, La, Ce, and Dy, were retained in the organic phase. Therefore, deionized water was considered as an appropriate scrubbing agent for removing impurities from the REE-loaded organic phase.

Table 4.2 Scrubbing efficiency from the REE-loaded organic phase using deionized water.

| | Al | Ca | Fe | Mn | Zn | Y | La | Ce | Dy |
|---|---|---|---|---|---|---|---|---|---|
| S/% | 98.7 | 98.6 | 99.2 | 98.9 | 99.8 | 3.8 | 4.6 | 3.5 | 3.2 |

### 4.3.4 Precipitation stripping

Precipitation stripping was employed to precipitate metal ions from a solution as solid compounds through the application of a stripping agent (Palden et al. 2019). In the process of precipitation stripping, oxalic acid concentration, precipitation time, and phase ratio were identified as different variables influencing the precipitation of REEs. Jorjani found that compared to oxalic acid concentration, precipitation time and phase ratio exerted negligible influences on the REE precipitation (Jorjani and Shahbazi 2016). Therefore, precipitation stripping of the REE-loaded organic phase obtained after scrubbing process was performed using oxalic acid with an A/O ratio of 1:1 at pH 2.5 by continuous mixing for 60 min (Dewulf, Riano, and Binnemans 2022; Jorjani and Shahbazi 2016).

The efficacy of oxalic acid concentrations, ranging from 0.005 to 0.1 mol/L, was investigated for the production of high purity REE oxalate. As shown in Figure 4.4, elevating the oxalic acid concentration from 0.005 mol/L to 0.01 mol/L led to a significant enhancement in the precipitation efficiency of four REEs. A concentration of 0.01 mol/L oxalic acid achieved precipitation of over 97% of REEs, while concentrations above 0.01 mol/L had a minimal impact on further precipitation. Consequently, 0.01 mol/L was determined to be the optimal oxalic acid concentration. The result showed almost 100% of REEs were finally precipitated under optimized conditions, which was a desired outcome. Therefore, if the assumption of neglecting the influences of precipitation time and phase ratio on REE precipitation was incorrect, it would also not exert a significant influence on the final result. In addition, the produced precipitate was digested for elemental analysis, and the result indicated REE oxalates were obtained with a purity of over 97%.

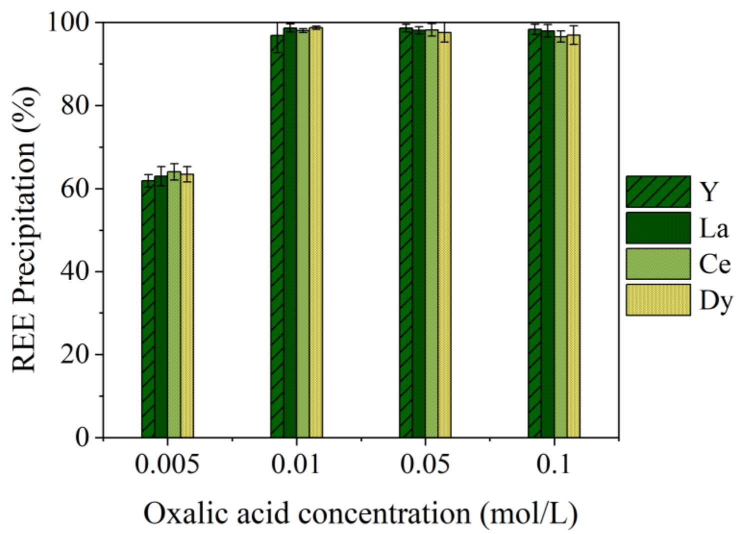


Figure 4.4 Effect of oxalic acid concentration on REE precipitation.

### 4.3.5 Struvite precipitation

The use of struvite precipitation is a common method for recovering nutrient elements, including nitrogen(N), P, and Mg, from liquid waste streams (Krishnamoorthy et al. 2021). In addition, struvite containing nutrients is a valuable fertilizer that is vital for plant growth (Ahmed et al. 2018). Almost 100% of P was retained in the raffinate following the extraction process.

Therefore, struvite precipitation was considered a sustainable method for the management of the raffinate obtained after the process of extraction. The effects of pH and Mg/P molar ratio on the recovery of P from the raffinate were examined in the following sections.

#### 4.3.5.1 Effect of pH

Figure 4.5(a) delineates the impact of pH on P recovery from the raffinate obtained after the extraction step at a fixed Mg/P ratio of 1. P recovery increased from 62.6% to 93.9% with the increase in pH value from 7.0 to 9.0. A negligible increase was observed as the pH value escalated from 7.0 to 9.0. However, when further increased pH from 10.0 to 12.0, P recovery decreased from 95.3% to 72.4%. With increasing the pH from 10.0 to 12.0, the concentration of $OH^-$ ions increased. Enhanced $OH^-$ competed with phosphate ions for binding with $Mg^{2+}$, resulting in the precipitation of $Mg(OH)_2$ and thus a decrease in P recovery (Stratful et al. 2001). These findings were consistent with prior work according to struvite precipitation from wastewater at different pH values (Zhou et al. 2015). In general, pH 9.0 represents the optimal condition for P recovery from the raffinate achieved after the extraction process.

Figure 4.5(b) shows the speciation of phosphate in solution, maintaining a constant Mg/P molar ratio of 1. Kumari and Bhuiyan found that Mg predominantly exists as $Mg^{2+}$ ions to form complexes with other components in wastewater (Bhuiyan et al., 2007; S. Kumari et al., 2019). $NH_4^+$ concentration decreased as the pH value increased due to the conversion of $NH_4^+$ to $NH_3$ at rising pH (D. Zhang et al., 2012). Figure 4.5(b) illustrates that $H_2PO_4^-$ and $HPO_4^{2-}$ are the prevalent phosphate species within the pH range of 7.0 to 10.0. However, as increasing the pH value from 10.0 to 12.0, an increase in the concentration of $PO_4^{3-}$ was observed. Additionally, the analysis from pH 8.0 to 11.0 demonstrates a predominance of $HPO_4^{2-}$ over $H_2PO_4^-$ and $PO_4^{3-}$, suggesting that in this specific pH range, the formation of struvite is optimally facilitated. This observation is elaborated upon in Equation (4.5), which describes the chemical mechanism underlying struvite crystallization under the above mentioned conditions.

$$Mg^{2+} + NH_4{}^{+} + HPO_4{}^{2-} + 6H_2O \rightarrow MgNH_4PO_4 \cdot 6H_2O + H^{+} \quad (4.5)$$

Considering maximizing the recovery of P, a pH value of 9.0 was selected as the preferred condition. In addition, the formation of struvite precipitate at pH 9.0 follows Equation (4.5).

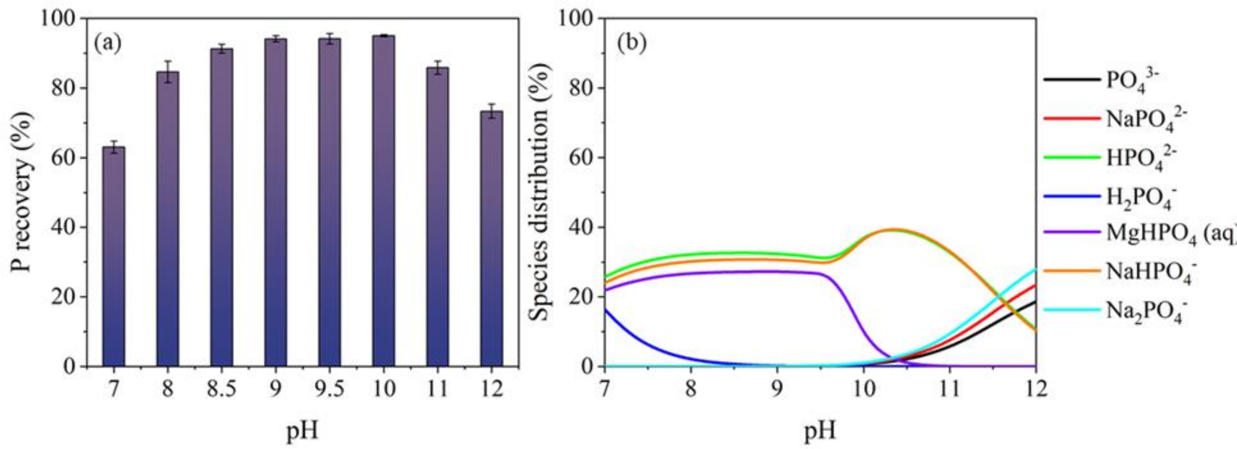


Figure 4.5 Effect of pH on the recovery of P (a); Species distribution of phosphate in the raffinate after the solvent process with a Mg/P ratio of 1 as a function of pH at 25 ºC (b).

#### 4.3.5.2 Effect of Mg/P molar ratio

The Mg/P molar ratio directly affects the stoichiometry and efficiency of the struvite precipitation reaction (Rahaman et al. 2008). The impact of the Mg/P molar ratio on the P recovery was investigated at a fixed pH value of 9.0. Figure 4.6 shows that P recovery escalates from 46.3% at Mg/P = 0.2 to 94.4% at Mg/P = 1.5, beyond which the recovery plateaued for ratios exceeding 1.5. Increased Mg/P molar ratio led to the enhanced availability of $Mg^{2+}$ for struvite precipitate formation. At a Mg/P molar ratio of 2.0, nearly all phosphate ions in the solution were reacted, and further addition of $Mg^{2+}$ did not contribute to higher P recovery.

In summary, an optimal recovery of 94.4% of P from the raffinate obtained after the extraction process was achieved by forming struvite precipitate at pH 9.0 with a Mg/P molar ratio of 1.5.

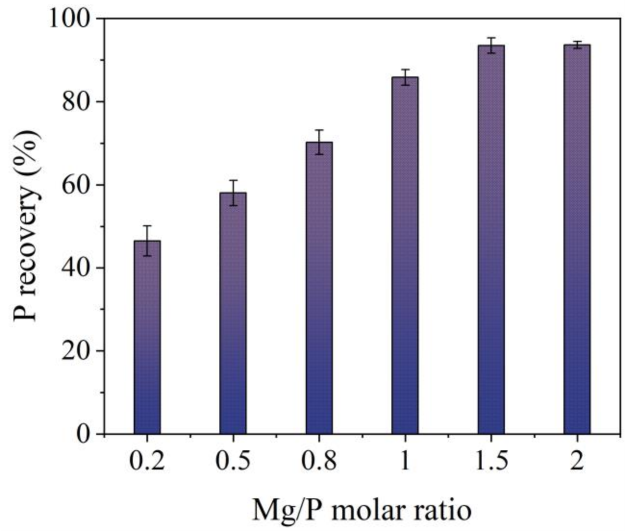


Figure 4.6 Effect of Mg/P molar ratio on the recovery of P.

#### 4.3.5.3 Struvite precipitate characterization

Figure 4.7(a) is the SEM image of the precipitate. The shape of the precipitate showed wedges and short columns, which agree with the typical shape of the struvite (Li et al. 2020). In addition, the XRD pattern of the precipitate is shown in Figure 4.7(b). Using Jade 6.0 software to analyze the XRD pattern, it clearly showed that diffraction peaks of the precipitate aligned with the standard patterns of struvite (PDF#15-0762), $Mg_3(PO_4)_2$ (PDF#71-1164), and $MgHPO_4 \cdot 3H_2O$ (PDF#01-0579). During the process of struvite precipitation, trace amounts of $Mg_3(PO_4)_2$ and $Mg_3(PO_4)_2$ were simultaneously generated with struvite precipitate (Tansel et al. 2018).

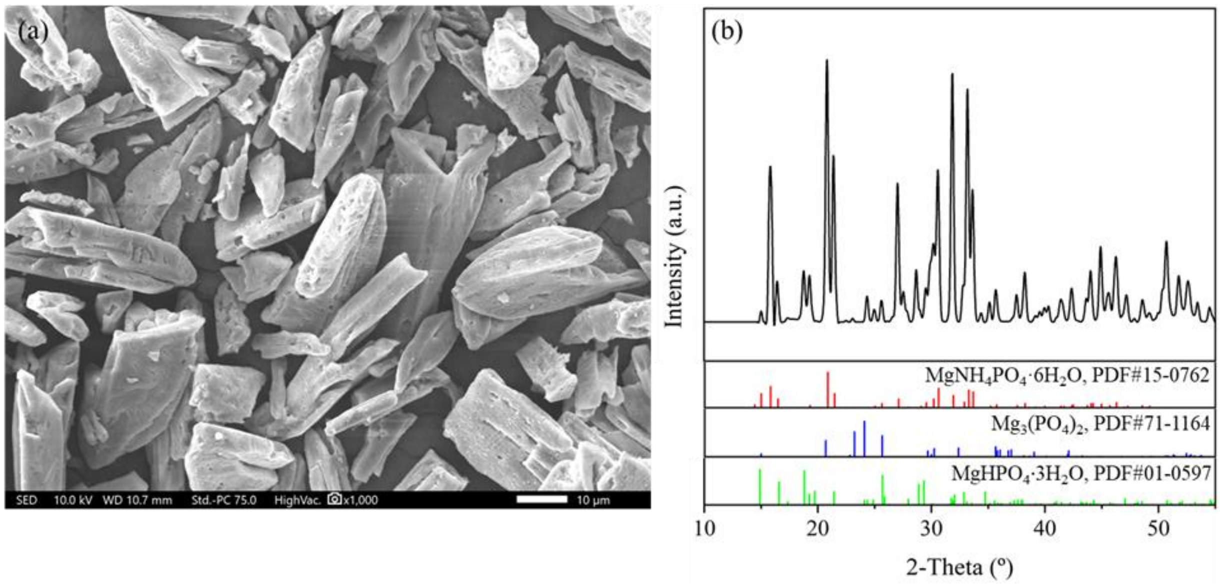


Figure 4.7 The structural characterization of the precipitate: SEM image (a); XRD pattern (b).

### 4.3.6 Flowsheet description

This study proposed a process flowsheet for the process of biocrudes is proposed in Figure 4.8 aiming at recovering REEs and producing struvite precipitate from biocrudes. As shown in Figure 4.8, 0.05 mol/L D2EHPA was used to extract REEs from biocrudes at pH 3.0 with an A/O ratio of 1:1. 95.6 % of REEs were extracted from biocrudes during this step. A majority of other impurities, including Al, Ca, Fe, Mn, and Zn, were also co-extracted with REEs, while Mg and P were retained in the raffinate. Deionized water was used as the scrubbing agent to separate other impurities from REEs. After the scrubbing step, over 98% of impurities were removed into the scrub raffinate, and over 96% of REEs were retained in the organic phase. The REE-loaded organic phase was subsequently subjected to the precipitation stripping step. Over 97% of REEs were precipitated into REE oxalates with the utilization of 0.01 mol/L oxalic acid. With the addition of $MgCl_2$, 94.4% of P in the raffinate was recovered to form struvite precipitate at pH 9.0 with a Mg/P molar ratio of 1.5. In addition, it was found that almost all of the organic carbon in biocrudes was water soluble and was retained in aqueous phases after extraction and struvite precipitation steps (Table 4.3).

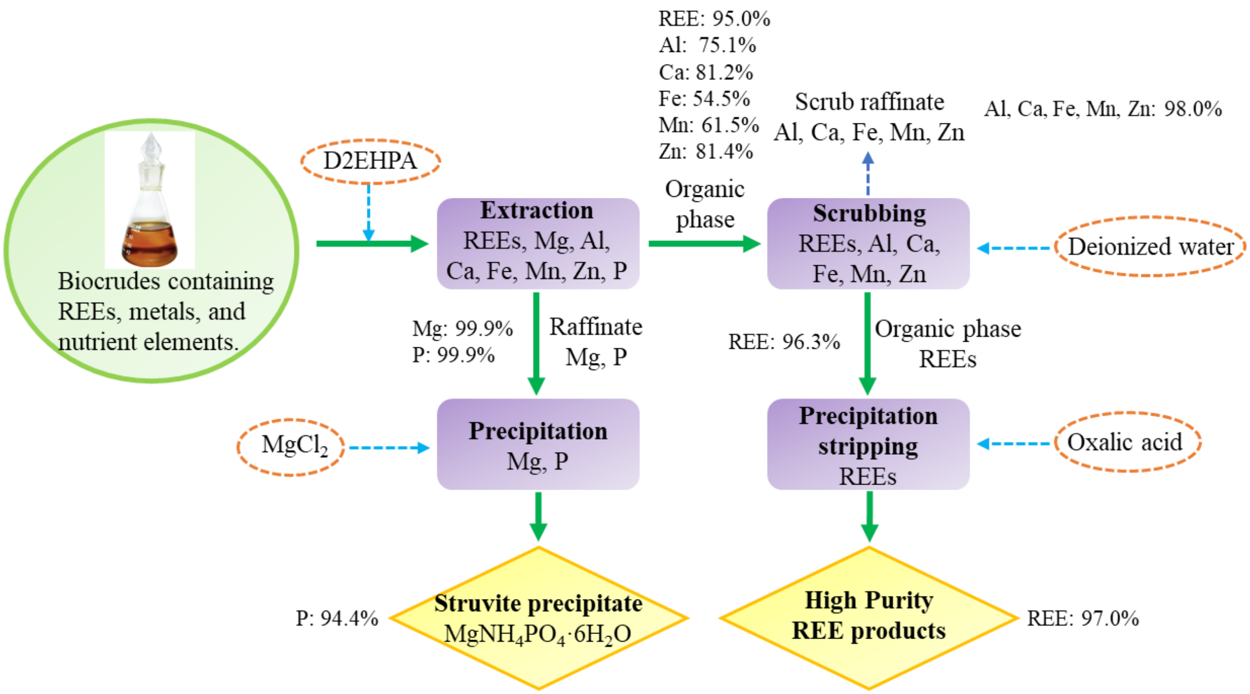


Figure 4.8 Flowsheet for REE recovery and struvite precipitate production from biocrudes.

Table 4.3 TOC of the aqueous phase.

| Sample | Biocrudes | Raffinate after extraction | Raffinate after struvite precipitation |
|---|---|---|---|
| TOC/mg/L | 111.9 | 109.0 | 94.21 |

## 4.4 Conclusion

Biocrudes obtained from treating REE hyperaccumulators in an acid-mediated MHTC system contains 6.44 mg/L REEs, 417.48 mg/L P, and other elements, which was a promising resource for valuable element recovery. The effect of pH, D2EHPA concentration, and A/O ratio on REE recovery from biocrudes was investigated during the extraction process. 95.6% of REEs were extracted using 0.05 mol/L D2EHPA with an A/O ratio of 1:1 at pH 3.0, while 75.1% of Al, 81.2% of Ca, 54.5% of Fe, 61.5% of Mn, and 81.3% of Zn were co-extracted with REEs into the organic phase.

In order to produce high purity REE products, deionized water was applied as a scrubbing agent to separate REEs from impurities from the organic phase. After the scrubbing step, over 98% of these impurities were removed from the organic phase, while over 96% of REEs were retained. Ultimately, precipitation stripping experiments with different oxalic acid concentrations were employed to maximize REE recovery. Over 97% of REEs were precipitated into REE oxalates using 0.01 mol/L oxalic acid as the stripping agent, and REE oxalates were obtained with a purity of over 97%.

Contrary to REEs, P remains solubilized in the raffinate after the extraction process. The effect of pH and Mg/P ratio on P recovery was investigated, and P was precipitated into struvite during this process. SEM revealed that the precipitate showing wedges and short columns was the typical shape of struvite. XRD analysis also revealed that struvite was produced during struvite precipitation. A process flowsheet was ultimately developed for the treatment of biocrudes aiming at recovering REEs and P from it into valuable products.

# Chapter 5 Summary and Perspectives

This study investigated a sustainable approach to the treatment of REE hyperaccumulators. REEs were efficiently extracted from hyperaccumulators using conventional hydrometallurgy and residual biomass was converted into hydrochar, an energy-rich fuel, with the application of MHTC. In addition, it was also found MHTC in the presence of acid was an effective way to extract REEs and produce hydrochar from hyperaccumulators. Solvent extraction and struvite precipitation were employed to recover REEs and phosphorus from biocrudes, yielding high-purity REE products and value-added byproducts (struvite). This research contributes a novel, efficient, and sustainable framework for REE hyperaccumulator treatment that aligns with circular economy principles by minimizing waste and maximizing resource reuse. It advances our understanding of employing sustainable methodologies for the treatment of hyperaccumulators aimed at recovering valuable elements and producing beneficial byproducts. From the perspective of broader impacts, this study extends well beyond the specific field of metal recovery, making substantial contributions to environmental sustainability, economic development, and technological innovation in mineral processing. It not only addresses the technical challenges associated with REE recovery but also promotes a broader application of these innovative techniques in resource management and waste reduction.

Perspectives for further improvement:

- Optimize extraction efficiency: Explore alternative, environmentally friendly lixiviants in conventional hydrometallurgy to efficiently extract REE from hyperaccumulators and minimize environmental impact. Future dissertations could develop novel syntheses of biodegradable lixiviants or modify existing ones to improve the leaching efficiency of REEs.
- Increase selectivity in solvent extraction: Investigate other green organic extractants to reduce the co-extraction of other impurities in biocrudes and minimize chemical usage. A

potential dissertation could focus on the synthesis and testing of new organic extractants, aiming to achieve high purity levels of REEs.

- Evaluate economic viability and scalability: Conduct a techno-economic analysis to assess the costs and feasibility of scaling up the process, considering resource availability, operational costs, and potential environmental benefits. Life-cycle assessments could also provide insight into the overall sustainability of the proposed methods. Future research might expand this analysis by incorporating life-cycle assessments to evaluate the environmental impacts throughout the entire process, from material sourcing to end-product disposal, thereby providing a holistic view of the sustainability of the methods.
- Apply this work to other elements: Extend the research framework to include the recovery of other critical and valuable elements from contaminated sites, such as heavy metals or transition metals, which can also be economically valuable and environmentally hazardous. A subsequent dissertation could apply the methods developed in this study to treat other elements-containing hyperaccumulators to extract these elements efficiently and derive value-added products.

# Reference


Afolabi, Oluwasola O. D., and M. Sohail. 2017. "Comparative Evaluation of Conventional and Microwave Hydrothermal Carbonization of Human Biowaste for Value Recovery." *Water Science and Technology* 75(12):2852–63.

Aguado, D., R. Barat, A. Bouzas, A. Seco, and J. Ferrer. 2019. "P-Recovery in a Pilot-Scale Struvite Crystallisation Reactor for Source Separated Urine Systems Using Seawater and Magnesium Chloride as Magnesium Sources." *Science of The Total Environment* 672:88–96. doi: https://doi.org/10.1016/j.scitotenv.2019.03.485.

Ahmed, Naveed, Soomin Shim, Seunggun Won, and Changsix Ra. 2018. "Struvite Recovered from Various Types of Wastewaters: Characteristics, Soil Leaching Behaviour, and Plant Growth." *Land Degradation & Development* 29(9):2864–79.

Alkan, Gözde, Bengi Yagmurlu, Seckin Cakmakoglu, Tobias Hertel, Şerif Kaya, Lars Gronen, Srecko Stopic, and Bernd Friedrich. 2018. "Novel Approach for Enhanced Scandium and Titanium Leaching Efficiency from Bauxite Residue with Suppressed Silica Gel Formation." *Scientific Reports* 8(1):5676.

Anderson, C. W. N., R. R. Brooks, A. Chiarucci, C. J. LaCoste, M. Leblanc, B. H. Robinson, R. Simcock, and R. B. Stewart. 1999. "Phytomining for Nickel, Thallium and Gold." *Journal of Geochemical Exploration* 67(1):407–15. doi: https://doi.org/10.1016/S0375-6742(99)00055-2.

Asati, Ambika, Mohnish Pichhode, and Kumar Nikhil. 2016. "Effect of Heavy Metals on Plants." *International Journal of Application or Innovation in Engineering & Management* 5(03):56–66. doi: 10.13140/RG.2.2.27583.87204.

Ashraf, Nermeen, Eduardo Santos Rodrigues, Eduardo de Almeida, Gabriel Sgarbiero Montanha, Cassio Hamilton Abreu-Junior, Milada Vítová, Rafael Henrique Lazzari Garcia, Hendrik Küpper, and Hudson Wallace Pereira de Carvalho. 2022. "Identification of Potential Plant Species Hyperaccumulating Light Rare Earth Elements (LREE) in a Mining Area in Minas Gerais, Brazil." *Environmental Science and Pollution Research* 29(60):90779–90. doi: 10.1007/s11356-022-22009-9.

Azizitorghabeh, Atefeh, Fereshteh Rashchi, Ataollah Babakhani, and Mehdi Noori. 2017. "Synergistic Extraction and Separation of Fe (III) and Zn (II) Using TBP and D2EHPA." *Separation Science and Technology* 52(3):476–86.

Bahcivanji, L., G. Gascó, J. Paz-Ferreiro, and A. Méndez. 2020. "The Effect of Post-Pyrolysis Treatment on Waste Biomass Derived Hydrochar." *Waste Management* 106:55–61. doi: 10.1016/j.wasman.2020.03.007.

Battsengel, Ariuntuya, Altansukh Batnasan, Kazutoshi Haga, and Atsushi Shibayama. 2018. "Selective Separation of Light and Heavy Rare Earth Elements from the Pregnant Leach Solution of Apatite Ore with D2EHPA." *Journal of Minerals and Materials Characterization and Engineering* 6(5):517–30.

Berazneva, Julia, Dominic Woolf, and David R. Lee. 2021. "Local Lignocellulosic Biofuel and Biochar Co-Production in Sub-Saharan Africa : The Role of Feedstock Provision in Economic Viability." *Energy Economics* 93:105031. doi: 10.1016/j.eneco.2020.105031.

Borai, E. H., A. M. Shahr El-Din, E. M. El Afifi, R. F. Aglan, and M. M. Abo-Aly. 2016. "Subsequent Separation and Selective Extraction of Thorium (IV), Iron (III), Zirconium (IV) and Cerium (III) from Aqueous Sulfate Medium." *South African Journal of Chemistry* 69:148–56.

Borghi, Alessandro, Roberto Cossio, Filippo Olmi, and Gloria Vaggelli. 1998. *Compositional X-Ray Maps of Metamorphic and Magmatic Minerals*. Springer.

Borra, Chenna Rao, Yiannis Pontikes, Koen Binnemans, and Tom Van Gerven. 2015. "Leaching of Rare Earths from Bauxite Residue (Red Mud)." *Minerals Engineering* 76:20–27.

Brewer, Aaron, Justyna Florek, and Freddy Kleitz. 2022. "A Perspective on Developing Solid-Phase Extraction Technologies for Industrial-Scale Critical Materials Recovery." *Green Chemistry* 24(7):2752–65.

Cai, Jiaxiao, Bin Li, Chaoying Chen, Jing Wang, Min Zhao, and Ke Zhang. 2016. "Hydrothermal Carbonization of Tobacco Stalk for Fuel Application." *Bioresource Technology* 220:305–11. doi: 10.1016/j.biortech.2016.08.098.

Cao, Xinde, Ying Chen, Xiaorong Wang, and Xihai Deng. 2001. "Effects of Redox Potential and PH Value on the Release of Rare Earth Elements from Soil." *Chemosphere* 44(4):655–61.

Carrier, Marion, Anne Loppinet-Serani, Christelle Absalon, Frederic Marias, Cyril Aymonier, and Michel Mench. 2011. "Conversion of Fern (Pteris Vittata L.) Biomass from a Phytoremediation Trial in Sub-and Supercritical Water Conditions." *Biomass and Bioenergy* 35(2):872–83.

Chai, Youzheng, Ma Bai, Anwei Chen, Liang Peng, Jihai Shao, Cui Shang, Cheng Peng, Jiachao

Zhang, and Yaoyu Zhou. 2022. "Thermochemical Conversion of Heavy Metal Contaminated Biomass: Fate of the Metals and Their Impact on Products." *Science of The Total Environment* 153426.

Chai, Youzheng, Anwei Chen, Ma Bai, Liang Peng, Jihai Shao, Jiayi Yuan, Cui Shang, Jiachao Zhang, Hongli Huang, and Cheng Peng. 2022a. "Valorization of Heavy Metal Contaminated Biomass: Recycling and Expanding to Functional Materials." *Journal of Cleaner Production* 366(June):132771. doi: 10.1016/j.jclepro.2022.132771.

Chai, Youzheng, Anwei Chen, Ma Bai, Liang Peng, Jihai Shao, Jiayi Yuan, Cui Shang, Jiachao Zhang, Hongli Huang, and Cheng Peng. 2022b. "Valorization of Heavy Metal Contaminated Biomass: Recycling and Expanding to Functional Materials." *Journal of Cleaner Production* 132771.

Channiwala, S. A., and P. P. Parikh. 2002. "A Unified Correlation for Estimating HHV of Solid, Liquid and Gaseous Fuels." *Fuel* 81(8):1051–63. doi: 10.1016/S0016-2361(01)00131-4.

Chen, Mengjun, Jinxiu Huang, Oladele A. Ogunseitan, Nengming Zhu, and Yan-min Wang. 2015. "Comparative Study on Copper Leaching from Waste Printed Circuit Boards by Typical Ionic Liquid Acids." *Waste Management* 41:142–47.

Chen, Wan Ting, Yuanhui Zhang, Jixiang Zhang, Lance Schideman, Guo Yu, Peng Zhang, and Mitchell Minarick. 2014. "Co-Liquefaction of Swine Manure and Mixed-Culture Algal Biomass from a Wastewater Treatment System to Produce Bio-Crude Oil." *Applied Energy* 128:209–16. doi: 10.1016/j.apenergy.2014.04.068.

Chen, Xueli, Yuxuan Zhang, Tao Hou, Lujia Han, and Weihua Xiao. 2018. "Catalysis Performance Comparison of a Brønsted Acid H2SO4 and a Lewis Acid Al2 (SO4) 3 in Methyl Levulinate Production from Biomass Carbohydrates." *Journal of Energy Chemistry* 27(2):552–58.

Chen, Yedan, Shuyi Ma, Shunyan Ning, Yilai Zhong, Xinpeng Wang, Toyohisa Fujita, and Yuezhou Wei. 2021. "Highly Efficient Recovery and Purification of Scandium from the Waste Sulfuric Acid Solution from Titanium Dioxide Production by Solvent Extraction." *Journal of Environmental Chemical Engineering* 9(5):106226.

Cheng, Kun, William T. Winter, and Arthur J. Stipanovic. 2012. "A Modulated-TGA Approach to the Kinetics of Lignocellulosic Biomass Pyrolysis/Combustion." *Polymer Degradation and Stability* 97(9):1606–15.

Chour, Zeinab, Baptiste Laubie, Jean Louis Morel, Ye Tao Tang, Marie Odile Simonnot, and Laurence Muhr. 2020. “Basis for a New Process for Producing REE Oxides from Dicranopteris Linearis.” *Journal of Environmental Chemical Engineering* 8(4):103961. doi: 10.1016/j.jece.2020.103961.

Chour, Zeinab, Baptiste Laubie, Jean Louis Morel, Yetao Tang, Rongliang Qiu, Marie Odile Simonnot, and Laurence Muhr. 2018. “Recovery of Rare Earth Elements from Dicranopteris Dichotoma by an Enhanced Ion Exchange Leaching Process.” *Chemical Engineering and Processing - Process Intensification* 130:208–13. doi: 10.1016/J.CEP.2018.06.007.

Ciszkowska, Malgorzata, Zbigniew Stojek, and Janet G. Osteryong. 1995. “Voltammetric Reduction of Polyprotic Acids at the Platinum Microelectrode: Dependence on Supporting Electrolyte.” *Journal of Electroanalytical Chemistry* 398(1–2):49–56.

Conti, Federica, Saqib S. Toor, Thomas H. Pedersen, Asbjørn H. Nielsen, and Lasse A. Rosendahl. 2018. “Biocrude Production and Nutrients Recovery through Hydrothermal Liquefaction of Wastewater Irrigated Willow.” *Biomass and Bioenergy* 118:24–31.

Cosio, Claudia, Enrico Martinoia, and Catherine Keller. 2004. “Hyperaccumulation of Cadmium and Zinc in Thlaspi Caerulescens and Arabidopsis Halleri at the Leaf Cellular Level.” *Plant Physiology* 134(2):716–25. doi: 10.1104/pp.103.031948.

Cui, Xiaoqiang, Jianwei Zhang, Xutong Wang, Minghui Pan, Qiang Lin, Kiran Yasmin Khan, Beibei Yan, Tingqiang Li, Zhenli He, and Xiaoe Yang. 2021. “A Review on the Thermal Treatment of Heavy Metal Hyperaccumulator: Fates of Heavy Metals and Generation of Products.” *Journal of Hazardous Materials* 405:123832.

Cui, Xiaoqiang, Jianwei Zhang, Xutong Wang, Minghui Pan, Qiang Lin, Kiran Yasmin Khan, Beibei Yan, Tingqiang Li, Zhenli He, Xiaoe Yang, and Guanyi Chen. 2021. “A Review on the Thermal Treatment of Heavy Metal Hyperaccumulator: Fates of Heavy Metals and Generation of Products.” *Journal of Hazardous Materials* 405(June 2020):123832. doi: 10.1016/j.jhazmat.2020.123832.

Dashti, Somayeh, Sina Shakibania, Fereshteh Rashchi, and Ahmad Ghahreman. 2021. “Synergistic Effects of Ionquest 801 and Cyanex 572 on the Solvent Extraction of Rare Earth Elements (Pr, Nd, Sm, Eu, Tb, and Er) from a Chloride Medium.” *Separation and Purification Technology* 279:119797.

Deep, Akash, and Jorge M. R. de Carvalho. 2008. "Review on the Recent Developments in the Solvent Extraction of Zinc." *Solvent Extraction and Ion Exchange* 26(4):375–404. doi: 10.1080/07366290802179267.

Demirbaş, Ahmet. 2000. "Mechanisms of Liquefaction and Pyrolysis Reactions of Biomass." *Energy Conversion and Management* 41(6):633–46.

Deng, Chen, Xihui Kang, Richen Lin, and Jerry D. Murphy. 2020. "Microwave Assisted Low-Temperature Hydrothermal Treatment of Solid Anaerobic Digestate for Optimising Hydrochar and Energy Recovery." *Chemical Engineering Journal* 395(April 2020):124999. doi: 10.1016/j.cej.2020.124999.

El Dessouky, S. I., Y. A. El-Nadi, I. M. Ahmed, E. A. Saad, and J. A. Daoud. 2008. "Solvent Extraction Separation of Zn(II), Fe(II), Fe(III) and Cd(II) Using Tributylphosphate and CYANEX 921 in Kerosene from Chloride Medium." *Chemical Engineering and Processing: Process Intensification* 47(2):177–83. doi: 10.1016/j.cep.2007.03.002.

Dewulf, Brecht, Sofia Riano, and Koen Binnemans. 2022. "Separation of Heavy Rare-Earth Elements by Non-Aqueous Solvent Extraction: Flowsheet Development and Mixer-Settler Tests." *Separation and Purification Technology* 290:120882.

Ding, ShiMing, Tao Liang, ChaoSheng Zhang, ZeChun Huang, YaNing Xie, and TongBin Chen. 2006. "Fractionation Mechanisms of Rare Earth Elements (REEs) in Hydroponic Wheat: An Application for Metal Accumulation by Plants." *Environmental Science & Technology* 40(8):2686–91.

Ding, Yan, Chuwen Guo, Shiru Qin, Baosu Wang, Peitao Zhao, and Xin Cui. 2022. "Effects of Process Water Recirculation on Yields and Quality of Hydrochar from Hydrothermal Carbonization Process of Rice Husk." *Journal of Analytical and Applied Pyrolysis* 166:105618.

Ding, Yung-Chin, Lin Chih-Chien, and Ta-Wui Cheng. 2015. "The Purification of Crude Zinc Oxide Using Scrubbing, Magnetic Separation, and Leaching Processes." *Separation Science and Technology* 50(15):2405–14.

Ding, Zhuhong, Lianyi Zhang, Huijing Mo, Yijun Chen, and Xin Hu. 2021. "Microwave-Assisted Catalytic Hydrothermal Carbonization of Laminaria Japonica for Hydrochars Catalyzed and Activated by Potassium Compounds." *Bioresource Technology* 341:125835. doi: 10.1016/J.BIORTECH.2021.125835.

Dinh, Truong, Zsolt Dobo, and Helga Kovacs. 2022a. “Phytomining of Noble Metals – A Review.” *Chemosphere* 286(P3):131805. doi: 10.1016/j.chemosphere.2021.131805.

Dinh, Truong, Zsolt Dobo, and Helga Kovacs. 2022b. “Phytomining of Rare Earth Elements – A Review.” *Chemosphere* 297(November 2021):134259. doi: 10.1016/j.chemosphere.2022.134259.

Dixon, D. G., and J. L. Hendrix. 1993. “A General Model for Leaching of One or More Solid Reactants from Porous Ore Particles.” *Metallurgical Transactions B* 24:157–69.

Donahue, Craig J., and Elizabeth A. Rais. 2009. “Proximate Analysis of Coal.” *Journal of Chemical Education* 86(2):222.

Dutta, Tanushree, Ki-hyun Kim, Minori Uchimiya, Eilhann E. Kwon, Byong-hun Jeon, Akash Deep, and Seong-taek Yun. 2016. “Global Demand for Rare Earth Resources and Strategies for Green Mining.” *Environmental Research* 150:182–90. doi: 10.1016/j.envres.2016.05.052.

Ebeling, J. M., and B. M. Jenkins. 1985. “Physical and Chemical Properties of Biomass Fuels.” *Transactions of the ASAE* 28(3):898–902.

Echevarria, Guillaume. 2018. *Agromining: Farming for Metals Extracting Unconventional Resources Using Plants*. Springer.

Elaigwu, Sunday E., and Gillian M. Greenway. 2016. “Microwave-Assisted and Conventional Hydrothermal Carbonization of Lignocellulosic Waste Material: Comparison of the Chemical and Structural Properties of the Hydrochars.” *Journal of Analytical and Applied Pyrolysis* 118:1–8.

Evcil, Tolgahan, Hamza Simsir, Suat Ucar, Kubilay Tekin, and Selhan Karagoz. 2020a. “Hydrothermal Carbonization of Lignocellulosic Biomass and Effects of Combined Lewis and Brønsted Acid Catalysts.” *Fuel* 279(June):118458. doi: 10.1016/j.fuel.2020.118458.

Evcil, Tolgahan, Hamza Simsir, Suat Ucar, Kubilay Tekin, and Selhan Karagoz. 2020b. “Hydrothermal Carbonization of Lignocellulosic Biomass and Effects of Combined Lewis and Brønsted Acid Catalysts.” *Fuel* 279:118458.

Fericelli, Paul D. 2011. “Comparison of Sludge Treatment by Gasification vs. Incineration.” in *Ninth LACCEI Latin American and Caribbean Conference (LACCEI’2011), Engineering for a Smart Planet, Innovation, Information Technology and Computational Tools for Sustainable Development*.

Finkelstein, Mark. 2000. *Twenty-First Symposium on Biotechnology for Fuels and Chemicals*.

Fisher, Travis, Mohammad Hajaligol, Bruce Waymack, and Diane Kellogg. 2002. “Pyrolysis Behavior and Kinetics of Biomass Derived Materials.” *Journal of Analytical and Applied Pyrolysis* 62(2):331–49.

Funke, Axel, and Felix Ziegler. 2010. “Hydrothermal Carbonization of Biomass: A Summary and Discussion of Chemical Mechanisms for Process Engineering.” *Biofuels, Bioproducts and Biorefining* 4(2):160–77.

Gao, Yang, Javier Remón, and Avtar S. Matharu. 2021. “Microwave-Assisted Hydrothermal Treatments for Biomass Valorisation: A Critical Review.” *Green Chemistry* 23(10):3502–25.

Gao, Ying, Yinghui Liu, Guangkuo Zhu, Jiayu Xu, Hui xu, Qiaoxia Yuan, Yuezhao Zhu, Jyotirmoy Sarma, Yinfeng Wang, Jing Wang, and Lian Ji. 2018. “Microwave-Assisted Hydrothermal Carbonization of Dairy Manure: Chemical and Structural Properties of the Products.” *Energy* 165:662–72. doi: 10.1016/j.energy.2018.09.185.

Gergoric, Marino, Christian Ekberg, Britt-Marie Steenari, and Teodora Retegan. 2017. “Separation of Heavy Rare-Earth Elements from Light Rare-Earth Elements via Solvent Extraction from a Neodymium Magnet Leachate and the Effects of Diluents.” *Journal of Sustainable Metallurgy* 3:601–10.

Gollakota, A. R. K., Nanda Kishore, and Sai Gu. 2018. “A Review on Hydrothermal Liquefaction of Biomass.” *Renewable and Sustainable Energy Reviews* 81(April 2017):1378–92. doi: 10.1016/j.rser.2017.05.178.

Guimarães, Alexandre Silva, Lucas Andrade Silva, Alexandre Moni Pereira, Julio Cesar Guedes Correia, and Marcelo Borges Mansur. 2020. “Purification of Concentrated Nickel Sulfuric Liquors via Synergistic Solvent Extraction of Calcium and Magnesium Using Mixtures of D2EHPA and Cyanex 272.” *Separation and Purification Technology* 239:116570.

Guo, Shuqing, Xiangyuan Dong, Tingting Wu, Fengjuan Shi, and Caixia Zhu. 2015. “Characteristic Evolution of Hydrochar from Hydrothermal Carbonization of Corn Stalk.” *Journal of Analytical and Applied Pyrolysis* 116:1–9.

Guo, Shuqing, Xiangyuan Dong, Tingting Wu, and Caixia Zhu. 2016. “Influence of Reaction Conditions and Feedstock on Hydrochar Properties.” *Energy Conversion and Management* 123:95–103. doi: 10.1016/j.enconman.2016.06.029.

Heilmann, Steven M., Lindsey R. Jader, Laurie A. Harned, Michael J. Sadowsky, Frederick J. Schendel, Paul A. Lefebvre, Marc G. Von Keitz, and Kenneth J. Valentas. 2011. "Hydrothermal Carbonization of Microalgae II. Fatty Acid, Char, and Algal Nutrient Products." *Applied Energy* 88(10):3286–90.

Hibbert, Sam, Kevin Welham, and Sharif H. Zein. 2019. "An Innovative Method of Extraction of Coffee Oil Using an Advanced Microwave System: In Comparison with Conventional Soxhlet Extraction Method." *SN Applied Sciences* 1:1–9.

Hidayah, Nur Nadiatul, and Sumaiya Zainal Abidin. 2018. "The Evolution of Mineral Processing in Extraction of Rare Earth Elements Using Liquid-Liquid Extraction: A Review." *Minerals Engineering* 121:146–57.

Hoekman, S. Kent, Amber Broch, and Curtis Robbins. 2011. "Hydrothermal Carbonization (HTC) of Lignocellulosic Biomass." *Energy & Fuels* 25(4):1802–10.

Housh, T., S. A. Bowring, and M. Villeneuve. 1985. "The Continental Crust: Its Composition and Evolution." *Journal of Geology* 97(6):735–47. doi: 10.1086/629355.

Huang, Xiaowei, Jinshi Dong, Liangshi Wang, Zongyu Feng, Qiannan Xue, and Xianglong Meng. 2017. "Selective Recovery of Rare Earth Elements from Ion-Adsorption Rare Earth Element Ores by Stepwise Extraction with HEH (EHP) and HDEHP." *Green Chemistry* 19(5):1345–52.

Jally, Bastien, Baptiste Laubie, Zeinab Chour, Laurence Muhr, Rongliang Qiu, Jean Louis Morel, Yetao Tang, and Marie Odile Simonnot. 2021a. "A New Method for Recovering Rare Earth Elements from the Hyperaccumulating Fern Dicranopteris Linearis from China." *Minerals Engineering* 166(March):106879. doi: 10.1016/j.mineng.2021.106879.

Jally, Bastien, Baptiste Laubie, Zeinab Chour, Laurence Muhr, Rongliang Qiu, Jean Louis Morel, Yetao Tang, and Marie Odile Simonnot. 2021b. "A New Method for Recovering Rare Earth Elements from the Hyperaccumulating Fern Dicranopteris Linearis from China." *Minerals Engineering* 166:106879. doi: 10.1016/J.MINENG.2021.106879.

Jankovská, I., V. Sloup, J. Száková, I. Langrová, and S. Sloup. 2016. "How the Tapeworm Hymenolepis Diminuta Affects Zinc and Cadmium Accumulation in a Host Fed a Hyperaccumulating Plant (Arabidopsis Halleri)." *Environmental Science and Pollution Research* 23(19):19126–33. doi: 10.1007/s11356-016-7123-1.

Ji, Bin, Qi Li, and Wencai Zhang. 2022. "Rare Earth Elements (REEs) Recovery from Coal

Waste of the Western Kentucky No. 13 and Fire Clay Seams. Part I: Mineralogical Characterization Using SEM-EDS and TEM-EDS." *Fuel* 307:121854.

Ji, Bin, and Wencai Zhang. 2021. "Rare Earth Elements (REEs) Recovery and Porous Silica Preparation from Kaolinite." *Powder Technology* 391:522–31.

Jiang, Si jie, Jingchun Sun, Gongsong Tong, Hao Ding, Jiewei Ouyang, Qiang Zhou, Yunxiang Fu, and Mei e. Zhong. 2022. "Emerging Disposal Technologies of Harmful Phytoextraction Biomass (HPB) Containing Heavy Metals: A Review." *Chemosphere* 290(November 2021):133266. doi: 10.1016/j.chemosphere.2021.133266.

Jorjani, Esmaeil, and Malek Shahbazi. 2016. "The Production of Rare Earth Elements Group via Tributyl Phosphate Extraction and Precipitation Stripping Using Oxalic Acid." *Arabian Journal of Chemistry* 9:S1532–39.

Jowitt, Simon M., Timothy T. Werner, Zhehan Weng, and Gavin M. Mudd. 2018. "Recycling of the Rare Earth Elements." *Current Opinion in Green and Sustainable Chemistry* 13:1–7. doi: https://doi.org/10.1016/j.cogsc.2018.02.008.

Jung, Min Jung, P. Venkateswaran, and Young Seak Lee. 2008. "Solvent Extraction of Nickel (II) Ions from Aqueous Solutions Using Triethylamine as Extractant." *Journal of Industrial and Engineering Chemistry* 14(1):110–15.

Kambo, Harpreet Singh, and Animesh Dutta. 2015a. "A Comparative Review of Biochar and Hydrochar in Terms of Production, Physico-Chemical Properties and Applications." *Renewable and Sustainable Energy Reviews* 45:359–78.

Kambo, Harpreet Singh, and Animesh Dutta. 2015b. "Comparative Evaluation of Torrefaction and Hydrothermal Carbonization of Lignocellulosic Biomass for the Production of Solid Biofuel." *Energy Conversion and Management* 105:746–55.

Kang, Kang, Sonil Nanda, Guotao Sun, Ling Qiu, Yongqing Gu, Tianle Zhang, Mingqiang Zhu, and Runcang Sun. 2019. "Microwave-Assisted Hydrothermal Carbonization of Corn Stalk for Solid Biofuel Production: Optimization of Process Parameters and Characterization of Hydrochar." *Energy* 186:115795. doi: 10.1016/j.energy.2019.07.125.

Kannan, Shrikalaa, Yvan Gariepy, and G. S. Vijay. Raghavan. 2017. "Optimization and Characterization of Hydrochar Produced from Microwave Hydrothermal Carbonization of Fish Waste." *Waste Management* 65:159–68. doi: 10.1016/j.wasman.2017.04.016.

Khaironie, Mohamed Takip, Markom Masturah, Meor Yusoff Meor Sulaiman, and

NAZARATUL ASHIFA ABDULLAH SALIM. 2014. “Solvent Extraction of Light Rare Earth Ions Using D2EHPA from Nitric Acid and Sulphuric Acid Solutions.” *Advanced Materials Research* 970:209–13.

Khoo, Choon Gek, Man Kee Lam, Abdul Rahman Mohamed, and Keat Teong Lee. 2020. “Hydrochar Production from High-Ash Low-Lipid Microalgal Biomass via Hydrothermal Carbonization: Effects of Operational Parameters and Products Characterization.” *Environmental Research* 188(March):109828. doi: 10.1016/j.envres.2020.109828.

Kim, Daegi, Kwanyong Lee, and Ki Young Park. 2014. “Hydrothermal Carbonization of Anaerobically Digested Sludge for Solid Fuel Production and Energy Recovery.” *Fuel* 130:120–25. doi: 10.1016/j.fuel.2014.04.030.

Kirkby, Ernest A. 2023. “Introduction, Definition, and Classification of Nutrients.” Pp. 3–9 in *Marschner’s Mineral Nutrition of Plants*. Elsevier.

Van Krevelen, D. W. 1950. “Graphical-Statistical Method for the Study of Structure and Reaction Processes of Coal.” *Fuel* 29:269–84.

Krishnamoorthy, Nageshwari, Baishali Dey, Yuwalee Unpaprom, Rameshprabu Ramaraj, Gaanty Pragas Maniam, Natanamurugaraj Govindan, Sivaraman Jayaraman, Thirugnanam Arunachalam, and Balasubramanian Paramasivan. 2021. “Engineering Principles and Process Designs for Phosphorus Recovery as Struvite: A Comprehensive Review.” *Journal of Environmental Chemical Engineering* 9(5):105579.

Kumar, Ramesh, and Parimal Pal. 2015. “Assessing the Feasibility of N and P Recovery by Struvite Precipitation from Nutrient-Rich Wastewater: A Review.” *Environmental Science and Pollution Research* 22:17453–64.

Kumari, Archana, Rekha Panda, Jin Young Lee, Thenepalli Thriveni, Manis Kumar Jha, and Devendra Deo Pathak. 2019. “Extraction of Rare Earth Metals (REMs) from Chloride Medium by Organo-Metallic Complexation Using D2EHPA.” *Separation and Purification Technology* 227(April):115680. doi: 10.1016/j.seppur.2019.115680.

Lai, Ying, Qiuquan Wang, Wenwu Yan, Limin Yang, and Benli Huang. 2005. “Preliminary Study of the Enrichment and Fractionation of REEs in a Newly Discovered REE Hyperaccumulator Pronephrium Simplex by SEC-ICP-MS and MALDI-TOF/ESI-MS.” *Journal of Analytical Atomic Spectrometry* 20(8):751–53. doi: 10.1039/b501766a.

Lang, Qianqian, Mengjun Chen, Yanchuan Guo, Zhengang Liu, and Chao Gai. 2019. “Effect of

Hydrothermal Carbonization on Heavy Metals in Swine Manure: Speciation, Bioavailability and Environmental Risk.” *Journal of Environmental Management* 234(November 2018):97–103. doi: 10.1016/j.jenvman.2018.12.073.

Larhed, Mats, Christina Moberg, and Anders Hallberg. 2002. “Microwave-Accelerated Homogeneous Catalysis in Organic Chemistry.” *Accounts of Chemical Research* 35(9):717–27.

Larsson, Kristian, Christian Ekberg, and Arvid Ødegaard-Jensen. 2013. “Dissolution and Characterization of HEV NiMH Batteries.” *Waste Management* 33(3):689–98.

Laubie, Baptiste, Zeinab Chour, Ye-Tao Tang, Jean-Louis Morel, Marie-Odile Simonnot, and Laurence Muhr. 2018. “REE Recovery from the Fern D. Dichotoma by Acid Oxalic Precipitation After Direct Leaching with EDTA BT - Extraction 2018.” Pp. 2659–67 in, edited by B. R. Davis, M. S. Moats, S. Wang, D. Gregurek, J. Kapusta, T. P. Battle, M. E. Schlesinger, G. R. Alvear Flores, E. Jak, G. Goodall, M. L. Free, E. Asselin, A. Chagnes, D. Dreisinger, M. Jeffrey, J. Lee, G. Miller, J. Petersen, V. S. T. Ciminelli, Q. Xu, R. Molnar, J. Adams, W. Liu, N. Verbaan, J. Goode, I. M. London, G. Azimi, A. Forstner, R. Kappes, and T. Bhambhani. Cham: Springer International Publishing.

Lee, Jongkeun, Kwanyong Lee, Donghwan Sohn, Young Mo Kim, and Ki Young Park. 2018. “Hydrothermal Carbonization of Lipid Extracted Algae for Hydrochar Production and Feasibility of Using Hydrochar as a Solid Fuel.” *Energy* 153:913–20. doi: 10.1016/j.energy.2018.04.112.

Lee, Jongkeun, and Ki Young Park. 2021. “Conversion of Heavy Metal-Containing Biowaste from Phytoremediation Site to Value-Added Solid Fuel through Hydrothermal Carbonization.” *Environmental Pollution* 269:116127. doi: 10.1016/j.envpol.2020.116127.

Lei, Qian, Shrikalaa Kannan, and Vijaya Raghavan. 2021. “Uncatalyzed and Acid-Aided Microwave Hydrothermal Carbonization of Orange Peel Waste.” *Waste Management* 126:106–18. doi: 10.1016/j.wasman.2021.02.058.

Li, Hong, Zhenyu Zhao, Christos Xiouras, Georgios D. Stefanidis, Xingang Li, and Xin Gao. 2019. “Fundamentals and Applications of Microwave Heating to Chemicals Separation Processes.” *Renewable and Sustainable Energy Reviews* 114:109316.

Li, Jin Tian, Hanumanth Kumar Gurajala, Long Hua Wu, Antony Van Der Ent, Rong Liang Qiu, Alan J. M. Baker, Ye Tao Tang, Xiao E. Yang, and Wen Sheng Shu. 2018.

“Hyperaccumulator Plants from China: A Synthesis of the Current State of Knowledge.” *Environmental Science and Technology* 52(21):11980–94. doi: 10.1021/acs.est.8b01060.

Li, Shiyu, Bin Ji, and Wencai Zhang. 2023. “A Review on the Thermochemical Treatments of Biomass: Implications for Hydrochar Production and Rare Earth Element Recovery from Hyperaccumulators.” *Chemosphere* 140140.

Li, Shiyu, Bin Ji, and Wencai Zhang. 2024. “Rare Earth Element Recovery and Hydrochar Evaluation from Hyperaccumulator by Acid Leaching and Microwave-Assisted Hydrothermal Carbonization.” *Minerals* 14(3).

Li, Shiyu, Thien Q. Tran, Qi Li, Bin Ji, Alexander S. Brand, and Wencai Zhang. 2023. “Zn Leaching Recovery and Mechanisms from End-of-Life Tire Rubber.” *Resources, Conservation and Recycling* 194:107004. doi: 10.1016/J.RESCONREC.2023.107004.

Li, Shiyu, and Wencai Zhang. 2024. “REE Recovery and Hydrochar Production from a Hyperaccumulator by Microwave-Assisted Hydrothermal Carbonization.” *Minerals Engineering* 208(October 2023):108595. doi: 10.1016/j.mineng.2024.108595.

Li, Shuaishuai, Wei Zeng, Huanhuan Xu, Ziyue Jia, and Yongzhen Peng. 2020. “Performance Investigation of Struvite High-Efficiency Precipitation from Wastewater Using Silicon-Doped Magnesium Oxide.” *Environmental Science and Pollution Research* 27(13):15463–74. doi: 10.1007/s11356-019-07589-3.

Li, Xingbin, Zhigan Deng, Cunxiong Li, Chang Wei, Minting Li, Gang Fan, and Hao Rong. 2015. “Direct Solvent Extraction of Indium from a Zinc Residue Reductive Leach Solution by D2EHPA.” *Hydrometallurgy* 156:1–5. doi: 10.1016/j.hydromet.2015.05.003.

Li, Xuewei, Xu Zhao, Juanjuan Zhang, Jingwei Hao, and Qiwu Zhang. 2022. “Struvite Crystallization by Using Active Serpentine: An Innovative Application for the Economical and Efficient Recovery of Phosphorus from Black Water.” *Water Research* 221:118678. doi: https://doi.org/10.1016/j.watres.2022.118678.

Li, Zheng, Xiaohua Li, Stijn Raiguel, and Koen Binnemans. 2018. “Separation of Transition Metals from Rare Earths by Non-Aqueous Solvent Extraction from Ethylene Glycol Solutions Using Aliquat 336.” *Separation and Purification Technology* 201:318–26. doi: https://doi.org/10.1016/j.seppur.2018.03.022.

Lie, Jenni, and Jhy Chern Liu. 2021. “Selective Recovery of Rare Earth Elements (REEs) from Spent NiMH Batteries by Two-Stage Acid Leaching.” *Journal of Environmental Chemical*

*Engineering* 9(5):106084. doi: 10.1016/j.jece.2021.106084.

Lima, Ana Teresa, and Lisbeth Ottosen. 2021. "Recovering Rare Earth Elements from Contaminated Soils: Critical Overview of Current Remediation Technologies." *Chemosphere* 265:129163. doi: 10.1016/j.chemosphere.2020.129163.

Liu, Chong, Wen-Shen Liu, Antony van der Ent, Jean Louis Morel, Hong-Xiang Zheng, Guo-Bao Wang, Ye-Tao Tang, and Rong-Liang Qiu. 2021. "Simultaneous Hyperaccumulation of Rare Earth Elements, Manganese and Aluminum in Phytolacca Americana in Response to Soil Properties." *Chemosphere* 282:131096.

Liu, Wen Shen, Antony Van Der Ent, Peter D. Erskine, Jean Louis Morel, Guillaume Echevarria, Kathryn M. Spiers, Emmanuelle Montargès-Pelletier, Rong Liang Qiu, and Ye Tao Tang. 2020. "Spatially Resolved Localization of Lanthanum and Cerium in the Rare Earth Element Hyperaccumulator Fern Dicranopteris Linearis from China." *Environmental Science and Technology* 54(4):2287–94. doi: 10.1021/acs.est.9b05728.

LIU, Ya nan, Zhao hui GUO, Yang SUN, Wei SHI, Zi yu HAN, Xi yuan XIAO, and Peng ZENG. 2017. "Stabilization of Heavy Metals in Biochar Pyrolyzed from Phytoremediated Giant Reed (Arundo Donax) Biomass." *Transactions of Nonferrous Metals Society of China (English Edition)* 27(3):656–65. doi: 10.1016/S1003-6326(17)60073-6.

LIU, Yan-jing, Ting-gui YAN, A. N. Yan, Wei ZHANG, and DONG Yang. 2021. "Influence of Water Leaching on Alkali-Induced Slagging Properties of Biomass Straw." *Journal of Fuel Chemistry and Technology* 49(12):1839–49.

Liu, Yanju, and Ravi Naidu. 2014. "Hidden Values in Bauxite Residue (Red Mud): Recovery of Metals." *Waste Management* 34(12):2662–73. doi: https://doi.org/10.1016/j.wasman.2014.09.003.

Liu, Yuyan, Shaoqiang Ma, and Jiawei Chen. 2018. "A Novel Pyro-Hydrochar via Sequential Carbonization of Biomass Waste: Preparation, Characterization and Adsorption Capacity." *Journal of Cleaner Production* 176:187–95. doi: 10.1016/j.jclepro.2017.12.090.

Liu, Zhengang, and Fu Shen Zhang. 2008. "Effects of Various Solvents on the Liquefaction of Biomass to Produce Fuels and Chemical Feedstocks." *Energy Conversion and Management* 49(12):3498–3504. doi: 10.1016/j.enconman.2008.08.009.

Lu, Jianwen, Jiaren Zhang, Zhangbing Zhu, Yuanhui Zhang, Yu Zhao, Ruirui Li, Jamison Watson, Baoming Li, and Zhidan Liu. 2017. "Simultaneous Production of Biocrude Oil and

Recovery of Nutrients and Metals from Human Feces via Hydrothermal Liquefaction." *Energy Conversion and Management* 134:340–46.

Lu, Xiaowei, Joseph R. V. Flora, and Nicole D. Berge. 2014. "Influence of Process Water Quality on Hydrothermal Carbonization of Cellulose." *Bioresource Technology* 154:229–39. doi: 10.1016/j.biortech.2013.11.069.

Lv, Yingwei, Yubo Liu, Baozhong Ma, Chengyan Wang, and Yongqiang Chen. 2023. "Preferential Extraction of Rubidium from High Concentration Impurity Solution by Solvent Extraction and Preparation of High-Purity Rubidium Salts." *Desalination* 545(September 2022):116162. doi: 10.1016/j.desal.2022.116162.

Ma, Ru, Sandile Fakudze, Shuai Liu, Yingyuan Wei, Jianqiang Chen, Jiangang Han, Chen Wang, and Jiaxin Wang. 2023. "Surfactants/Citric Acid Catalyzed Hydrothermal Carbonization of Pomelo Peel for Solid Fuels: Conversion Mechanism and Combustion Performance." *Fuel* 342(January). doi: 10.1016/j.fuel.2023.127762.

Mai, Carsten, and Holger Militz. 2004. "Modification of Wood with Silicon Compounds. Inorganic Silicon Compounds and Sol-Gel Systems: A Review." *Wood Science and Technology* 37:339–48.

Majima, Hiroshi, Toshio Izaki, and Sumiko Sanuki. 1985. "Reductive Stripping of Fe (III)-Loaded D2EHPA with the Aqueous Solutions Containing Sulfur Dioxide." *Metallurgical Transactions B* 16:187–94.

Mäkelä, Mikko, Verónica Benavente, and Andrés Fullana. 2015. "Hydrothermal Carbonization of Lignocellulosic Biomass: Effect of Process Conditions on Hydrochar Properties." *Applied Energy* 155:576–84. doi: 10.1016/j.apenergy.2015.06.022.

Martinez-Fernandez, Jose S., and Shulin Chen. 2017. "Sequential Hydrothermal Liquefaction Characterization and Nutrient Recovery Assessment." *Algal Research* 25:274–84.

Marx, S., I. Chiyanzu, and N. Piyo. 2014. "Influence of Reaction Atmosphere and Solvent on Biochar Yield and Characteristics." *Bioresource Technology* 164:177–83. doi: 10.1016/j.biortech.2014.04.067.

Misch, David, Doris Gross, Qing Huang, Federica Zaccarini, and R. F. Sachsenhofer. 2016. "Light and Trace Element Composition of Carboniferous Coals from the Donets Basin (Ukraine): An Electron Microprobe Study." *International Journal of Coal Geology* 168:108–18.

Mohammadi, Maryam, Kerstin Forsberg, Lars Kloo, Joaquin Martinez De La Cruz, and Åke Rasmuson. 2015. "Separation of Nd (III), Dy (III) and Y (III) by Solvent Extraction Using D2EHPA and EHEHPA." *Hydrometallurgy* 156:215–24.

Mokoena, By K., L. S. Mokhahlane, and S. Clarke. 2022. "Effects of Acid Concentration on the Recovery of Rare Earth Elements from Coal Fly Ash." *International Journal of Coal Geology* 259(May):104037. doi: 10.1016/j.coal.2022.104037.

Moldoveanu, Georgiana A., and Vladimiros G. Papangelakis. 2012. "Recovery of Rare Earth Elements Adsorbed on Clay Minerals: I. Desorption Mechanism." *Hydrometallurgy* 117:71–78.

Muhmood, Atif, Shubiao Wu, Jiaxin Lu, Zeeshan Ajmal, Hongzhen Luo, and Renjie Dong. 2018. "Nutrient Recovery from Anaerobically Digested Chicken Slurry via Struvite: Performance Optimization and Interactions with Heavy Metals and Pathogens." *Science of The Total Environment* 635:1–9. doi: https://doi.org/10.1016/j.scitotenv.2018.04.129.

Muraina, H. O., J. K. Odusote, and A. A. Adeleke. 2017. "Physical Properties of Biomass Fuel Briquette from Oil Palm Residues." *Journal of Applied Sciences and Environmental Management* 21(4):777–82.

Mwewa, Brian, Margreth Tadie, Sehliselo Ndlovu, Geoffrey S. Simate, and Elias Matinde. 2022. "Recovery of Rare Earth Elements from Acid Mine Drainage: A Review of the Extraction Methods." *Journal of Environmental Chemical Engineering* 10(3):107704.

Naderi, Mohadese, and Masoud Vesali-naseh. 2021. "Hydrochar-Derived Fuels from Waste Walnut Shell through Hydrothermal Carbonization : Characterization and Effect of Processing Parameters." 1443–51.

Nizamuddin, Sabzoi, Humair Ahmed Baloch, G. J. Griffin, N. M. Mubarak, Abdul Waheed Bhutto, Rashid Abro, Shaukat Ali Mazari, and Brahim Si Ali. 2017. "An Overview of Effect of Process Parameters on Hydrothermal Carbonization of Biomass." *Renewable and Sustainable Energy Reviews* 73(February):1289–99. doi: 10.1016/j.rser.2016.12.122.

Nizamuddin, Sabzoi, Sundus Saeed Qureshi, Humair Ahmed Baloch, Muhammad Tahir Hussain Siddiqui, Pooja Takkalkar, Nabisab Mujawar Mubarak, Deepa K Dumbre, Gregory J. Griffin, Srinivasan Madapusi, and Akshat Tanksale. 2019. "Microwave Hydrothermal Carbonization of Rice Straw: Optimization of Process Parameters and Upgrading of Chemical, Fuel, Structural and Thermal Properties." *Materials* 12(3):403.

Nizamuddin, Sabzoi, Sundus Saeed Qureshi, Humair Ahmed Baloch, Muhammad Tahir Hussain Siddiqui, Pooja Takkalkar, Nabisab Mujawar Mubarak, Deepa K. Dumbre, Gregory J. Griffin, Srinivasan Madapusi, and Akshat Tanksale. 2019. "Microwave Hydrothermal Carbonization of Rice Straw: Optimization of Process Parameters and Upgrading of Chemical, Fuel, Structural and Thermal Properties." *Materials* 12(3). doi: 10.3390/ma12030403.

Nizamuddin, Sabzoi, Muhammad Tahir Hussain Siddiqui, Humair Ahmed Baloch, Nabisab Mujawar Mubarak, Gregory Griffin, Srinivasan Madapusi, and Akshat Tanksale. 2018. "Upgradation of Chemical, Fuel, Thermal, and Structural Properties of Rice Husk through Microwave-Assisted Hydrothermal Carbonization." *Environmental Science and Pollution Research* 25(18):17529–39. doi: 10.1007/s11356-018-1876-7.

Njira, Keston O. W., and J. Nabwami. 2015. "A Review of Effects of Nutrient Elements on Crop Quality." *African Journal of Food, Agriculture, Nutrition and Development* 15(1):9777–93.

Palden, Thupten, Mercedes Regadío, Bieke Onghena, and Koen Binnemans. 2019. "Selective Metal Recovery from Jarosite Residue by Leaching with Acid-Equilibrated Ionic Liquids and Precipitation-Stripping." *ACS Sustainable Chemistry & Engineering* 7(4):4239–46.

Parikh, Jigisha, S. A. Channiwala, and G. K. Ghosal. 2007. "A Correlation for Calculating Elemental Composition from Proximate Analysis of Biomass Materials." *Fuel* 86(12–13):1710–19. doi: 10.1016/J.FUEL.2006.12.029.

Parshetti, Ganesh K., S. Kent Hoekman, and Rajasekhar Balasubramanian. 2013. "Chemical, Structural and Combustion Characteristics of Carbonaceous Products Obtained by Hydrothermal Carbonization of Palm Empty Fruit Bunches." *Bioresource Technology* 135:683–89.

Phytolaccaceae, Roxb. 2017. "Chemosphere Biochar Provides a Safe and Value-Added Solution for Hyperaccumulating Plant Disposal : A Case Study of Phytolacca Acinosa." *Chemosphere* 178:59–64. doi: 10.1016/j.chemosphere.2017.02.121.

Pollard, A. Joseph, Roger D. Reeves, and Alan J. M. Baker. 2014. "Facultative Hyperaccumulation of Heavy Metals and Metalloids." *Plant Science* 217–218:8–17. doi: 10.1016/j.plantsci.2013.11.011.

Qian, Feng, Xiangdong Zhu, Yuchen Liu, Quan Shi, Longhua Wu, Shicheng Zhang, Jianmin Chen, and Zhiyong Jason Ren. 2018. "Influences of Temperature and Metal on Subcritical

Hydrothermal Liquefaction of Hyperaccumulator: Implications for the Recycling of Hazardous Hyperaccumulators." *Environmental Science and Technology* 52(4):2225–34. doi: 10.1021/acs.est.7b03756.

Rabemanolontsoa, Harifara, and Shiro Saka. 2016. "Various Pretreatments of Lignocellulosics." *Bioresource Technology* 199:83–91.

Rahaman, M. S., N. Ellis, and D. S. Mavinic. 2008. "Effects of Various Process Parameters on Struvite Precipitation Kinetics and Subsequent Determination of Rate Constants." *Water Science and Technology* 57(5):647–54.

Rech, Ioná, Paul J. A. Withers, Davey L. Jones, and Paulo S. Pavinato. 2018. "Solubility, Diffusion and Crop Uptake of Phosphorus in Three Different Struvites." *Sustainability* 11(1):134.

Reed, S. J. B., and A. Buckley. 1998. "Rare-Earth Element Determination in Minerals by Electron-Probe Microanalysis: Application of Spectrum Synthesis." *Mineralogical Magazine* 62(1):1–8.

Ren, Zhang, Meng, Liu, and Yuan Dai. 2007. "Extraction Equilibria of Copper (II) with D2EHPA in Kerosene from Aqueous Solutions in Acetate Buffer Media." *Journal of Chemical & Engineering Data* 52(2):438–41.

Reza, M. Toufiq, Joan G. Lynam, M. Helal Uddin, and Charles J. Coronella. 2013. "Hydrothermal Carbonization: Fate of Inorganics." *Biomass and Bioenergy* 49:86–94. doi: 10.1016/j.biombioe.2012.12.004.

Robinson, B. H., R. R. Brooks, A. W. Howes, J. H. Kirkman, and P. E. H. Gregg. 1997. "The Potential of the High-Biomass Nickel Hyperaccumulator Berkheya Coddii for Phytoremediation and Phytomining." *Journal of Geochemical Exploration* 60(2):115–26. doi: https://doi.org/10.1016/S0375-6742(97)00036-8.

Sciarria, T. Pepè, S. Zangarini, F. Tambone, L. Trombino, S. Puig, and F. Adani. 2023. "Phosphorus Recovery from High Solid Content Liquid Fraction of Digestate Using Seawater Bittern as the Magnesium Source." *Waste Management* 155:252–59.

Seehar, Tahir H., Saqib S. Toor, Ayaz A. Shah, Asbjørn H. Nielsen, Thomas H. Pedersen, and Lasse A. Rosendahl. 2021. "Catalytic Hydrothermal Liquefaction of Contaminated Construction Wood Waste for Biocrude Production and Investigation of Fate of Heavy Metals." *Fuel Processing Technology* 212:106621. doi: 10.1016/J.FUPROC.2020.106621.

Sena, Madeline, Matthew Seib, Daniel R. Noguera, and Andrea Hicks. 2021. "Environmental Impacts of Phosphorus Recovery through Struvite Precipitation in Wastewater Treatment." *Journal of Cleaner Production* 280:124222.

Sevilla, Marta, and Antonio B. Fuertes. 2009. "The Production of Carbon Materials by Hydrothermal Carbonization of Cellulose." *Carbon* 47(9):2281–89.

Shao, Yuchao, Yuyang Long, Hengyi Wang, Dongyun Liu, Dongsheng Shen, and Ting Chen. 2019. "Hydrochar Derived from Green Waste by Microwave Hydrothermal Carbonization." *Renewable Energy* 135:1327–34.

Shao, Yuchao, Wenjing Lu, Yanjun Meng, Dan Zhou, Ying Zhou, Dongsheng Shen, and Yuyang Long. 2021. "The Formation of 5-Hydroxymethylfurfural and Hydrochar during the Valorization of Biomass Using a Microwave Hydrothermal Method." *Science of The Total Environment* 755:142499.

Shao, Yuchao, Hao Tan, Dongsheng Shen, Ying Zhou, Zhiyuan Jin, Dan Zhou, Wenjing Lu, and Yuyang Long. 2020. "Synthesis of Improved Hydrochar by Microwave Hydrothermal Carbonization of Green Waste." *Fuel* 266(September 2019):117146. doi: 10.1016/j.fuel.2020.117146.

Shen, Ruixia, Jianwen Lu, Zonglu Yao, Lixin Zhao, and Yulong Wu. 2021. "The Hydrochar Activation and Biocrude Upgrading from Hydrothermal Treatment of Lignocellulosic Biomass." *Bioresource Technology* 342:125914.

Sheoran, V., A. S.Sheoran, and P. Poonia. 2013. "Phytomining of Gold: A Review." *Journal of Geochemical Exploration* 128:42–50. doi: 10.1016/j.gexplo.2013.01.008.

Sheoran, V., A. S. Sheoran, and P. Poonia. 2009. "Phytomining: A Review." *Minerals Engineering* 22(12):1007–19. doi: 10.1016/j.mineng.2009.04.001.

Al Shra'Ah, Ahmad, and Robert Helleur. 2014. "Microwave Pyrolysis of Cellulose at Low Temperature." *Journal of Analytical and Applied Pyrolysis* 105:91–99. doi: 10.1016/j.jaap.2013.10.007.

Smolders, Erik, and Fien Degryse. 2002. "Fate and Effect of Zinc from Tire Debris in Soil." *Environmental Science and Technology* 36(17):3706–10. doi: 10.1021/es025567p.

Song, Huijuan, Jun Zhou, Shilong He, Qiao Ma, Liang Peng, Miaogen Yin, Hui Lin, and Qingru Zeng. 2023. "Efficient Removal of Heavy Metals from Contaminated Sunflower Straw by an Acid-Assisted Hydrothermal Process." *International Journal of Environmental Research* *and Public Health* 20(2):1311.

Stratful, I., M. D. Scrimshaw, and J. N. Lester. 2001. "Conditions Influencing the Precipitation of Magnesium Ammonium Phosphate." *Water Research* 35(17):4191–99.

Su, Hongcai, Xuanyou Zhou, Rendong Zheng, Zhihao Zhou, Yan Zhang, Gaojun Zhu, Caimeng Yu, Dwi Hantoko, and Mi Yan. 2021. "Hydrothermal Carbonization of Food Waste after Oil Extraction Pre-Treatment: Study on Hydrochar Fuel Characteristics, Combustion Behavior, and Removal Behavior of Sodium and Potassium." *Science of the Total Environment* 754:142192.

Sun, Huijuan, Abdul Nayeem Mohammed, and Yang Liu. 2020. "Phosphorus Recovery from Source-Diverted Blackwater through Struvite Precipitation." *Science of the Total Environment* 743:140747.

Sun, Jing, Wenlong Wang, and Qinyan Yue. 2016. "Review on Microwave-Matter Interaction Fundamentals and Efficient Microwave-Associated Heating Strategies." *Materials* 9(4):231.

Sun, Shichang, Xiaofei Huang, Junhao Lin, Rui Ma, Lin Fang, Peixin Zhang, and Junle Qu. 2018. "Study on the Effects of Catalysts on the Immobilization Efficiency and Mechanism of Heavy Metals during the Microwave Pyrolysis of Sludge." *Waste Management* 77:131–39. doi: 10.1016/j.wasman.2018.04.046.

Sun, Wei, Bin Ji, Sultan Ahmed Khoso, Honghu Tang, Runqing Liu, Li Wang, and Yuehua Hu. 2018. "An Extensive Review on Restoration Technologies for Mining Tailings." *Environmental Science and Pollution Research* 25(34):33911–25. doi: 10.1007/s11356-018-3423-y.

Tag, Asli Toptas, Gozde Duman, and Jale Yanik. 2018. "Influences of Feedstock Type and Process Variables on Hydrochar Properties." *Bioresource Technology* 250:337–44.

Talboys, Peter J., James Heppell, Tiina Roose, John R. Healey, Davey L. Jones, and Paul J. A. Withers. 2016. "Struvite: A Slow-Release Fertiliser for Sustainable Phosphorus Management?" *Plant and Soil* 401:109–23.

Talebi, A., A. Marra, A. Cesaro, V. Belgiorno, and I. Norli. 2018. "The Recovery of Rare Earth Metals from WEEE Leaching Solution via Liquid-Liquid Extraction." *Glob. Nest J* 20:719–24.

Tang, Xing, Junnan Wei, Ning Ding, Yong Sun, Xianhai Zeng, Lei Hu, Shijie Liu, Tingzhou Lei, and Lu Lin. 2017. "Chemoselective Hydrogenation of Biomass Derived 5-

Hydroxymethylfurfural to Diols: Key Intermediates for Sustainable Chemicals, Materials and Fuels." *Renewable and Sustainable Energy Reviews* 77:287–96. doi: https://doi.org/10.1016/j.rser.2017.04.013.

Tansel, Berrin, Griffin Lunn, and Oscar Monje. 2018. "Struvite Formation and Decomposition Characteristics for Ammonia and Phosphorus Recovery: A Review of Magnesium-Ammonia-Phosphate Interactions." *Chemosphere* 194:504–14.

Tu, Ren, Yan Sun, Yujian Wu, Xudong Fan, Shuchao Cheng, Enchen Jiang, and Xiwei Xu. 2021. "Selective Production of Furfural and Phenols from Rice Husk: The Influence of Synergetic Pretreatments with Different Order." *Renewable Energy* 168:297–308. doi: 10.1016/j.renene.2020.12.011.

Ul Saqib, Najam, Ajit K. Sarmah, and Saeid Baroutian. 2019. "Effect of Temperature on the Fuel Properties of Food Waste and Coal Blend Treated under Co-Hydrothermal Carbonization." *Waste Management* 89:236–46. doi: 10.1016/J.WASMAN.2019.04.005.

Vafaei, Mostafa, and Ali Allahverdi. 2017. "Durability of Geopolymer Mortar Based on Waste-Glass Powder and Calcium Aluminate Cement in Acid Solutions." *Journal of Materials in Civil Engineering* 29(10):4017196.

Wang, Li, Bin Ji, Yuehua Hu, Runqing Liu, and Wei Sun. 2017. "A Review on in Situ Phytoremediation of Mine Tailings." *Chemosphere* 184:594–600. doi: 10.1016/j.chemosphere.2017.06.025.

Wang, Liuwei, Nanthi S. Bolan, Daniel C. W. Tsang, and Deyi Hou. 2020. "Green Immobilization of Toxic Metals Using Alkaline Enhanced Rice Husk Biochar: Effects of Pyrolysis Temperature and KOH Concentration." *Science of the Total Environment* 720:137584. doi: 10.1016/j.scitotenv.2020.137584.

Wang, Shengsen, Bin Gao, Yuncong Li, Yong Sik Ok, Chaofeng Shen, and Shengguo Xue. 2017. "Biochar Provides a Safe and Value-Added Solution for Hyperaccumulating Plant Disposal: A Case Study of Phytolacca Acinosa Roxb. (Phytolaccaceae)." *Chemosphere* 178:59–64. doi: 10.1016/j.chemosphere.2017.02.121.

Wang, Tengfei, Yunbo Zhai, Yun Zhu, Caiting Li, and Guangming Zeng. 2018. "A Review of the Hydrothermal Carbonization of Biomass Waste for Hydrochar Formation: Process Conditions, Fundamentals, and Physicochemical Properties." *Renewable and Sustainable Energy Reviews* 90:223–47.

Wang, Yu-jie, Yi Yu, Hua-jun Huang, Cheng-long Yu, Han-sun Fang, Chun-huo Zhou, Xin Yin, Wei-hua Chen, and Xin-chun Guo. 2022. "Efficient Conversion of Sewage Sludge into Hydrochar by Microwave-Assisted Hydrothermal Carbonization." *Science of the Total Environment* 803:149874.

Wang, Zhong-Min, Jeff Wagner, Sutapa Ghosal, Gagandeep Bedi, and Stephen Wall. 2017. "SEM/EDS and Optical Microscopy Analyses of Microplastics in Ocean Trawl and Fish Guts." *Science of the Total Environment* 603:616–26.

Wehbie, M., Guilhem Arrachart, C. Arrambide Cruz, I. Karamé, L. Ghannam, and S. Pellet-Rostaing. 2017. "Organization of Diglycolamides on Resorcinarene Cavitand and Its Effect on the Selective Extraction and Separation of HREEs." *Separation and Purification Technology* 187:311–18.

Wei, Ning, Donghai Xu, Botian Hao, Shuwei Guo, Yang Guo, and Shuzhong Wang. 2021. "Chemical Reactions of Organic Compounds in Supercritical Water Gasification and Oxidation." *Water Research* 190:116634.

Westerholm, M., S. Isaksson, O. Karlsson Lindsjö, and A. Schnürer. 2018. "Microbial Community Adaptability to Altered Temperature Conditions Determines the Potential for Process Optimisation in Biogas Production." *Applied Energy* 226:838–48.

Wiedner, Katja, Christophé Naisse, Cornelia Rumpel, Alessandro Pozzi, Peter Wieczorek, and Bruno Glaser. 2013. "Chemical Modification of Biomass Residues during Hydrothermal Carbonization–What Makes the Difference, Temperature or Feedstock?" *Organic Geochemistry* 54:91–100.

Wilk, Małgorzata, Aneta Magdziarz, Izabela Kalemba-Rec, and Monika Szymańska-Chargot. 2020. "Upgrading of Green Waste into Carbon-Rich Solid Biofuel by Hydrothermal Carbonization: The Effect of Process Parameters on Hydrochar Derived from Acacia." *Energy* 202:117717.

Wilson, A. Matthew, Phillip J. Bailey, Peter A. Tasker, Jennifer R. Turkington, Richard A. Grant, and Jason B. Love. 2014. "Solvent Extraction: The Coordination Chemistry behind Extractive Metallurgy." *Chemical Society Reviews* 43(1):123–34.

Wu, Jun, Jian Lu, Leiming Li, Xiuyun Min, Zhenhua Zhang, and Yongming Luo. 2019. "Distribution, Pollution, and Ecological Risks of Rare Earth Elements in Soil of the Northeastern Qinghai–Tibet Plateau." *Human and Ecological Risk Assessment* 25(7):1816–

31. doi: 10.1080/10807039.2018.1475215.

Wu, Shengxi, Liangshi Wang, Patrick Zhang, Hassan El-Shall, Brij Moudgil, Xiaowei Huang, Longsheng Zhao, Lifeng Zhang, and Zongyu Feng. 2018. “Simultaneous Recovery of Rare Earths and Uranium from Wet Process Phosphoric Acid Using Solvent Extraction with D2EHPA.” *Hydrometallurgy* 175:109–16.

Xiang, Qian, Y. Y. Lee, Pär O. Pettersson, and Robert W. Torget. 2003. “Heterogeneous Aspects of Acid Hydrolysis of α-Cellulose.” Pp. 505–14 in *Biotechnology for Fuels and Chemicals: The Twenty-Fourth Symposium*. Springer.

Xiao, Ling Ping, Zheng Jun Shi, Feng Xu, and Run Cang Sun. 2012. “Hydrothermal Carbonization of Lignocellulosic Biomass.” *Bioresource Technology* 118:619–23. doi: 10.1016/j.biortech.2012.05.060.

Xie, Feng, Ting An Zhang, David Dreisinger, and Fiona Doyle. 2014. “A Critical Review on Solvent Extraction of Rare Earths from Aqueous Solutions.” *Minerals Engineering* 56:10–28.

Yang, Wei, Hui Wang, Meng Zhang, Jiayu Zhu, Jie Zhou, and Shengji Wu. 2016. “Fuel Properties and Combustion Kinetics of Hydrochar Prepared by Hydrothermal Carbonization of Bamboo.” *Bioresource Technology* 205:199–204.

Yang, Xinbo, and Rick Q. Honaker. 2020. “Leaching Kinetics of Rare Earth Elements from Fire Clay Seam Coal.” *Minerals* 10(6):491.

Yin, Xiangbo, Christine Martineau, Isabelle Demers, Nathan Basiliko, and Nicole J. Fenton. 2021. “The Potential Environmental Risks Associated with the Development of Rare Earth Element Production in Canada.” 377(March):354–77.

Yu, Xinyang, Ruirui Zhang, Siyuan Yang, Cheng Liu, Guichun He, Haolin Wang, and Jingliang Wang. 2020. “Short Communication A Novel Decanedioic Hydroxamic Acid Collector for the Fl Otation Separation of Bastnäsite from Calcite.” *Minerals Engineering* 151(May 2019):106306. doi: 10.1016/j.mineng.2020.106306.

Yuan, Xingzhong, Jingyu Wang, Guangming Zeng, Huajun Huang, Xiaokai Pei, Hui Li, Zhifeng Liu, and Minghui Cong. 2011a. “Comparative Studies of Thermochemical Liquefaction Characteristics of Microalgae Using Different Organic Solvents.” *Energy* 36(11):6406–12. doi: 10.1016/j.energy.2011.09.031.

Yuan, Xingzhong, Jingyu Wang, Guangming Zeng, Huajun Huang, Xiaokai Pei, Hui Li, Zhifeng

Liu, and Minghui Cong. 2011b. "Comparative Studies of Thermochemical Liquefaction Characteristics of Microalgae Using Different Organic Solvents." *Energy* 36(11):6406–12.

Zeng, Qiang, Shuzhen Li, Wei Sun, Liang Hu, Hui Zhong, and Zhiguo He. 2021. "Eco-Friendly Leaching of Rubidium from Biotite-Containing Minerals with Oxalic Acid and Effective Removal of Hg2+ from Aqueous Solution Using the Leaching Residues." *Journal of Cleaner Production* 306:127167. doi: 10.1016/j.jclepro.2021.127167.

Zhang, Hedong, Zuopeng Gao, Wenya Ao, Jing Li, Guangqing Liu, Jie Fu, Chunmei Ran, Xiao Mao, Qinhao Kang, Yang Liu, and Jianjun Dai. 2017. "Microwave-Assisted Pyrolysis of Textile Dyeing Sludge Using Different Additives." *Journal of Analytical and Applied Pyrolysis* 127(August):140–49. doi: 10.1016/j.jaap.2017.08.014.

Zhang, Jianwei, Yuting Wang, Xutong Wang, Wenzhu Wu, Xiaoqiang Cui, Zhanjun Cheng, Beibei Yan, Xiaoe Yang, Zhenli He, and Guanyi Chen. 2022. "Hydrothermal Conversion of Cd/Zn Hyperaccumulator (Sedum Alfredii) for Heavy Metal Separation and Hydrochar Production." *Journal of Hazardous Materials* 423:127122.

Zhang, Sheng, Fei Wang, Zhiya Mei, Lukai Lv, and Yong Chi. 2021. *Status and Development of Sludge Incineration in China*. Vol. 12. Springer Netherlands.

Zhang, Wencai, and Rick Honaker. 2020. "Process Development for the Recovery of Rare Earth Elements and Critical Metals from an Acid Mine Leachate." *Minerals Engineering* 153:106382.

Zhang, Wencai, and Aaron Noble. 2020a. "Mineralogy Characterization and Recovery of Rare Earth Elements from the Roof and Floor Materials of the Guxu Coalfield." *Fuel* 270(February):117533. doi: 10.1016/j.fuel.2020.117533.

Zhang, Wencai, and Aaron Noble. 2020b. "Mineralogy Characterization and Recovery of Rare Earth Elements from the Roof and Floor Materials of the Guxu Coalfield." *Fuel* 270:117533.

Zhang, Wencai, Aaron Noble, Bin Ji, and Qi Li. 2022. "Effects of Contaminant Metal Ions on Precipitation Recovery of Rare Earth Elements Using Oxalic Acid." *Journal of Rare Earths* 40(3):482–90.

Zhang, Xiufeng, Zhifeng Qin, Tahani Aldahri, Shan Ren, and Weizao Liu. 2020. "Solvent Extraction of Rubidium from a Sulfate Solution with High Concentrations of Rubidium and Potassium Using 4-Tert-Butyl-2-(α-Methylbenzyl)-Phenol." *Journal of the Taiwan Institute* *of Chemical Engineers* 116:43–50.

Zhang, Zhikun, Zongyuan Zhu, Boxiong Shen, and Lina Liu. 2019. “Insights into Biochar and Hydrochar Production and Applications: A Review.” *Energy* 171:581–98.

Zhou, Shaoqi, and Yanyu Wu. 2012. “Improving the Prediction of Ammonium Nitrogen Removal through Struvite Precipitation.” *Environmental Science and Pollution Research* 19(2):347–60. doi: 10.1007/s11356-011-0520-6.

Zhou, Zhen, Dalong Hu, Weichao Ren, Yuzeng Zhao, Lu-Man Jiang, and Luochun Wang. 2015. “Effect of Humic Substances on Phosphorus Removal by Struvite Precipitation.” *Chemosphere* 141:94–99.

Zhu, Xiangdong, Feng Qian, Chuifan Zhou, Lijie Li, Quan Shi, Shicheng Zhang, and Jianmin Chen. 2019. “Inherent Metals of a Phytoremediation Plant Influence Its Recyclability by Hydrothermal Liquefaction.” *Environmental Science & Technology* 53(11):6580–86.

Zhuang, Xiuzheng, Yanpei Song, Hao Zhan, Xiaotao T. Bi, Xiuli Yin, and Chuangzhi Wu. 2020. “Pyrolytic Conversion of Biowaste-Derived Hydrochar: Decomposition Mechanism of Specific Components.” *Fuel* 266:117106. doi: 10.1016/J.FUEL.2020.117106.

Zielinski, Margot, Laurent Cassayre, Philippe Destrac, Nicolas Coppey, Gilles Garin, and Béatrice Biscans. 2020. “Leaching Mechanisms of Industrial Powders of Spent Nickel Metal Hydride Batteries in a Pilot-scale Reactor.” *ChemSusChem* 13(3):616–28.